A BAYESIAN STATISTICAL EVALUATION OF THE COMPETITION INDICES USED IN EUCALYPTUS TREE GROWTH MODELING

by

SAMUEL MNISI

DISSERTATION

Submitted in fulfilment of the requirements for the degree of

MASTER OF SCIENCE

in

STATISTICS

in the

FACULTY OF SCIENCE AND AGRICULTURE

(School of Mathematical and Computer Sciences)

at the

UNIVERSITY OF LIMPOPO

SUPERVISOR: Dr K.D Moloi

CO-SUPERVISOR: Dr J Hugo (Nelson Mandela University)

2023

Declaration

I, Samuel Mnisi, the undersigned, hereby declare that the work contained in this dissertation submitted to the University of Limpopo, for the qualification of Master of Science in Statistics is my own independent work and has not been submitted by me for a qualification at this or any other institution of higher learning. Further, I confirm that all the reference materials contained therein have been acknowledged to the fullest.

Signature ……  …… **Date** ...**29/10/2023**……

Abstract

Eucalyptus is the most frequently planted genus tree in the world which is grown in more than 100 different countries. It is a subfamily of the Myrtaceae family with approximately 800 species of flowering evergreen trees and bushes. Since it offers wood for applications such as manufacturing pulp and solid wood, eucalyptus tree farming is especially significant in South Africa, where it is one of the most important sources of income. The study aims to evaluate the individual tree growth as well as competition present in eucalyptus plantations measured as a function of the growth rate during a particular growth period. The study used confidential secondary data, which were collected from a eucalyptus grandis cross with eucalyptus urophylla seedlings planted in the Kwa-Zulu Natal midlands in South Africa. The data were collected from the year 2000 to 2010 by the Institute for Commercial Forestry Research (ICFR) with trial number W184/03. For this study, one plot was randomly selected from all the plots planted for trail number W184/03. This randomly selected plot was plot 9 with a specified planting density of 1959 stems planted per hectare. A re-purposed Bayesian mixed effects variance component model, known as the Sire-Model in animal breeding problems, was used to determine the marginal posterior distributions of unknown parameters and provided the estimates. The re-purposing and subsequent use of the Bayesian Sire Model in individual tree growth modelling, was originally proposed by Kepe, Little and Hugo during the 61st Annual Conference of the South African Statistical Association, held from 27 – 29 November 2019 at the Nelson Mandela University in Port Elizabeth, South Africa (Programme and Abstracts, SASA 2019). Estimated tree growth indices were determined and used to make probability statements in order to rank the individually selected trees based on the amount of growth observed. A tree growth index is a measurement of a tree's average growth performance in relation to the average growth performance of all trees on the same plot. For this study specifically, the growth index was not calculated in relation to all the trees on the same plot, it was calculated in relation to the trees in the selected buffer. The marginal posterior densities were observed using a sampling-based approach known as the Gibbs sampler. MATLAB R2022b was used to obtain the results. Since the DBH is taken at a standard height of 1.37 meters above the ground and is therefore constant across measurements. The study used descriptive

statistics analysis using the tree DBH to determine average growth instead of using the circumference of the trees. The findings of a descriptive statistics revealed that plot 9 had maximum DBH of 23.4 cm. According to literature, competition starts to set in after canopy closure (Morley *et al*., 2008). By considering the previously mentioned growth curve, it can be seen that after growth periods 3 (after year 3), the gradient of the growth curve reduced, suggesting that canopy closure took place during, or just after, period 3. The marginal posterior densities of four trees namely tree 182, tree 184, tree 214, and tree 216 for the variance components and random effects were estimated using the Gibbs Sampler where competition between the trees was assumed, as well as for the case where it was assumed that no competition takes place. An identity matrix was utilised in Gibbs sampling when it was assumed that there is no competition between the trees. A distance independent competition index called Lorimer (1983), was used to generate a matrix that was used in Gibbs sampling when it was assumed that there is competition between the trees. Results assuming no competition, revealed that the estimated marginal posterior densities of the error variance and tree variance, were slightly positively skewed and severely positively skewed, respectively. The estimated marginal posterior density for the growth index for trees 182, 184, 214 and 216 were symmetrical and all the equal tails credibility intervals contained zero. This indicated that there was no significant difference in the average growth of these selected trees from plot 9 with a density of 1959. However, the marginal posterior densities of the fixed effects indicated that there was a significant difference in the average growth rates of the selected trees from plot 9 since their equal tails credibility intervals did not contain zero. This therefore indicated that the specific treatment applied, had a significant effect. Results when competition was assumed, revealed that the estimated marginal posterior densities of the error variance as well as tree variance, were again positively and severely positively skewed. The estimated marginal posterior density for the growth indices for tree 182, tree 184, tree 214 and tree 216 were also symmetrical and, similar to the case when no competition was assumed, their equal tails credibility intervals also contained zero. However, when competition between the trees was considered, the growth indices for tree 182, tree 184, tree 214 and tree 216 however appeared to be lower than the case when no competition was assumed. Given that the results were based on a

distance-independent competition index, it is advised that an investigation be conducted using a distance-dependent index as well.

Dedication

I would like to dedicate this dissertation to my son Kopano and my parents, Malani Zacharia and Mmaseme Hilda Mnisi for their tolerant support, endurance, and continuous encouragement.

Acknowledgements

Firstly, I wish to thank my Heavenly Father for the grace, wisdom, and strength He has bestowed upon me and the ability He gave me to complete this dissertation. My sincere appreciation and thanks to my supervisor Dr Khehla Daniel Moloi and my co-supervisor Dr Johan Hugo for their guidance, support, and patience throughout this dissertation. I am grateful to Mr Lulama Kepe from Nelson Mandela University for his unfailing support, assistance, and fruitful discussions throughout the study. I would also like to thank my partner for her understanding and encouragement during the course of the study. A special appreciation and gratitude to National Research Foundation (NRF) for funding my research and the Institute for Commercial Forestry Research (ICFR) for their contribution in this dissertation in terms of providing dataset. Finally, I would like to thank my friends and family for their moral support and encouragement.

Table of Content

List of Figures

List of Tables

List of Special Symbols

θ	Unknown Parameter for Θ_0 and Θ_1
Θ	Vector Parameter
K_ε	Normalisation constant
ρ	Intraclass Correlation
g_j	Basal area of the competitor tree
d_j	DBH of the competitor tree
d_i	DBH of the subject tree
G	Basal area of the trees within the plot.
l_{ij}	Distance between the competitor j and the subject tree i
d_j	DBH of the competitor tree
d_i	DBH of the subject tree
S	Plot area
y	Response vector (current growth rate of a tree)
$\boldsymbol{\beta}$	Vector of corresponding fixed effect coefficients
Z	Design matrix of covariates whose effects are assumed to be random
$\boldsymbol{u}$	Vector of random effect coefficients (or growth rate indices)
$\boldsymbol{\varepsilon}$	Vector of random errors that is independent of X, Z
Sdr	Lorimer (1983) competition index
Heg	Hegyi competition index

List of Distributions

$P(\Theta\|Y)$	Posterior Probability Distribution
$P(\theta)$	Prior Probability Distribution
$P(Y\|\Theta)$	Likelihood Function
$f(Y)$	Marginal Distribution
$f(\Theta\|Y) \propto f(\mathrm{Y}\|\Theta)$	Posterior Density
$y = X\boldsymbol{\beta} + Z\boldsymbol{u} + \boldsymbol{\varepsilon}$	Bayesian Linear Mixed Model
$P(\boldsymbol{u}\|\sigma_s^2, \boldsymbol{A})$	Prior Distribution of The Vector $\boldsymbol{u}$
$p(\boldsymbol{\beta}, \boldsymbol{u}, \sigma_s^2, \sigma_\varepsilon^2\|y)$	Joint Posterior Distribution

List of Acronyms

AIC	Akaike's Information Criterion
BLA	Basal Area Larger
ICFR	Institute for Commercial Forestry Research
CIs	Competition Indices
CSIR	Council for Scientific and Industrial Research
CV	Coefficient of Variation
DBH	Diameter at Breast Height
Hm	Modified Hegyi
HT	Total Height
MCMC	Markov Chain Monte Carlo
NICIS	National Integrated Cyberinfrastructure System
PLP	Post-Logging Period
Pm	Probability of Mortality
RIL	Reduced Impact Logging
SASA	South African Statistical Association
SAS	Statistical Analysis System
SWWA	South-West Western Australia

Conference/Workshop Attended

Conference

1. Mnisi, S., Hugo, J. and Moloi, K.D. A Bayesian statistical evaluation of the competition indices used in eucalyptus tree growth modelling. Presented during the 13th Annual Faculty of Science and Agriculture Postgraduate Research Day held at Bolivia Lodge, Limpopo, South Africa, September 2023.

Workshop

1. Research workshop conducted for Master's and Doctoral candidates at Magoebaskloof hotel in 2023, Limpopo Province, South Africa.

2. Research Publication Writing Retreat funded by the Department of Statistics and Operations Research at The Coach Hotel Tzaneen in 2023, Limpopo Province, South Africa.

3. Research workshop using MATLAB Online and Simulink Online conducted by MATLAB Expo for 2 days in 2022.

CHAPTER 1

INTRODUCTION

1.1 Background of the Study

Eucalyptus is a flowering evergreen tree and bush that belongs to the Myrtaceae family, the subfamily Myrotideae, and has over eight hundred species (Bayle, 2019). Eucalyptus is a genus name derived from eu- + Greek kalyptos, covered from kalyptein to conceal; derived from the conical covering of the buds (Mugayi, 2019). Although this tree is native to Australia, there are a few species in New Guinea, Indonesia and the Philippines (Paine *et al*., 2011; Zegeye, 2010). The trees survived a broad group of herbivores prevalent in their native environment after being spread over the world as seeds. In the last 30 years, however, some herbivore species native to the eucalyptus range have invaded several eucalyptus-growing locations in North America, Europe, Africa, Asia and South America (Paine *et al*., 2011).

Figure 1.1: Eucalyptus Trees (Source: Picture of Eucalyptus Tree, Australian plantation)

In 1875, the country's first plantations of exotic species, primarily pine and eucalyptus, were planted after it was realised that demand for timber had outstripped supply from indigenous forests (Albaugh *et al*., 2013). Eucalyptus tree farming is particularly important in South Africa, as it provides timber for pulp manufacture and solid wood applications, making it one of the country's most important sources of revenue (Melesse and Zewotir, 2017). Eucalyptus grandis, eucalyptus nitens, eucalyptus smithii, eucalyptus macarthuri, and eucalyptus dunnii are the five commercially produced species that make up most eucalyptus plantations in South Africa (Melesse and Zewotir, 2017).

Eucalyptus is the world's most widely planted genus, with eucalyptus plantations in over one hundred nations (Zegeye, 2010). Their remarkable adaptability, development and diversity have made them a global renewable fibre and energy resource (Myburg *et al*., 2014). Eucalyptus species are widely farmed for their oil, gum, pulp, lumber, medicinal and aesthetic value, among other things (Batish *et al*., 2008). The tree grows well and quickly even in poor soil. However, fast-growing tree plantations, on the other hand, can degrade soil quality if they are not adequately maintained (Mugayi, 2019). This is especially true of eucalyptus trees, which harm the ecosystem and ecology by drowning water resources, enhancing environmental destruction, suppressing forest, reducing soil nutrients, and causing distress to nearby agricultural crops (Bayle, 2019).

According to Dale (1985), tree growth models simulate forest ecosystem growth and development by increasing the size of each simulated tree in the forest on a yearly or more frequent basis. These models are often referred to as 'tree models' because they are based on the birth, growth and death of individual trees, and the properties of individual trees that are aggregated to define the tree stand. This study applies a Bayesian approach to model tree growth in eucalyptus plantations.

1.2 Problem Statement

The need for wood for industrial and fuel purposes has increased, especially in emerging nations due to population growth (Zerga, 2015). Forest plantations are

being developed all over the world to address the problem of increasing demand for wood (Chu *et al*., 2019). However, there is competition among the trees, leading to a decrease in reproduction, growth and survival of the competing trees. Trees compete for light, space, nutrients and moisture when they start to increase in size and age (Bhandari *et al*., 2021). Soil quality decline is frequently attributed to poor land use and soil management, which leaves the soil with little or no vegetation. When poorly planned and managed, fast-growing tree plantings can also lead to deterioration in soil quality (Mugayi, 2019).

According to Zegeye (2010), the negative effects of eucalyptus on the environment, which are mostly because of poor management, are far less than the benefits. Another evidence by İlseven and Başta ş (2018) revealed how botanists, ecologists, foresters and geographers see eucalyptuses as a potential danger for the environment, which can be considered as an asset instead. Hence, further studies are necessary to examine the effects of the plant and its implications on the environment (Vecchio, 2016).

Competition is one of several interlinked biotic and abiotic elements that affect a forest community's structure (Sahney *et al*. 2010). In most cases, competition implies the exploitation of available resources. For example, plants compete for finite resources such as light, water and nutrients that are necessary for their survival (Berger *et al*., 2008). They compete for resources both above and below ground; below-ground competition includes a broader range of resources, such as water and all essential mineral nutrients, whereas above-ground competition is focused on a single resource: light (Rubio *et al*., 2001).

Any measure that describes the level of competition generated by nearby trees on the productivity and growth capability of the subject tree is referred to as a competition index (CI) (Mohammed and Röhle, 2011). To evaluate the level of competition between the trees, this study used a distance-independent competition index called Lorimer (1983) which will be discussed briefly in section 3.8 and the results will be discussed in section 4.8.

1.3 Rationale

Competition among trees within a stand arises when there are not enough resources, such as light, space, water and soil nutrients to meet all the needs of the tree population for optimum growth (Mary and Oluremi, 2019). Due to intense competition and a reduction in the number of accessible resources for each tree, mortality results (Mohammed and Röhle, 2011), especially in forest areas that are managed and show different growth changing aspects when compared to natural areas that are not professionally managed (de Oliveira *et al.,* 2021). Perry (1985) highlighted that competition has an impact on both individual growth and how that growth is distributed, with much of the direct effect of competition on growth mediated through its effects on the amount of carbon fixed per unit leaf area, as well as crown size and structure. This study will briefly explain how competition indices can be used to explain individual tree competition present in eucalyptus plantations.

1.4 Aim and objectives of the study

1.4.1 Aim

The study aims to evaluate the individual tree growth present in eucalyptus plantations measured as a function of the growth rate during a particular growth period.

1.4.2 Objectives

The objectives of the study are to:

i. Use a Bayesian re-purposed mixed effect variance component model, known as the sire-model in animal breeding problems to determine the marginal posterior distributions of unknown parameters and to provide the growth index estimates based on the selected distance independent individual tree competition.

ii. Use the estimated growth indices and other treatment regimens, to determine posterior probabilities in order to establish tree growth position amongst the selected individual eucalyptus trees.

1.5 Significance of the Study

To better understand ecological dynamics, through the use of a re-purposed Bayesian Animal Breeding Model. The findings of this study will help us better understand how the Bayesian inference provides a unique and logical way of mixing prior data with information within a strong choice hypothetical framework. The study will also demonstrate how the Bayesian inference can be used to update personal beliefs about random events when new data becomes available. Because most research papers in ecological studies focus primarily on frequentist (or classical) inference, the outcomes of this study may contribute to a better understanding of Bayesian reasoning.

1.6 Structure of the Dissertation

The structure of the dissertation is described in this section. Five chapters, including references, make up the research study. The background of the study, problem statement, rationale, aim and objectives, and significance of the study are all covered in Chapter 1. Chapter 2 looks at previous research on comparable and related subjects. The research methodologies used in data analysis are described in Chapter 3. The data is analysed, and the results are illustrated in graphs and tables in Chapter 4. A short discussion of the results, followed by concluding remarks and recommendations for future research, are presented in Chapter 5.

CHAPTER 2

LITERATURE REVIEW

2.1 Introduction

This chapter reviews books, journals, thesis and other materials that are pertinent to the study of tree growth modelling. South Africa is one of the countries where research studies under consideration were done. In the conclusion of the chapter, findings from several studies are examined, summarised, and connections between the researcher's work are established.

2.2 Competition Indices

Berger *et al*. (2008) argued that competition is a critical process in plant populations and communities. In agreement, Peet and Christensen (1987) also concurred that competition is a key basic ecological process in population survival, growth dynamics and tree replacement. Competition, according to Weigelt and Jolliffe (2003) is an essential component in biology that is being studied in a variety of environments and for a variety of objectives. Its intensity and significance vary depending on the size and composition of neighbouring trees, as well as nutrient gradients (Luu, 2013). Because mathematical indices allow researchers to quantify and express several attributes of plant competition, such as competition intensity and importance, competitive effects and responses, and the outcome of competition, they can help researchers to summarise, interpret and display results from plant competition experiments (Weigelt and Jolliffe, 2003).

Competition indices (CIs) for tree development and survival are divided into two types: distance-independent (non-spatial) and distance-dependent (spatial) indices (Dong *et al*., 2021). They are widely used as explanatory variables in individual tree growth models because competition between trees is important in determining plant development (Kahriman *et al*., 2018). Distance-independent indices rely purely on non-spatial information about the total tree size and number inside a particular region, so they do not need to know the location of every tree in the plot (Contreras *et al*., 2011). The distance-dependent competition indices, on the other hand, require data that can only be calculated once the location of the trees within the plot is known,

such as tree spacing (Orso *et al*., 2020). The relative locations of neighbouring trees are factored into distance-dependent indices (Contreras *et al*., 2011).

In Curitiba, Paraná state, Brazil, Orso *et al*. (2020) investigated the impact of different plot sizes and competitor selection radii on distance-independent and distance-dependent competition indices and evaluated many adjustments to previously produced indices. Their research study employed data from two stem mapping measurements taken over a six-year span to determine diameter, canopy stratum and crown quality. For varying plot sizes and competitor selection radii, the statistical software R was used to construct both distance-independent and dependent indices. The performance of plot sizes and neighbourhood radii with annual diameter growth was assessed using Spearman's rank correlation. Those with the highest correlation coefficient were included in a stepwise regression to estimate diameter growth. The results showed that when the plot size or radius rose, the correlation increased for all the indicators. At varied plot sizes or competition radii, both distance-independent and distance-dependent competition indices affected the connection with diameter growth. Furthermore, their research study found that the best distance-independent competition index was the Basal Area in Larger Trees (BAL), and the best distance-dependent competition index was the modified Hegyi index (Hm). A 50 m x 50 m square plot was the optimal plot size for distance-independent indices, while the best competition radius for distance-dependent indices was 20 m.

The impacts of resource competition, according to de Oliveira *et al*. (2021), are poorly understood, particularly in regions subjected to forest management, which exhibit unique growth patterns when compared to unmanaged natural areas. The goal of de Oliveira *et al*. (2021) study was to estimate, evaluate and select the best fit competition indices (CI) for individual trees in an eastern Amazon managed forest. Their research study was based on data from eighteen one-hectare permanent plots that were followed for 12 years following Reduced Impact Logging (RIL). A total of twenty-three indicators were investigated for the competition analysis. Graphical analyses and linear correlation coefficients (r) between each index and variables, basal area growth (G), probability of mortality (Pm) and post-logging period, were used to calculate CIs (PLP). The distance-independent index for BAL (Basal Area

Larger) fared the best, according to the findings. The best interactions with the variables investigated for the distance-dependent and semi-independent indices occurred at radii of 15 and 20 m from the object tree. Curto (2020) and Dong (2021), who concluded that distance-independent (non-spatial) CIs outperformed distance-dependent (spatial) CIs, backed up this claim. Maleki *et al*. (2015) found that spatial indices were better growth predictors than non-spatial indices in a study aimed at quantifying and describing the influence of neighbours on the diameter growth of silver birch trees.

2.3 Competition from Neighbouring Trees

Competition from nearby trees has a detrimental influence on the growth of an individual tree in general; however, the level of competition is likely to vary depending on the size and proximity of the tree and its competitors (Bhandari *et al*., 2021). Luu (2013) investigated the effect of neighbourhood uniformity on the growth of individual eucalyptus monoculture trees. The data of the study came from a eucalyptus plantation in Aracruz, Espirito Santo, Brazil (40005W, 19049 S), which was grown on an Ultisol soil with 37 percent clay and $pH = 4$ at a height of twelve meters. At the ages of 17th month and 48th month, all trees in the stand were mapped and measured for diameters at breast height (DBH) and total heights (HT).

The researcher utilised R (R development Core Team 2010) to find and calculate nearby trees, distances, and coefficients of variation (CV) for each focal tree, as well as R2jags and JAGS 3.1.0 (Just Another Gibbs Sampler) to estimate parameters. The study employed a log-transform of growth to fit the models and uninformative priors for parameter estimation to optimise the likelihood and account for heteroscedasticity and non-normality in the residuals. The convergence of models was assessed using the Rhat value. All models and their parameters converged satisfactorily (Rhat less than 1.05), with Akaike's Information Criterion (AIC) values ranging from 1533 (highest value, least information) to 1120 (lowest value, most information) (smallest value, highest information). The corrected correlation (R^2) values varied only 3% between the models and across the neighbourhood radii (range from 0.43 to 0.46). The study also found that tree size uniformity in the neighbourhood had a significant impact on individual clonal Eucalyptus tree growth,

and that these impacts grew stronger as the age of the stand grew older because stand and neighbourhood tree sizes got less uniform.

In a study done in Mexico, Quiñonez-Barraza *et al*. (2018) modelled the growth of diameter at breast height (DBH) and assessed neighbourhood effects for four species groups in mixed-species stands. The study was based on information gathered from 44 stem-mapped re-measurement plots in mixed-species stands in Durango, Mexico. Pinus (seven species), other conifers (three species), other broadleaves (four species), and Quercus (four species) were the four groupings (eight species). Twelve competition indices (CIs) were created using four ways to identify neighbouring trees. There were comparisons of neighbouring tree selection methods and CIs, as well as tests of assumptions about neighbourhood effects. Except for the quercus group, all species groups showed a considerable reduction in diameter growth due to intra-species competition. The pinus, other conifers, and quercus species groups all demonstrated significant and negative neighbourhood effects on the other broadleaves species group, but not the other way around. The quercus species had a negative neighbourhood influence on the pinus and other conifer species, but not the other way around. The species groupings of pinus and other conifers showed negative neighbourhood impacts on each other. All the age independent DBH growth models that were fitted to the data fit the data well (adjusted coefficient of determination larger than 0.977).

2.4 Tree Growth Modelling

Tree growth models enlarge each simulated tree in the forest on an annual or more frequent basis to estimate the growth and development of forest ecosystems. Because they are based on the birth, growth and death of specific trees, these models are frequently referred to as "tree models" (Dale *et al*., 1985). In heterogeneous forests, tree-level growth models are becoming more popular because they can account for underlying mechanisms like competition (Orso *et al*., 2020). The growth of a single tree in a forest is influenced by a variety of factors, including its size, age, and stand density. Understanding how these elements influence individual growth can aid in terms of a better understanding of forest growth and dynamics in general (Bhandari *et al*., 2021).

Martins *et al*. (2014) assessed and verified the best-fitting diameter and height growth models for individual trees in eucalyptus forests in Brazil. The researchers used data from 48 permanent plots of unthinned eucalyptus grandis eucalyptus urophylla hybrid stands in northern Brazil from 1997 to 2003. The adjusted coefficient of determination, standard error of estimate as a percentage, trend, root mean square error and Akaike Information Criterion were used to evaluate the diameter and height growth models. The nonlinear estimation procedure from Statistica software (Statsoft, version 7.0, 2008), which uses a variant of the Gauss-Newton method to estimate the parameters of nonlinear regression by the least squares method, and the SAS software model procedure (Statistical Analysis System, version 8.0, 2001), with maximum likelihood fitting for nonlinear estimation. In comparison to the other models, the Lundqvist–Korf model provided the most accurate estimates for diameter and height growth, with better statistical values, closer proximity to observed values, and a better distribution of residual percentages.

Bhandari *et al*. (2021) investigated the growth of individual jarrah trees in Southwest Western Australia (SWWA) (eucalyptus marginata). The study investigated how well individual tree growth could be explained by considering tree size at the start of the growth period; whether this explanation could be improved by accounting for competition from neighbouring trees in various ways; how many neighbouring trees or what neighbourhood distance needed to be considered when accounting for competition; and whether the neighbouring tree growth could be a useful indicator of competition. The plots were thinned for the first time in 1965 (when they were 40 years old) and measured for the last time in 2010. The maximum likelihood approach in the nlme package in R was used to calculate the model's parameters. The findings showed that the size of the tree had a substantial impact on growth. When competition was added to the models, the results improved, according to R^2 (which ranged from 0.31 to 0.68). Competition from the 10 to 12 nearest competitors, or competitors within 10 meters of the base of the subject tree was considered to improve diameter growth explanation. The study recommends factoring neighbourhood competition when projecting growth and investigating thinning treatments to reduce the influence of competition on development.

2.5 Brief Literature Review about Techniques used in the Study

2.5.1 Bayesian Statistical Inference

The numerical approximation of analytically difficult integrals is required for Bayesian inferences, which are widely employed for probabilistic ecological modelling (Qian *et al*., 2003). The process of fitting a probability model to a collection of data and summarising the outcome using a probability distribution on model parameters and unobserved quantities such as forecasts for new observations is known as Bayesian inference (Gelman *et al*., 2014). According to Rupp *et al*. (2004), Bayesian methods were first introduced to social and behavioural researchers in an article by Edwards *et al*. in 1963. Bayesian inference methods offer an alternative form of data analysis that addresses many of the problems in traditional hypothesis testing while also allowing for the incorporation of uncertainty (Wade, 2000). Probability distributions are frequently used in Bayesian statistics to apply to more than just data. They can be used to express prior uncertainty in model parameters and then updated with new data to generate posterior probability distributions (Rupp *et al*., 2004; Gearhart, 2018). Data are treated as fixed variables in the Bayesian inference, which is used to update prior beliefs about the likelihood of a hypothesis (Westera, 2021). Without making any assumptions about the distribution of parameters, Bayesian frameworks frequently use Markov chain Monte Carlo (MCMC) methods to sample parameter space and to generate posterior predictions from the product of the likelihood function and prior distribution (King *et al*., 2019).

2.5.2 Markov Chain Monte Carlo Sampling

Bayesian techniques based on MCMC are currently included as standard features in several statistical software packages (Westera, 2021). The idea of the MCMC sampling method was first suggested by Metropolis *et al*. in 1953 as a method for the efficient modelling of energy levels of atoms in a crystalline structure (Brooks, 1998; Hastings, 1970). Following that, Hastings (1970) modified the approach to focus on statistical issues. The Bayesian inference aims to keep a complete posterior probability distribution over a set of random variables. However, maintaining and using this distribution frequently necessitates computing integrals, which is problematic for most non-trivial models (Yildirim, 2012). Brooks (1998) showed that MCMC approaches can directly give a solution for sampling from marginal posterior

distributions while implicitly computing the integrals. Starting with a series of trial values (e.g., means, regressions, genetic variances, genetic and environmental effects, etc.), the MCMC approach constructs a Markov Chain on the parameter of unknown quantities such that, after an initial series of iterations, successive iterations represent samples from an unknown joint distribution (Eaves *et al*., 2005). Because MCMC methods are useful for sampling from multivariate distributions that are generally difficult to sample from, a researcher can simulate a series of dependent random draws from models that are sometimes quite complex (Gearhart, 2018). To put it another way, MCMC is a general method for solving the difficult problem of numerical integration (Qian *et al*., 2003).

When there are many parameters or when the prior distribution is noninformative, direct Monte Carlo integration sampling from the posterior is unsuccessful. The posterior distribution is then used to produce samples using Markov Chain Monte Carlo (MCMC) methods. A Markov chain is put up using the posterior distribution as its long-run distribution in the context of MCMC approaches. The Metropolis-Hastings and Gibbs sampler algorithms can help with this. The Markov chain is run long enough till it hits the limiting (long-run) distribution in MCMC methods. As a result, each value obtained after the first run-in time is equivalent to a random pick from the posterior distribution (Sehlabana, 2020).

2.5.3 Gibbs Sampling

The block-wise Metropolis-Hastings algorithm is the foundation for Gibbs sampling. Assume that we use the genuine conditional density instead of the candidate density at each step for each block of parameters provided others. This implies the following:

$$q\left(\theta_j, \theta_j^T \middle| \theta_{-j}\right) > f\left(\theta_j \middle| \theta_{-j}, y\right).$$

Therefore, at step *n* for block θ_j, the acceptance probability is given by:

$$\alpha\left(\theta_j^{(n-1)}, \theta_j^{T(n)}, \theta_1^{(n)}, \ldots, \theta_{j-1}^{(n)}, \theta_{j+1}^{(n-1)}, \ldots \theta_j^{(n-1)}\right)$$

$$= \min\left[1, \frac{f(\theta_j^T|\theta_{-j}, y)q(\theta_j^T|\theta_{-j})}{f(\theta_j|\theta_{-j}, y)q(\theta_j, \theta_j^T|\theta_{-j})}\right] = 1.$$

The candidate will always be accepted at each step. Gibbs sampling is a special case of block-wise Metropolis-Hastings algorithm. This is a case where each candidate block is drawn from its true conditional density provided that all the other blocks given are at their recently drawn values (Zanella, 2020).

Without having to determine the density, Gibbs sampling is a numerical integration technique for indirectly creating random variables from a marginal distribution. Gibbs sampling is a widely used MCMC method for building a Markov chain for a target density (Gearhart, 2018). It is a simulation tool that allows you to get samples from a non-normalised joint density function (Gelfand, 2000). According to Brooks (1998), Gelfand (2000) and Rupp *et al*. (2004), in 1984 Geman and Geman originally presented the Gibbs sampler as an MCMC tool in the context of picture restoration. In 1989 Besag and York brought it to the statistics literature (Brooks, 1998). Gelfand and Smith in 1990 made the sampling approach more widely known (Rupp *et al*., 2004). Gibbs sampling is based on the idea of generating posterior samples by sweeping through each variable (or block of variables) to sample from its conditional distribution while keeping the remaining variables at their current values (Yildirim, 2012).

2.5.4 Mixed Effects Models

In order to analyse data sets having both fixed-effect variables and random-effect factors, as well as numerical covariates, the mixed-effect model offers a flexible tool that enables results to be generalised to the populations sampled by the random-effect factors. Two or more random-effect elements can be directly incorporated into mixed-effect models (Baayen, 2012). In a statistical study, the random variation in the sample is managed using random effects, whereas the independent variables are modelled using fixed effects (Linck and Cunnings, 2015). The re-purposing and subsequent use of the Bayesian mixed effects variance component model known as a sire-model,

specifically for use in individual tree growth modelling as presented by Mr L. Kepe, Prof K. Little and Dr J. Hugo during the 61st Animal conference of the South African Statistical Association (SASA), will be discussed in more detail in Chapter 3.

CHAPTER 3

RESEARCH METHODOLOGY

3.1 Introduction

This chapter describes the broad profound framework of the methods used in the study. The area of study and how the data used in the study were generated are outlined in section 3.2. This is followed by Section 3.3 in which the Bayesian inference method of estimation is discussed. Bayesian mixed effect models and the Posterior inference are outlined in section 3.4 and 3.5, respectively. Section 3.6 describes density estimation of function for variance components and section 3.7 describes competition indices. Lastly, section 3.8 describes the analysis of competition between individual trees using competition index called Lorimer (1983).

3.2 Study Area and Data Collection

3.2.1 Study Area

South Africa, which is located on the southernmost tip of Africa, is diverse and appealing. Botswana, Mozambique, Namibia and Zimbabwe all share borders with the country. The climate and weather in South Africa are pleasant, with bright sunny days for most of the year. From November to February, the summers are here. Hot weather with afternoon thunderstorms characterises the country. Winters are moderate and dry in general. Eastern Cape, Free State, Gauteng, KwaZulu-Natal, Limpopo, Mpumalanga, Northern Cape, Northwest and Western Cape are the nine provinces that make up South Africa. Limpopo province, which includes five districts: Capricorn, Mopani, Sekhukhune, Vhembe, and Waterberg, is the subject of this study.

Figure 3.1: South African Map

3.2.2 Data Collection

This study was conducted using confidential secondary data which were collected from a eucalyptus grandis cross with eucalyptus urophylla seedlings planted in the Kwa-Zulu Natal midlands in South Africa. The data were collected for the years 2000 to 2010 by the Institute for Commercial Forestry Research (ICFR) using trail number W184/03. The study consisted of two replicates, the diameter at breast height, which was measured for each tree. The growth rate stated as the change in growth from one growth season to the next at different phases in the life of the trees represents the dependent variable for this study. The independent variables are the tree plot density, height, DBH, soil type, soil moisture, rainfall, relative humidity and the tree's position in the plot.

3.3 Bayesian Inference

The theorem stated by Reverend Thomas Bayes is the foundation of the Bayesian framework. The framework integrates knowledge of a distribution's model parameters with information about those parameters included in the observed data. Bayes' theorem is used to achieve this combination. The theorem arises from the relationship between the unconditional and conditional probability functions of the distribution. Because the true values of parameters are uncertain under the classical framework, the Bayesian framework treats the parameters as random variables. Suppose that the parameter vector $\Theta = (\theta_1, \dots, \theta_I)$ is a random variable, and $Y = y_1, \dots, y_J$ denotes the variable depending on Θ. The parameter Θ is unobservable. However, the inference about this parameter is based on Bayes' theorem when given the observed data Y. The Bayesian universe is made up of all possible ordered pairs of the parameter vector Θ and all possible values of the observed random variable Y .These pairs can be generally denoted by (θ_i, y_j) for $i = 1, \dots, I$ and $j = 1, \dots J$. Each event $(\theta = \theta_1), \dots, (\theta = \theta_J)$ partitions the Bayesian universe even though the events that have occurred remain unknown. Each event $(y = y_1), \dots, (y = y_J)$ is always observed. Hence, the events that have occurred are always known. The Bayes' theorem in this context is given by:

$$P(\Theta|Y) = \frac{P(Y|\Theta) * P(\theta)}{P(Y)}, \tag{3.1}$$

where

$P(\Theta|Y) =$ the posterior probability distribution that represents the knowledge about the parameters after inference.

$P(\theta) =$ the prior probability distribution, which represents the prior knowledge about the parameter Θ before inference.

$P(Y|\Theta) =$ the likelihood function that represents the relationship between the observed data and the parameter Θ.

$P(Y)$ = the marginal likelihood function which represents a normalisation factor. We change the notations in (3.1) for simplicity. Suppose that $f(.)$ is a probability distribution encompassing the observable random variable Y, and $g(.)$ be the probability distribution containing only the unobservable random variable parameter Θ. Hence the Bayes' theorem in (3.1) will be given by:

$$f(\Theta|Y) = \frac{f(Y|\Theta)*g(\theta)}{f(Y)}, \tag{3.2}$$

where

$f(Y)$ is the marginal distribution of a random variable Y, given by:

$$f(Y) = \int f(Y|\Theta) * g(\Theta)d\theta. \tag{3.3}$$

Now, $f(Y)$ in (3.3) does not depend on the parameter Θ because it is obtained by averaging over all the possible values of Θ. Hence (3.2) can be written as:

$$f(\Theta|Y) \propto f(\mathrm{Y}|\Theta), \tag{3.4}$$

which indicates the posterior density of Θ up to some unknown constant. Therefore, in the Bayesian universe, each joint probability can be found by using the multiplication rule denoted by:

$$f(\theta_i|y_j) \propto g(\theta_i) * f(y_i|\theta_i). \tag{3.5}$$

3.4 Bayesian Mixed Effects Models

This research study will focus on the mixed effect models, which have been discussed and implemented from the Bayesian viewpoint (Nazir *et al*, 2011). Mixed effect models are fundamental tools for the analysis of longitudinal data, panel data and cross-

sectional data. They are widely used by various fields of social sciences, medical and biological sciences. However, the complex nature of these models has made variable selection and parameter estimation a challenging problem (Peng and Lu, 2012).

The model that this study will focus on is a Bayesian re-purposed mixed effect variance component model, known as the Sire-Model in animal breeding problems. The process of adapting an existing model, system, or technology for a new or different application than it was originally intended is referred to as "re-purposing". In Bayesian modelling, model parameters are given prior distributions, observed data are incorporated, and the prior distributions are updated using Bayes' theorem to provide posterior distributions (Dunson, 2001). This approach allows for the quantification of uncertainty and the integration of prior knowledge into the analysis (Sumner *et al*., 2009). A sire model is a statistical technique used in animal breeding to calculate the genetic merit or value of male animals (sires) for particular attributes. Typically, it includes the offspring's performance history, the dam's performance history, and genetic data on the sire (Sun *et al.*, 2009). However, this study will use the re-purposed Bayesian Sire model, as proposed by Kepe *et al*. (2019), to determine the marginal posterior distributions of unknown parameters and to provide the growth index estimate based on the selected individual tree competition.

In matrix notation, the resulting mixed linear model can be written as:

$$y = X\boldsymbol{\beta} + Z\boldsymbol{u} + \boldsymbol{\varepsilon} \tag{3.6}$$

where

y is the $n \times 1$ response vector (current growth rate of a tree).

$X(n \times p) = \left(X_0, X_1, \dots, X_{p-1}\right)$: is the design matrix of covariates whose effects are assumed to be fixed.

$\boldsymbol{\beta}(p \times 1) = (\boldsymbol{\beta}_0, \boldsymbol{\beta}_1, \dots, \boldsymbol{\beta}_p)'$: is the vector of corresponding fixed effect coefficients (specific growth period, number of normal growing trees around a specific tree, and, whether a specific tree was suppressed or not).

$Z(n \times q) = (Z_0, Z_1, \dots, Z_q)$: is the design matrix of covariates whose effects are assumed to be random.

$\boldsymbol{u}(q \times 1) = (u_0, u_1, \dots, u_q)'$: is the vector of random effect coefficients (or growth rate indices of specific target or subject trees).

$\boldsymbol{\varepsilon}(n \times 1) = (\varepsilon_0, \varepsilon_1, \dots, \varepsilon_n)'$: is the vector of random errors that is independent of X, Z and $\boldsymbol{u}$. Typically, a linear mixed model makes the following distributional assumptions,

$\boldsymbol{\varepsilon} \sim N(0, \sigma_\varepsilon^2 \boldsymbol{I}_n)$,

$\boldsymbol{u} \sim N(0, \sigma_\varepsilon^2 \boldsymbol{A})$,

where $\boldsymbol{I}_n$ is the identity matrix of order n and A is $q \times q$ nonnegative relationship matrix. The unknown sire and error variance components are given by σ_s^2 and σ_ε^2 respectively. The idea is to use Bayesian methods and Gibbs sampling to estimate σ_ε^2, σ_s^2, $\boldsymbol{u}$, and $\boldsymbol{\beta}$ (Hugo, 1998). Since it will initially be assumed that there is no relationship or competition between the trees, matrix $\mathbf{A}$ will be represented by an identity matrix. The known and widely used distance independent competition index, called the Lorimer (1983) index between the individual trees, will also be determined and incorporated into the model using this numerator relationship matrix $\mathbf{A}$.

3.4.1 Likelihood Function

Consider model (3.6). The likelihood function can be given by:

$$P(\boldsymbol{y}|\boldsymbol{u}, \boldsymbol{\beta}, \sigma_\varepsilon^2) = \frac{1}{(2\pi\sigma_\varepsilon^2)^{\frac{n}{2}}} \exp\left\{-\frac{1}{2\sigma_s^2}(y - X\boldsymbol{\beta} - Z\boldsymbol{u})'(y - X\boldsymbol{\beta} - Z\boldsymbol{u})\right\} \quad (3.7)$$

i.e.

$$(\boldsymbol{y}|\boldsymbol{u}, \boldsymbol{\beta}, \sigma_\varepsilon^2) \sim N(X\boldsymbol{\beta} + Zu; \sigma_\varepsilon^2 \boldsymbol{I}_n)$$

(Box and Tiao, 1973).

3.4.2 Prior Distribution

Prior distributions indicate the parameters' prior knowledge before the data is observed (van de Schoot *et.al*, 2021). Bayesian inferential techniques rely heavily on this distribution. As a result, the strength of a posterior distribution is determined by the strength of the previous distribution and the amount of data available (Sehlabana, 2020).

According to Glickman and Dyk (2007), there are two main techniques to choosing a prior distribution. The first strategy entails selecting an informative prior distribution. With this method, the statistician constructs a prior distribution that accurately reflects his (and experts') ideas about the unknown parameters based on his (and experts') understanding of the substantive problem, maybe based on other data, as well as elicited expert opinion, if possible. The construction of a non-informative prior distribution that indicates ignorance about the model parameters is the second basic technique of picking a prior distribution. This type of distribution is also known as objective, ambiguous and diffuse, as well as a reference prior distribution.

3.4.3 Informative Prior Distribution

An informative prior distribution is one in which prior beliefs have a significant impact on the information contained in the observed data. As a result, inferences about model parameters drawn from observed data and conclusions drawn from the prior distribution disagree. Choosing a distribution for unknown parameters and specifying the parameters in the selected distribution that represents prior knowledge about the unknown parameters are two common methods for selecting an informative prior distribution. This means that the prior distribution chosen must reflect prior knowledge of the parameters. When choosing previous distributions for location parameters, this is even more critical. Conjugate priors are another name for informative priors (Sehlabana, 2020).

3.4.4 Non-informative Prior Distribution

When prior knowledge of the parameters is imprecise or unclear, non-informative prior distributions are employed. As a result, converting such information into a useful prior is tough. This type of prior provides unambiguous information and enables the probabilistic interpretation of probability data. Uniform probability distributions or the Jefrey's prior are used as non-informative priors in most circumstances. The uniform probability distribution chosen as a prior probability distribution must be defined on the parameter's support. When compared to the observed data, the non-informative priors have less effect on the posterior distribution. Vague, diffuse, flat, weak, or reference prior distributions are all terms used to describe these priors (Sehlabana, 2020). Given in equation 3.6, uniform prior distributions are assigned to $\boldsymbol{\beta}$ and σ_{ε}^{2} due to lack of prior knowledge about the vector of fixed effects and the error variance (Hugo, 1998).

Therefore,

$$P(\boldsymbol{\beta}, \sigma_{\varepsilon}^{2}) \propto Constant$$

Further, the prior distribution of the vector $\boldsymbol{u}$ can be given by

$$P(\boldsymbol{u}|\sigma_{s}^{2}, \boldsymbol{A}) = \frac{1}{(2\pi\sigma_{\varepsilon}^{2})^{\frac{q}{2}}|A|^{\frac{1}{2}}} \exp\left\{-\frac{1}{2\sigma_{s}^{2}}(\boldsymbol{u})' A^{-1}(\boldsymbol{u})\right\} \quad (3.8)$$

i.e.

$$u|\sigma_{s}^{2}, A \sim N(0, ; \sigma_{s}^{2}\boldsymbol{A})$$

3.5 Posterior Distribution

The posterior distribution of a parameter vector θ given the data observed Y is calculated by applying Bayes' theorem. We should also keep in mind that the posterior is the result of combining observed data with prior knowledge of the parameter of interest θ. As a result, the posterior contains all relevant information

about the parameter θ. The posterior distribution is used exclusively in the Bayesian framework for inference (Sehlabana, 2020).

3.5.1 Joint Posterior Distribution

It is always possible to calculate the joint posterior density of unknown parameters given the likelihood function and the prior distributions. The joint posterior distribution is provided by:

$$p(\boldsymbol{\beta}, \boldsymbol{u}, \sigma_s^2, \sigma_\varepsilon^2 | y) \propto Likelihood\ function \times Prior\ distributions$$

Therefore

$$p(\boldsymbol{\beta}, \boldsymbol{u}, \sigma_s^2, \sigma_\varepsilon^2 | y) \propto \frac{1}{(\sigma_\varepsilon^2)^{\frac{n}{2}}(\sigma_s^2)^{\frac{q}{2}}} \exp\left\{-\frac{1}{2\sigma_s^2}(y - X\boldsymbol{\beta} - Z\boldsymbol{u})'(y - X\boldsymbol{\beta} - Z\boldsymbol{u})\right\}$$
$$\times \exp\left\{-\frac{1}{2\sigma_s^2}(\boldsymbol{u})'A^{-1}(\boldsymbol{u})\right\} \quad (3.9)$$

where $\mathbf{A}$ is the numerator relationship matrix (Hugo, 1998).

3.5.2 Full Conditional Posterior Densities

The Gibbs sampler cannot be applied without complete conditional posterior densities of all the unknown parameters. If all other variables in the joint posterior density are taken as known, then each of the full conditional densities can be computed (Hugo,1998).

Following Hugo (1998), it can be shown that the conditional distribution of $\boldsymbol{\beta}$ i.e., $p(\boldsymbol{\beta}|\sigma_s^2, \sigma_\varepsilon^2, y, \boldsymbol{u})$ can be obtained from the joint posterior distribution given by $p(\boldsymbol{\beta}, u, \sigma_s^2, \sigma_\varepsilon^2|y)$, by excluding all the terms in the exponent that do not contain $\boldsymbol{\beta}$, then we get:

$$\frac{1}{2\sigma_\varepsilon^2}(y - X\boldsymbol{\beta} - Z\boldsymbol{u})'(y - X\boldsymbol{\beta} - Z\boldsymbol{u})$$

$$= \frac{1}{2\sigma_\varepsilon^2}(X\boldsymbol{\beta} - \boldsymbol{y} + Z\boldsymbol{u})'(X\boldsymbol{\beta} - y + Z\boldsymbol{u})$$

$$= \frac{1}{2\sigma_\varepsilon^2}[(X\boldsymbol{\beta} - (\boldsymbol{y} - Z\boldsymbol{u})]'\,[(X\boldsymbol{\beta} - (y - Z\boldsymbol{u})]$$

$$= \frac{1}{2\sigma_\varepsilon^2}[\boldsymbol{\beta}'X'X\boldsymbol{\beta} - \boldsymbol{\beta}'X'(y - Z\boldsymbol{u}) - (y - Z\boldsymbol{u})'X\boldsymbol{\beta} + (y - Z\boldsymbol{u})'(y - Z\boldsymbol{u})]$$

$$\frac{1}{2\sigma_\varepsilon^2}[\boldsymbol{\beta}'X'X\boldsymbol{\beta} - \boldsymbol{\beta}'X'(y - Z\boldsymbol{u}) - (y - Z\boldsymbol{u})'X\boldsymbol{\beta} + y'y - 2\boldsymbol{u}'Z'y + \boldsymbol{u}'Z'Z\boldsymbol{u}].$$

By noticing that $\boldsymbol{\beta}'X'(y - Z\boldsymbol{u})$ and $(y - Z\boldsymbol{u})'X\boldsymbol{\beta}$ are scalars and by excluding the given terms, we get:

$$= \frac{1}{2\sigma_\varepsilon^2}[\boldsymbol{\beta}'X'X\boldsymbol{\beta} - 2\boldsymbol{\beta}'X'(y - Z\boldsymbol{u}) + \boldsymbol{u}'Z'Z\boldsymbol{u}].$$

By applying add and subtract technique:

$$\boldsymbol{\beta}'X'X\boldsymbol{\beta} - 2\boldsymbol{\beta}'X'(y - Z\boldsymbol{u})$$

$$= \boldsymbol{\beta}'X'X\boldsymbol{\beta} - 2\boldsymbol{\beta}'X'(y - Z\boldsymbol{u}) + (y - Z\boldsymbol{u})'X(X'X)^{-1}(y - Z\boldsymbol{u}) - (y - Z\boldsymbol{u})'X(X'X)^{-1}X'(y - Z\boldsymbol{u})$$

$$= \{\boldsymbol{\beta}'(X'X) - (y - Z\boldsymbol{u})'X\}\{\boldsymbol{\beta} - (X'X)^{-1}X'(y - Z\boldsymbol{u})\}$$

$$= \{\boldsymbol{\beta}' - (y - Z\boldsymbol{u})'X(X'X)^{-1}\}(X'X)\{\boldsymbol{\beta} - (X'X)^{-1}X'(y - Z\boldsymbol{u})\}.$$

This result can be defined as a vector normal distribution. Therefore, the conditional distribution of $\boldsymbol{\beta}$ is given by:

$$p(\boldsymbol{\beta}\,|\sigma_s^2, \sigma_\varepsilon^2, y, \boldsymbol{u}, \boldsymbol{A}) = p(\boldsymbol{\beta}\,|\sigma_\varepsilon^2, y, \boldsymbol{u}) \sim N_p[(X'X)^{-1}X'(y - Z\boldsymbol{u}); \sigma_\varepsilon^2(X'X)^{-1}]$$

$$\text{for } -\infty \leq \boldsymbol{\beta} \leq \infty$$

The conditional distribution of $\boldsymbol{u}, p(\boldsymbol{\beta}\,|\sigma_s^2, \sigma_\varepsilon^2, y, \boldsymbol{u}, \boldsymbol{A})$, can be obtained by excluding the terms that do not contain $\boldsymbol{u}$ (Hugo,1998):

Therefore,

$$\frac{1}{2\sigma_\varepsilon^2}(y-X\boldsymbol{\beta}-Z\boldsymbol{u})'(y-X\boldsymbol{\beta}-Z\boldsymbol{u})+\frac{1}{2\sigma_s^2}(\boldsymbol{u})'A^{-1}(\boldsymbol{u})$$

$$=\frac{1}{2}\left\{\frac{1}{\sigma_\varepsilon^2}\{[(y-X\boldsymbol{\beta})'-\boldsymbol{u}'Z']\}\{(y-X\boldsymbol{\beta})-Z\boldsymbol{u}\}+\frac{1}{\sigma_s^2}(\boldsymbol{u})'A^{-1}(\boldsymbol{u})\right\}$$

$$=\frac{1}{2}\left\{\frac{1}{\sigma_\varepsilon^2}[\boldsymbol{u}'Z'Z\boldsymbol{u}-\boldsymbol{u}'Z'(y-X\boldsymbol{\beta})-(y-X\boldsymbol{\beta})'Z\boldsymbol{u}+(y-X\boldsymbol{\beta})'(y-X\boldsymbol{\beta})]+\right.$$

$$\left.\frac{1}{\sigma_s^2}(\boldsymbol{u}'A^{-1}\boldsymbol{u})\right\}.$$

$$=\frac{1}{2}\left\{\frac{1}{\sigma_\varepsilon^2}[\boldsymbol{u}'Z'Z\boldsymbol{u}-\boldsymbol{u}'Z'(y-X\boldsymbol{\beta})-(y-X\boldsymbol{\beta})'Z\boldsymbol{u}]+\frac{1}{\sigma_s^2}(\boldsymbol{u}'A^{-1}\boldsymbol{u})\right\}$$

$$=\frac{1}{2}\left\{\left[\frac{1}{\sigma_\varepsilon^2}\boldsymbol{u}'Z'Z\boldsymbol{u}+\frac{1}{\sigma_s^2}(\boldsymbol{u}'A^{-1}\boldsymbol{u})\right]-\left(\frac{1}{\sigma_\varepsilon^2}\boldsymbol{u}'Z'\right)(y-X\boldsymbol{\beta})-(y-X\boldsymbol{\beta})'\left(\frac{1}{\sigma_\varepsilon^2}Z\boldsymbol{u}\right)\right\}$$

$$=\frac{1}{2}\left\{\left[\left(\frac{1}{\sigma_\varepsilon^2}\boldsymbol{u}'\boldsymbol{u}\right)\left(Z'Z+\frac{\sigma_\varepsilon^2}{\sigma_s^2}A^{-1}\right)\right]-\left(\frac{1}{\sigma_\varepsilon^2}\boldsymbol{u}'Z'\right)(y-X\boldsymbol{\beta})-(y-X\boldsymbol{\beta})'\left(\frac{1}{\sigma_\varepsilon^2}Z\boldsymbol{u}\right)\right\}$$

By applying add and subtract technique:

$$=\frac{1}{2}\left\{\left[\left(\frac{1}{\sigma_\varepsilon^2}\boldsymbol{u}'\boldsymbol{u}\right)\left(Z'Z+\frac{\sigma_\varepsilon^2}{\sigma_s^2}A^{-1}\right)\right]-\left(\frac{1}{\sigma_\varepsilon^2}\boldsymbol{u}'Z'\right)(y-X\boldsymbol{\beta})-(y-X\boldsymbol{\beta})'\left(\frac{1}{\sigma_\varepsilon^2}Z\boldsymbol{u}\right)+\right.$$

$$\left[(y-X\boldsymbol{\beta})'\left(\frac{1}{\sigma_\varepsilon^2}Z\right)\left(Z'Z+\frac{\sigma_\varepsilon^2}{\sigma_s^2}A^{-1}\right)^{-1}Z'(y-X\boldsymbol{\beta})\right]-\left[(y-X\boldsymbol{\beta})'\left(\frac{1}{\sigma_\varepsilon^2}Z\right)\left(Z'Z+\right.\right.$$

$$\left.\left.\frac{\sigma_\varepsilon^2}{\sigma_s^2}A^{-1}\right)^{-1}Z'(y-X\boldsymbol{\beta})\right]\Big\}$$

$$=\frac{1}{2}\left\{\left[\left(\frac{1}{\sigma_\varepsilon^2}\boldsymbol{u}'\right)\left(Z'Z+\frac{\sigma_\varepsilon^2}{\sigma_s^2}A^{-1}\right)-(y-X\boldsymbol{\beta})'\left(\frac{1}{\sigma_\varepsilon^2}Z\right)\right]\times\left[\boldsymbol{u}-\left(Z'Z+\right.\right.\right.$$

$$\left.\left.\left.\frac{\sigma_\varepsilon^2}{\sigma_s^2}A^{-1}\right)^{-1}Z'(y-X\boldsymbol{\beta})\right]\right\}$$

$$=\frac{1}{2}\left\{\left[\boldsymbol{u}'-(y-X\boldsymbol{\beta})'Z\left(Z'Z+\frac{\sigma_\varepsilon^2}{\sigma_s^2}A^{-1}\right)^{-1}\right]\frac{1}{\sigma_\varepsilon^2}\left(Z'Z+\frac{\sigma_\varepsilon^2}{\sigma_s^2}A^{-1}\right)\times\left[\boldsymbol{u}-\left(Z'Z+\right.\right.\right.$$

$$\left.\left.\left.\frac{\sigma_\varepsilon^2}{\sigma_s^2}A^{-1}\right)^{-1}Z'(y-X\boldsymbol{\beta})\right]\right\}$$

$$=\frac{1}{2}\left\{\left[\boldsymbol{u}-(y-X\boldsymbol{\beta})'Z\left(Z'Z+\frac{\sigma_\varepsilon^2}{\sigma_s^2}A^{-1}\right)^{-1}\right]\frac{1}{\sigma_\varepsilon^2}\left(Z'Z+\frac{\sigma_\varepsilon^2}{\sigma_s^2}A^{-1}\right)\times\left[\boldsymbol{u}-\left(Z'Z+\right.\right.\right.$$

$$\left.\left.\left.\frac{\sigma_\varepsilon^2}{\sigma_s^2}A^{-1}\right)^{-1}Z'(y-X\boldsymbol{\beta})\right]\right\}.$$

This result can also be defined as a vector normal distribution. Therefore, the conditional distribution of $\boldsymbol{u}$ is given by:

$$p(\boldsymbol{u}|\boldsymbol{\beta},\sigma_s^2,\sigma_\varepsilon^2,A,y)\sim N_q\left[\left(Z'Z+\frac{\sigma_\varepsilon^2}{\sigma_s^2}A^{-1}\right)^{-1}Z'(y-X\boldsymbol{\beta});\ \sigma_\varepsilon^2\left(Z'Z+\frac{\sigma_\varepsilon^2}{\sigma_s^2}A^{-1}\right)\right]$$

for $-\infty \leq \boldsymbol{u} \leq \infty$

The conditional distribution of σ_s^2 is an inverse Gamma distribution given by:

$$p(\sigma_s^2|\boldsymbol{u},\boldsymbol{\beta},\sigma_\varepsilon^2,A,y)=\boldsymbol{p}(\sigma_s^2|\boldsymbol{u})=K_s\left(\frac{1}{\sigma_s^2}\right)^{\frac{q}{2}}\exp\left(-\frac{1}{2\sigma_s^2}\boldsymbol{u}'A^{-1}\boldsymbol{u}\right)$$

where $\sigma_s^2 \geq 0$ and $\mathbf{A}$ is the numerator relationship matrix. K_s is the normalisation constant. The normalisation constant can be determined by integrating $p(\sigma_s^2|\boldsymbol{u},y)$ with respect to σ_s^2 and by letting the integral to be one (Hugo, 1998).

The procedure is as follows:

Let $\frac{\boldsymbol{u}'A^{-1}\boldsymbol{u}}{\sigma_s^2}=v$.

Therefore

$$\sigma_s^2 v=\boldsymbol{u}'A^{-1}\boldsymbol{u}\ ,$$

thus

$$\sigma_s^2=(\boldsymbol{u}'A^{-1}\boldsymbol{u})v^{-1},$$

and

$$\frac{d\sigma_s^2}{dv} = -(\boldsymbol{u}'A^{-1}\boldsymbol{u})v^{-2}.$$

But

$$\left|\frac{d\sigma_s^2}{dv}\right| = |-(\boldsymbol{u}'A^{-1}\boldsymbol{u})v^{-2}| = (\boldsymbol{u}'A^{-1}\boldsymbol{u})v^{-2}$$

and therefore

$$|d\sigma_s^2| = |-(\boldsymbol{u}'A^{-1}\boldsymbol{u})v^{-2}dv| = (\boldsymbol{u}'A^{-1}\boldsymbol{u})v^{-2}dv.$$

Now, determine

$$\int_0^\infty p(\sigma_s^2|\boldsymbol{u}, y)d\sigma_s^2$$

and let the integral be equal to one.

Therefore

$$\int_0^\infty p(\sigma_s^2|\boldsymbol{u}, y)d\sigma_s^2 = 1$$

which means that

$$K_s\left\{\int_0^\infty \left(\frac{1}{\sigma_s^2}\right)^{\frac{q}{2}} \exp\left(-\frac{1}{2\sigma_s^2}(\boldsymbol{u}'A^{-1}\boldsymbol{u})d\sigma_s^2\right)\right\} = 1$$

$$K_s\left\{\int_0^\infty [v(\boldsymbol{u}'A^{-1}\boldsymbol{u})^{-1}]^{\frac{q}{2}} \exp\left[-\frac{1}{2}(v(\boldsymbol{u}'A^{-1}\boldsymbol{u})^{-1})(\boldsymbol{u}'A^{-1}\boldsymbol{u})\right](\boldsymbol{u}'A^{-1}\boldsymbol{u})v^{-2}dv\right\} = 1$$

$$K_s\left\{\int_0^\infty (v)^{\frac{q}{2}}(\boldsymbol{u}'A^{-1}\boldsymbol{u})^{-\frac{q}{2}} \exp\left[-\frac{1}{2}v\right](\boldsymbol{u}'A^{-1}\boldsymbol{u})v^{-2}dv\right\} = 1$$

$$K_s\left\{(\boldsymbol{u}'A^{-1}\boldsymbol{u})^{-\frac{q}{2}}(\boldsymbol{u}'A^{-1}\boldsymbol{u})[\int_0^\infty (v)^{\frac{q}{2}-2}e^{-\frac{1}{2}v}dv]\right\}=1$$

$$K_s\left\{(\boldsymbol{u}'A^{-1}\boldsymbol{u})^{-\frac{q}{2}+1}[\int_0^\infty (v)^{\frac{q}{2}-2}e^{-\frac{1}{2}v}dv]\right\}=1$$

$$K_s\left\{(\boldsymbol{u}'A^{-1}\boldsymbol{u})^{-\frac{q}{2}+1}[\int_0^\infty (v)^{\frac{1}{2}(q-2)-1}e^{-\frac{1}{2}v}dv]\right\}=1$$

$$K_s\left\{(\boldsymbol{u}'A^{-1}\boldsymbol{u})^{-\frac{1}{2}(q-2)}[\int_0^\infty (v)^{\frac{1}{2}(q-2)-1}e^{-\frac{1}{2}v}dv]\right\}=1.$$

$\int_0^\infty (v)^{\frac{1}{2}(q-2)-1}e^{-\frac{1}{2}v}dv$ is a χ^2_{q-2}.

Therefore

$$\int_0^\infty (v)^{\frac{1}{2}(q-2)-1}e^{-\frac{1}{2}v}dv = 2^{\frac{1}{2}(q-2)}\Gamma\left(\frac{q-2}{2}\right)$$

and

$$K_s\left\{(\boldsymbol{u}'A^{-1}\boldsymbol{u})^{-\frac{1}{2}(q-2)}\times 2^{\frac{1}{2}(q-2)}\Gamma\left(\frac{q-2}{2}\right)\right\}=1$$

$$K_s\left\{\left(\frac{2}{\boldsymbol{u}'A^{-1}\boldsymbol{u}}\right)^{\frac{1}{2}(q-2)}\Gamma\left(\frac{q-2}{2}\right)\right\}=1\ .$$

The conditional distribution of σ_ε^2 is also an inverse Gamma distribution given by:

$$p(\sigma_\varepsilon^2|\boldsymbol{u},\boldsymbol{\beta},\sigma_s^2,A,y)=K_\varepsilon(\sigma_\varepsilon^2)^{-\frac{n}{2}}\exp\left\{-\frac{1}{2\sigma_\varepsilon^2}(y-X\boldsymbol{\beta}-Z\boldsymbol{u})'(y-X\boldsymbol{\beta}-Z\boldsymbol{u})\right\}$$

for $\sigma_\varepsilon^2>0$

K_ε is the normalisation constant that can be determined by integrating $p(\sigma_\varepsilon^2|\boldsymbol{u},\boldsymbol{\beta},\sigma_s^2,y)$ with respect to σ_ε^2 and by letting the integral to be equal to one (Hugo, 1998).

Let $\frac{(y-X\boldsymbol{\beta}-Z\boldsymbol{u})'(y-X\boldsymbol{\beta}-Z\boldsymbol{u})}{\sigma_\varepsilon^2} = w.$

Therefore

$$\sigma_\varepsilon^2 = \frac{(y-X\boldsymbol{\beta}-Z\boldsymbol{u})'(y-X\boldsymbol{\beta}-Z\boldsymbol{u})}{w} = (y - X\boldsymbol{\beta} - Z\boldsymbol{u})'(y - X\boldsymbol{\beta} - Z\boldsymbol{u})w^{-1}$$

and

$$d\sigma_\varepsilon^2 = -(y - X\boldsymbol{\beta} - Z\boldsymbol{u})'(y - X\boldsymbol{\beta} - Z\boldsymbol{u})w^{-2}dw.$$

Therefore

$$\frac{d\sigma_\varepsilon^2}{dw} = -(y - X\boldsymbol{\beta} - Z\boldsymbol{u})'(y - X\boldsymbol{\beta} - Z\boldsymbol{u})w^{-2}.$$

But

$$\left|\frac{d\sigma_\varepsilon^2}{dw}\right| = |-(y - X\boldsymbol{\beta} - Z\boldsymbol{u})'(y - X\boldsymbol{\beta} - Z\boldsymbol{u})w^{-2}| = (y - X\boldsymbol{\beta} - Z\boldsymbol{u})'(y - X\boldsymbol{\beta} - Z\boldsymbol{u})w^{-2}$$

and therefore

$$|d\sigma_\varepsilon^2| = |-(y - X\boldsymbol{\beta} - Z\boldsymbol{u})'(y - X\boldsymbol{\beta} - Z\boldsymbol{u})w^{-2}dw|$$
$$= (y - X\boldsymbol{\beta} - Z\boldsymbol{u})'(y - X\boldsymbol{\beta} - Z\boldsymbol{u})w^{-2}dw.$$

Now, determine

$$\int_0^\infty p(\sigma_\varepsilon^2|\boldsymbol{u}, \boldsymbol{\beta}, \sigma_s^2, A, y)d\,\sigma_\varepsilon^2$$

and let the integral to be equal to one.

Then

$$\int_0^{\infty} p(\sigma_\varepsilon^2|\boldsymbol{u},\boldsymbol{\beta},\sigma_s^2,A,y)d\,\sigma_\varepsilon^2 = 1$$

$$K_\varepsilon\{\int_0^{\infty}(\sigma_\varepsilon^2)^{-\frac{n}{2}}\exp\left[-\frac{1}{2\sigma_\varepsilon^2}(y-X\boldsymbol{\beta}-Z\boldsymbol{u})'(y-X\boldsymbol{\beta}-Z\boldsymbol{u})\right]d\sigma_\varepsilon^2\} = 1$$

$$K_\varepsilon\left\{\int_0^{\infty}\left[\frac{(y-X\boldsymbol{\beta}-Z\boldsymbol{u})'(y-X\boldsymbol{\beta}-Z\boldsymbol{u})}{w}\right]^{-\frac{n}{2}} exp\left[-\frac{1}{2}\frac{w}{(y-X\boldsymbol{\beta}-Z\boldsymbol{u})'(y-X\boldsymbol{\beta}-Z\boldsymbol{u})}\times(y-X\boldsymbol{\beta}-\right.\right.$$

$$\left.\left.Z\boldsymbol{u})'(y-X\boldsymbol{\beta}-Z\boldsymbol{u})\right]\times(y-X\boldsymbol{\beta}-Z\boldsymbol{u})'(y-X\boldsymbol{\beta}-Z\boldsymbol{u})w^{-2}dw\right\} = 1$$

$$K_\varepsilon\left\{\int_0^{\infty}[(y-X\boldsymbol{\beta}-Z\boldsymbol{u})'(y-X\boldsymbol{\beta}-Z\boldsymbol{u})]^{-\frac{n}{2}}\left(\frac{1}{w}\right)^{-\frac{n}{2}} exp\left[-\frac{1}{2}w\right]\times(y-X\boldsymbol{\beta}-\right.$$

$$\left.Z\boldsymbol{u})'(y-X\boldsymbol{\beta}-Z\boldsymbol{u})w^{-2}dw\right\} = 1$$

$$K_\varepsilon\left\{\int_0^{\infty}[(y-X\boldsymbol{\beta}-Z\boldsymbol{u})'(y-X\boldsymbol{\beta}-Z\boldsymbol{u})]^{-\frac{n}{2}+1}(w)^{\frac{n}{2}}(w)^{-2}exp\left[-\frac{1}{2}w\right]dw\right\} = 1$$

$$K_\varepsilon\left\{\int_0^{\infty}[(y-X\boldsymbol{\beta}-Z\boldsymbol{u})'(y-X\boldsymbol{\beta}-Z\boldsymbol{u})]^{-\frac{n}{2}+1}(w)^{\frac{n}{2}-2}exp\left[-\frac{1}{2}w\right]dw\right\} = 1$$

$$K_\varepsilon\left\{[(y-X\boldsymbol{\beta}-Z\boldsymbol{u})'(y-X\boldsymbol{\beta}-Z\boldsymbol{u})]^{-\frac{n}{2}+1}\int_0^{\infty}(w)^{\frac{n}{2}-2}exp\left[-\frac{1}{2}w\right]dw\right\} = 1$$

$$K_\varepsilon\left\{[(y-X\boldsymbol{\beta}-Z\boldsymbol{u})'(y-X\boldsymbol{\beta}-Z\boldsymbol{u})]^{-\frac{n}{2}+1}\int_0^{\infty}(w)^{\frac{1}{2}(n-2)-1}exp\left[-\frac{1}{2}w\right]dw\right\} = 1$$

$$K_\varepsilon\left\{[(y-X\boldsymbol{\beta}-Z\boldsymbol{u})'(y-X\boldsymbol{\beta}-Z\boldsymbol{u})]^{-\frac{1}{2}(n-2)}\int_0^{\infty}(w)^{\frac{1}{2}(n-2)-1}exp\left[-\frac{1}{2}w\right]dw\right\} = 1$$

But

$\int_0^{\infty}(w)^{\frac{1}{2}(n-2)-1}exp\left[-\frac{1}{2}w\right]dw$ is a χ^2_{n-2}.

Therefore

$$\int_0^{\infty}(w)^{\frac{1}{2}(n-2)-1}exp\left[-\frac{1}{2}w\right]dw = 2^{\frac{1}{2}(n-2)}\Gamma\left(\frac{n-2}{2}\right)$$

and

$$K_{\varepsilon}\left\{[(y-X\boldsymbol{\beta}-Z\boldsymbol{u})'(y-X\boldsymbol{\beta}-Z\boldsymbol{u})]^{-\frac{1}{2}(n-2)}\int_0^{\infty}(w)^{\frac{1}{2}(n-2)-1}exp\left[-\frac{1}{2}w\right]dw\right\}$$

$$=K_{\varepsilon}\left\{[(y-X\boldsymbol{\beta}-Z\boldsymbol{u})'(y-X\boldsymbol{\beta}-Z\boldsymbol{u})]^{-\frac{1}{2}(n-2)}\times 2^{\frac{1}{2}(n-2)}\Gamma\left(\frac{n-2}{2}\right)\right\}=1.$$

Therefore

$$K_{\varepsilon}\left\{\left[\frac{1}{(y-X\boldsymbol{\beta}-Z\boldsymbol{u})'(y-X\boldsymbol{\beta}-Z\boldsymbol{u})}\right]^{\frac{1}{2}(n-2)}\times 2^{\frac{1}{2}(n-2)}\Gamma\left(\frac{n-2}{2}\right)\right\}=1$$

and

$$K_{\varepsilon}\left\{\left[\frac{2}{(y-X\boldsymbol{\beta}-Z\boldsymbol{u})'(y-X\boldsymbol{\beta}-Z\boldsymbol{u})}\right]^{\frac{1}{2}(n-2)}\times \Gamma\left(\frac{n-2}{2}\right)\right\}=1$$

which means that

$$K_{\varepsilon}=\left[\frac{(y-X\boldsymbol{\beta}-Z\boldsymbol{u})'(y-X\boldsymbol{\beta}-Z\boldsymbol{u})}{2}\right]^{\frac{1}{2}(n-2)}\frac{1}{\Gamma\left(\frac{n-2}{2}\right)}.$$

Therefore, in order to implement the Gibbs sampling scheme, the aforementioned full conditional distributions are necessary (Hugo, 1998).

3.6 Density Estimation of Function for Variance Components

The posterior density of any function of the original parameters can be made through the transformation of random variables. This can be done without rerunning the Gibbs sampler, provided appropriate samples are saved. This section will give descriptions of the variance ratio (Hugo, 1998).

3.7 Competition Indices

Competition indices can also be used to measure competition for each subject tree. These indices can be distance-independent or distance-dependent. Distance-independent models do not need tree coordinates, since they are just functions of stand-level variables or the subject tree's starting dimensions. But distance-dependent models need the dimensions and relative locations of multiple neighbours to determine. In data field measurements, distance-independent indices are simple to compute and less challenging (Rivas *et al*., 2005).

For non-spatial index (distance-independent index) consider, Lorimer (1983):

$$Sdr_{ij} = \frac{\left(\frac{\left(\sum_{j\neq i}^{n} d_j\right)}{d_i}\right)}{S} \qquad (3.10)$$

Although Hegyi is mentioned here, it was not considered for this study. This study focused on distance independent indices. For spatial indices (distance-dependent index) consider, Hegyi (1974):

$$Heg = \sum_{j\neq i}^{n}\left(\frac{d_j}{d_i * l_{ij}}\right) \qquad (3.11$$

3.8 Analysis of Competition Between Individual Trees Using Lorimer (1983)

To investigate the effect of competition on the growth of individual trees, the study used a non-spatial index named Lorimer to evaluate competition between individual eucalyptus trees. The index Lorimer sums up the diameter (d) of the neighbouring trees divided by the subject tree (d) in the plot (ha^{-1}) (Maleki *et al*., 2015). The non-spatial index Lorimer (1983) is given by:

$$Sdr_{ij} = \frac{\left(\frac{\left(\sum_{j\neq i}^{n} d_j\right)}{d_i}\right)}{S}$$

where

$d_j =$ DBH of the competitor tree (cm).

$d_i =$ DBH of the subject tree (cm).

$S =$ Plot area $(m^2 ha^{-1})$.

$l_{ij} =$ Distance between the competitor j and the subject tree i (m).

When analysing the competition between the individual trees, the circumferences of the competitor tree and the subject tree (d_j and d_i) will be used instead of the DBHs. When using circumference as compared to diameter, the observed variability may be slightly higher. A growing tree increases the volume of the trunk as well as its diameter. Circumference may be a better measure of real growth when DBH appears to be small. Therefore, it is suggested that the use of circumference, may be able to detect small changes in growth more effectively. This implies that the equation of the non-spatial index Lorimer (1983) will now be given by:

$$Sdr_{ij} = \frac{\left(\frac{\left(\sum_{j\neq i}^{n} c_j\right)}{c_i}\right)}{S} \tag{3.12}$$

The above non-spatial competition index will be used to generate a square matrix that will replace the numerator relationship matrix $\mathbf{A}$ and then use the specified Bayesian methods and Gibbs sampling to estimate the marginal posterior densities of variance components and mixed effects. To calculate the entries for the new numerator relationship matrix $\mathbf{A}$, the Lorimer (1983) competition index will be used to sum up the circumferences of the neighbouring trees from a selected buffer of a plot and divide this sum by the circumference of the subject tree i. This is then divided by the area covered by the selected trees from the buffer. The diagonal entries of the new matrix must be greater than 1 in order to satisfy the conditions of the Sire model. According to Hugo (1998), a diagonal entry for the numerator relationship matrix $\mathbf{A}$ is calculated by determining $(1 + F_i)$, where F_i represents the inbreeding coefficient of animal i. For this study, the inbreeding coefficient for animal i, will be replaced by the

competition experienced by selected tree i located on the specified buffer zone calculated using the Lorimer index.

3.9 Generating a matrix $\mathbf{A}$ using the Lorimer (1983) competition index

This section shows a layout of how the distant-independent competition index from equation 3.12 will be used to generate the new $\mathbf{A}$ matrix step by step. In place of an identity matrix $\mathbf{A}$ used when no competition between neighbouring trees is assumed, this new matrix will be used when it is considered that there is competition among the trees. The individual values determined to form the numerator relationship matrix $\mathbf{A}$, represent the distance-independent competition between the selected buffer of trees calculated using the Lorimer (1983) distance-independent competition index. The diagonal elements (a_{ii}) (i.e., when $i = j$) of the new numerator relationship matrix for the subject or target tree (i.e the (i^{th}) tree), (a_{ii}) is then given by $1 + 0.25(Sdr_i)$ (Hugo, 1998). To calculate Sdr_i in this case, determine the sum of the circumferences of the trees surrounding tree i, and then divide by circumference of tree i. The mentioned fraction is then divided by the area in the randomly selected buffer covered by all the trees surrounding tree i, including the area covered by tree i as well. The off-diagonal elements in the numerator relationship matrix $\mathbf{A}$, represents the competition between the i^{th} tree (subject tree) and the j^{th} tree (competitor tree) and is then given by $a_{ij} = 0.5Sdr_i + 0.25Sdr_j$ (Hugo, 1998). In order to calculate Sdr_i to form the off diagonal elements of the numerator relationship matrix $\mathbf{A}$, use the circumferences of all the trees in the buffer directly surrounding the two target trees, i.e tree i and tree j, and calculate the distance-independent Lorimer Index where, depending on the specific off-diagonal element that is determined, the circumference of either the i^{th} or j^{th} tree is removed from the sum, and is then used to divide the sum of the remaining circumferences, with. This fraction is then divided by the total area of the randomly selected buffer covered by the 15 highlighted trees. The following figures below shows how $\mathbf{A}$ was computed.

168	185	200	217	232
169	**184**	201	**216**	233
170	183	202	215	234
171	**182**	203	**214**	235
172	181	204	213	236

Figure 3. 2: Buffer Zone of 25 Trees Randomly Selected on Plot 9

Figure 3.2 shows the buffer that was selected from plot 9 with tree density of 1959. The randomly selected buffer consisted of 25 trees with four target trees being tree number 182, tree number 184, tree number 214 and tree number 216.

168	185	200	217	232
169	**184**	201	**216**	233
170	183	202	215	234
171	**182**	203	**214**	235
172	181	204	213	236

Figure 3. 3: Selected Trees Surrounding Target Tree 182 on the Buffer zone Randomly Selected on Plot 9

Figure 3.3 shows the same buffer as indicated in Figure 3.2, with the exception that only 9 trees, specifically tree 182, and trees directly surrounding tree 182, were also highlighted. This figure therefore indicates trees that were used specifically to generate one of the diagonal elements of the numerator relationship matrix $\mathbf{A}$, namely diagonal element a_{11} of the numerator relationship matrix. Tree 182, located in the middle of the group of 9 trees, represents the subject or target tree of the shaded group of 9 trees indicated in Figure 3.3.

168	185	200	217	232
169	**184**	201	**216**	233
170	183	202	215	234
171	**182**	203	**214**	235
172	181	204	213	236

Figure 3. 4: Selected Trees Surrounding Target Tree 184 on the Buffer zone Randomly Selected on Plot 9

Figure 3.4 shows the same buffer as indicated in Figure 3.2, with the exception that only 9 trees, specifically tree 184, and trees directly surrounding tree 184, were also highlighted. As a result, the trees shown in this figure were specifically selected to generate one of the diagonal elements of the numerator relationship matrix $\mathbf{A}$, namely diagonal element a_{22} of the numerator relationship matrix $\mathbf{A}$. The subject or target

tree of the nine trees shaded in Figure 3.4 is represented by Tree 184, which is in the middle of the group.

168	185	200	217	232
169	**184**	201	**216**	233
170	183	202	215	234
171	**182**	203	**214**	235
172	181	204	213	236

Figure 3. 5: Selected Trees Surrounding Target Tree 214 on the Buffer zone Randomly Selected on Plot 9

Figure 3.5 displays the same buffer as Figure 3.2, with the difference that only 9 trees, including tree 214 and the trees directly surrounding tree 214, were additionally highlighted. This figure therefore indicates trees that were used specifically to generate one of the diagonal elements of the numerator relationship matrix $\mathbf{A}$, namely diagonal element a_{33} of the numerator relationship matrix $\mathbf{A}$. Tree 214, located in the middle of the group of 9 trees, represents the subject or target tree of the shaded group of 9 trees indicated in Figure 3.5.

168	185	200	217	232
169	**184**	201	**216**	233
170	183	202	215	234
171	**182**	203	**214**	235
172	181	204	213	236

Figure 3. 6: Selected Trees Surrounding Target Tree 216 on the Buffer zone Randomly Selected on Plot 9

Figure 3.6 indicates the same buffer as Figure 3.2, with the difference that just 9 trees, particularly tree 216 and trees directly surrounding tree 216, were also highlighted. As a result, this figure shows the trees that were specifically used to create diagonal element of the numerator relationship matrix $\mathbf{A}$, namely diagonal element a_{44} of the numerator relationship matrix. Tree 216, located in the middle of the group of 9 trees, represents the subject or target tree of the shaded group of 9 trees indicated in Figure 3.6.

168	185	200	217	232
169	**184**	201	**216**	233
170	183	202	215	234
171	**182**	203	**214**	235
172	181	204	213	236

Figure 3. 7: Selected Trees Surrounding Target Tree 182 and Tree 184on the Buffer zone Randomly Selected on Plot 9

Figure 3.7 indicates the same randomly selected buffer as indicated in Figure 3.2, with the exception that only 15 trees were highlighted. The 15 trees were selected, since the highlighted group specifically contains both tree 182 and tree 184, where both these trees represent subject or target trees, and trees specifically located around these two mentioned target trees. This figure therefore indicates trees that were used specifically to generate one of the off-diagonal elements of the numerator relationship matrix $\mathbf{A}$, namely off-diagonal element a_{12} of the numerator relationship matrix. Tree 182, in this case, represents the subject or target tree, while tree 184, represents the competitor tree. In order to calculate a_{21}, use tree 184 as target or subject tree, while tree 182 will now be used as the competitor tree.

168	185	200	217	232
169	**184**	201	**216**	233
170	183	202	215	234
171	**182**	203	**214**	235
172	181	204	213	236

Figure 3. 8: Selected Trees Surrounding Target Tree 184 and Tree 216 on the Buffer zone Randomly Selected on Plot 9

Figure 3.8 indicates the same randomly selected buffer as indicated in Figure 3.2, with the exception that only 15 trees were highlighted. The 15 trees were selected, since the highlighted group specifically contains both tree 184 and tree 216, where both these trees represent subject or target trees, and trees specifically located around these two mentioned target trees. Figure 3.8 therefore indicates trees that were used specifically to generate one of the off-diagonal elements of the numerator relationship matrix $\mathbf{A}$, namely off-diagonal element a_{24} of the numerator relationship matrix. Tree 184, in this case, represents the subject or target tree, while tree 216, represents the competitor tree. In order to calculate a_{42}, use tree 216 as target or subject tree, while tree 184 will now be used as the competitor tree.

168	185	200	217	232
169	**184**	201	**216**	233
170	183	202	215	234
171	**182**	203	**214**	235
172	181	204	213	236

Figure 3. 9: Selected Trees Surrounding Target Tree 182 and Tree 214 on the Buffer zone Randomly Selected on Plot 9

Figure 3.9 shows the same randomly chosen buffer as Figure 3.2, with the difference that only 15 trees were highlighted. The 15 trees were selected, since the highlighted group specifically contains both tree 182 and tree 214, where both these trees represent subject or target trees, and trees specifically located around these two mentioned target trees. This figure therefore indicates trees that were used specifically to generate one of the off-diagonal elements of the numerator relationship matrix $\mathbf{A}$, namely off-diagonal element a_{13} of the numerator relationship matrix. Tree 182, in this case, represents the subject or target tree, while tree 214, represents the competitor tree. In order to calculate a_{31}, use tree 214 as target or subject tree, while tree 182 will now be used as the competitor tree.

168	185	200	217	232
169	**184**	201	**216**	233
170	183	202	215	234
171	**182**	203	**214**	235
172	181	204	213	236

Figure 3. 10: Selected Trees Surrounding Target Tree 214 and Tree 216 on the Buffer zone Randomly Selected on Plot 9

Figure 3.10 indicates the same randomly selected buffer as indicated in Figure 3.2, with the exception that only 15 trees were highlighted. The 15 trees were selected, since the highlighted group specifically contains both tree 214 and tree 216, where both these trees represent subject or target trees, and trees specifically located around these two mentioned target trees. This figure therefore indicates trees that were used specifically to generate one of the off-diagonal elements of the numerator relationship matrix $\mathbf{A}$, namely off-diagonal element a_{34} of the numerator relationship matrix. Tree 214, in this case, represents the subject or target tree, while tree 216,

represents the competitor tree. In order to calculate a_{43}, use tree 216 as target or subject tree, while tree 214 will now be used as the competitor tree.

168	185	200	217	232
169	**184**	201	**216**	233
170	183	202	215	234
171	**182**	203	**214**	235
172	181	204	213	236

Figure 3. 11: Selected Trees Surrounding Target Tree 184 and Tree 214 on the Buffer zone Randomly Selected on Plot 9

Figure 3.11 indicates the same randomly selected buffer as indicated in Figure 3.2, with the exception that 17 different trees were now highlighted, since tree 202 is included twice. The 17 trees were selected, since the two highlighted groups specifically contains both tree 184 and tree 214, where both these trees represent subject or target trees, and trees specifically located around these two mentioned target trees. Here, note as mentioned, tree 202 is included in both highlighted groups and should therefore only be counted once. This figure therefore indicates trees that were used specifically to generate ~~a~~ one of the off-diagonal elements of the numerator relationship matrix $\mathbf{A}$, namely off-diagonal element a_{23} of the numerator relationship matrix. Tree 184, in this case, represents the subject or target tree, while tree 214, represents the competitor tree. In order to calculate a_{32}, use tree 214 as target or subject tree, while tree 184 is this time used as the competitor tree. Remember, that in this case, when dividing with the total area covered by the selected 17 trees, only count the area covered by tree 202, once.

168	185	200	217	232
169	**184**	201	**216**	233
170	183	202	215	234
171	**182**	203	**214**	235
172	181	204	213	236

Figure 3. 12: Selected Trees Surrounding Target Tree 182 and Tree 216 on the Buffer zone Randomly Selected on Plot 9

Figure 3.12 indicates the same randomly selected buffer as indicated in Figure 3.2, with the exception that 17 different trees were now highlighted, since tree 202 is included twice. The 17 trees were selected, since the two highlighted groups

specifically contains both tree 182 and tree 216, where both these trees represent subject or target trees, and trees specifically located around these two mentioned target trees. Similar to Figure 3.11, tree 202 is included in both highlighted groups and should therefore only be counted once. Figure 3.12 therefore indicates trees that were used specifically to generate one of the off-diagonal elements of the numerator relationship matrix $\mathbf{A}$, namely off-diagonal element a_{14} of the numerator relationship matrix. Tree 182, in this case, represents the subject or target tree, while tree 216, represents the competitor tree. In order to calculate a_{41}, use tree 216 as target or subject tree, while tree 182 is this time used as the competitor tree. Also in this case, when dividing with the total area covered by the selected 17 trees, only count the area covered by tree 202, once.

The outcomes of the analysis using the distance-independent Lorimer competition index, will be presented in Chapter 4 section 4.8.

CHAPTER 4

RESULTS FROM THE STUDY

4.1 Introduction

This chapter presents the data analysis and results of the study. The results are obtained through the application of the methodology outlined in Chapter 3. MATLAB R2022b was used to analyse the data and results are presented as follows:

4.2 Characterisation of the Plots

Table 4. 1: Mensuration of Treatments

Plot Number	Plot Dimension	Treatments	Planting Spacing(m)	Area per tree (m^2)	Density	Mortality (%)
Plot 9	16 x 16	1	2.26 x 2.26	5.1	1959	0

In Table 4.1, the characteristics of the randomly selected Plot 9 from Trail number W184/03, are given. From Table 4.1 it can be seen that on plot 9 only 256 trees were planted in rows of 16 x 16 stems. To clarify, although on plot 9 there were only 256 stems planted and not the 1959 stems as indicated in the planting density, plot 9 was set up with spacing between the trees similar to a plot with a planting density of 1959 stems per hectare. Therefore, the area allocated per tree on plot 9, was $5.1m^2$ $(2.26m\ x\ 2.26m)$. This area per tree is therefore the same as the area allocated per tree on a plot, 1 hectare in size with a planting density of 1959 stems per hectare. Also note that on plot 9, no trees died, although some trees may have experienced suppressed growth, either naturally, or through human intervention as part of the trial.

Table 4. 2: Individual Plot Layout (12 x 12 measured trees plot^{-1})

	S	S	S	S	S	S	S	S	S	S	S	S	S	S	S	S	S	S	
S	1 x	2 x	3 x	4 x	5 x	6 x	7 x	8 x	9 x	10 x	11 x	12 x	13 x	14 x	15 x	16 x	17 x	18 x	S
S	2 x	x	x	x	x	x	x	x	x	x	x	x	x	x	x	x	x	x	S
S	3 x	x	x	x	x	x	x	x	x	x	x	x	x	x	x	x	x	x	S
S	4 x	x	x	x	x	x	x	x	x	x	x	x	x	x	x	x	x	x	S
S	5 x	x	x	x	x	x	x	x	x	x	x	x	x	x	x	x	x	x	S
S	6 x	x	x	x	x	x	x	x	x	x	x	x	x	x	x	x	x	x	S
S	7 x	x	x	x	x	x	x	x	x	x	x	x	x	x	x	x	x	x	S
S	8 x	x	x	x	x	x	x	x	x	x	x	x	x	x	x	x	x	x	S
S	9 x	x	x	x	x	x	x	x	x	x	x	x	x	x	x	x	x	x	S
S	10 x	x	x	x	x	x	x	x	x	x	x	x	x	x	x	x	x	x	S
S	11 x	x	x	x	x	x	x	x	x	x	x	x	x	x	x	x	x	x	S
S	12 x	x	x	x	x	x	x	x	x	x	x	x	x	x	x	x	x	x	S
S	13 x	x	x	x	x	x	x	x	x	x	x	x	x	x	x	x	x	x	S
S	14 x	x	x	x	x	x	x	x	x	x	x	x	x	x	x	x	x	x	S
S	15 x	x	x	x	x	x	x	x	x	x	x	x	x	x	x	x	x	x	S
S	16 x	x	x	x	x	x	x	x	x	x	x	x	x	x	x	x	x	x	S
S	17 x	x	x	x	x	x	x	x	x	x	x	x	x	x	x	x	x	x	S
S	18 x	x	x	x	x	x	x	x	x	x	x	x	x	x	x	x	x	x	S
	S	S	S	S	S	S	S	S	S	S	S	S	S	S	S	S	S	S	

Table 4.2 represents a practical layout of plot 9, indicating specifically where trees are located according to the specific assigned number of the individual trees. Note also that trees are numbered according to a snake pattern, with for example, tree 16 located directly next to tree 17 and tree 32 for example, located directly next to tree 1. Also, **x**

represents the specific position a tree is planted on the allocated area of $5.1m^2$. In the layout above, **S** represents a boundary zone or fire break where no trees are planted. This is done in an attempt to kill the fire front in order to protect the trees planted on plot 9, in the event of a fire breaking out.

4.3 Descriptive Statistics

Descriptive statistics analysis was obtained using the tree DBH to obtain variation, centralisation, and distribution of the data to check when the tree competition starts to set in eucalyptus plantations from three different plots. The mean is used to measure the central tendency of the data while the standard deviation is utilised to measure the variation of the data.

4.3.1 Descriptive Statistics of the DBH for Plot 9

Table 4. 3: Descriptive Statistics of the Tree Diameter at Breast Hight (DBH) for Plot 9

Time Period (yrs.)	Minimum	Maximum	Mean	Standard Deviation (SD)	Coefficient of Variation (C.V)
Year 1	0	2.4	0.9223	0.6174	66.9358
Year 2	0.4	6.9	4.7996	1.1561	24.0869
Year 3	1.8	13.5	10.5695	1.8088	17.113
Year 4	1.8	16.9	12.6918	2.4534	19.3305
Year 5	1.8	18.7	13.7141	2.9631	21.6064
Year 6	1.8	20.3	14.2887	3.3615	23.5256
Year 7	1.8	22.2	14.6594	3.5829	24.4412
Year 8	1.8	22.3	15.1148	3.8676	25.5879
Year 9	1.8	22.3	15.6133	4.1031	26.2792
Year 10	1.8	23.7	15.759	4.2555	27.0039

In Table 4.3 descriptive statistics of the tree diameter at breast hight (DBH), for trees planted on plot 9, are given for the 10-year period from 2000 to 2009. Measurements

were taken at the same time period during each consecutive year in order to ensure that the time period in between measurements (growth period), were the same. By considering the minimum DBH measurement during the consecutive growth periods, it can be seen that no growth took place in some trees from year 3 onwards. These trees did not die however, but experienced suppressed growth, either naturally, or through human intervention as part of the trial. Note also that a minimum DBH value of $0\ cm$ is possible during growth period 1, since some of the trees may not have reached breast hight during that growth period. By considering the maximum DBH, it can be seen that maximum DBH consistently increased over the 10-year period, except for the periods between years 7 to 10 (growth periods 7 -10) when maximum DBH remained relatively constant. This may be explained by trees either approaching maturity, or due to a possible peak in competition experienced between the trees on plot 9. The mean, standard deviation, and coefficient of variation were calculated using the measured DBH values of all 256 stems planted on plot 9. These values were calculated for all 10 consecutive years. From Table 4.3, it can be seen that there was an increase in the average DBH for a 10 growth periods, although the average growth started slowing down from year 4 onwards. From Table 4.3 it can also be seen that the standard deviation increased as well during the consecutive growth periods over the 10-year period. This may be explained due to the suppressed growth experienced by some of the trees on the plot from period 3 onwards, since the DBH values of these trees were located further away from the mean DBH as growth progressed during the 10-year period. By considering the coefficient of variation (CV) provided in Table 4.3, a higher CV value would indicate a higher level of dispersion of DBH values around the mean DBH during a specific growth period. It can therefore be seen that the highest variability in growth was observed during the first growth period. Variability in DBH around the mean however decreased as the trees increased in size up to the end of growth period 3. This may indicate the period when canopy closure took place. According to literature, competition starts to set in, in the growth period following canopy closure. As competition sets in, a gradual increase in variability may be expected, since some trees may grow quicker than others as a result of competition between neighbouring trees. This gradual increase can also be observed in the coefficient of variation during the 7-year period following canopy closure.

4.3.2 DBH Average for Plot 9

The following figure depict the same means from Table 4.3 of plot 9.

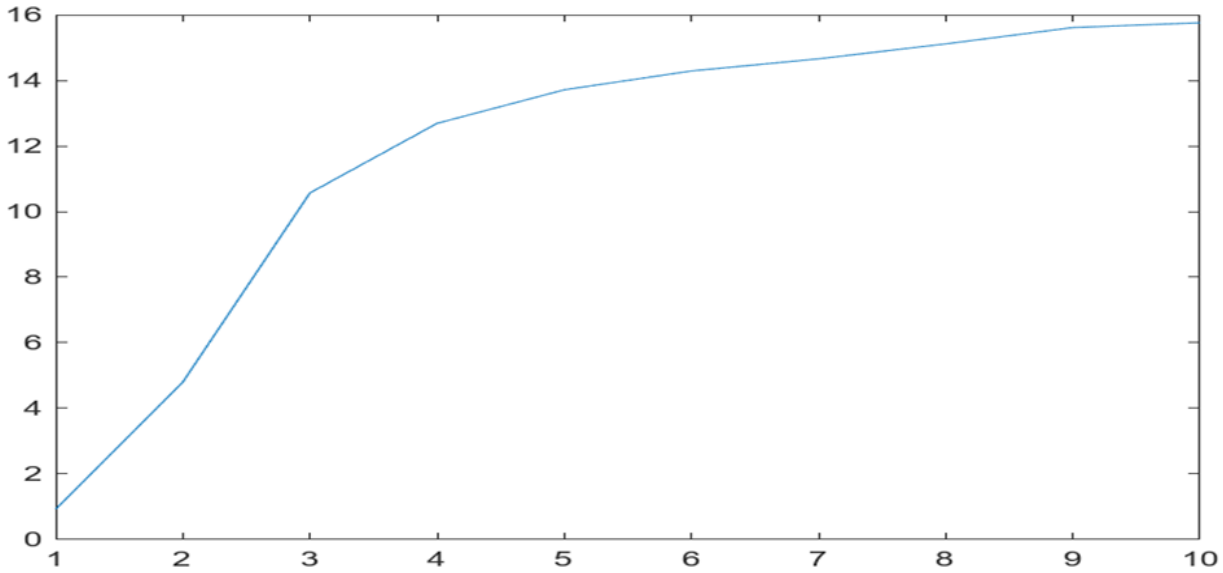

Figure 4.1: Plot representing the Average Growth measured in DBH of all 256 Stems Planted on Plot 9 for the 10 Growth Periods

According to Morley *et al*. (2008) canopy closure should take place at around year 3, or during growth period 2-3 (year 2). It is also suggested that competition between trees start to set in after canopy closure, since individual trees will start to compete more for available resources. When competition sets in, average growth on plots will therefore gradually start to decrease. From Figure 4.1, it can be seen that the average growth of the 256 stems planted on plot 9, measured in DBH, increased substantially during the first 3 years after planting. After year 2, i.e., during year 3 (growth period 3-4) however, average growth gradually decreased. As mentioned in literature, this gradual decrease observed was expected and may be due to individual trees competing for resources.

4.4 Gibbs Sampling Procedure

Initially, it has been assumed that there is no relationship between the trees. The numerator relationship matrix will therefore be represented by an identity matrix. Since the numerator relationship matrix $\mathbf{A}$ has been set up, and the full conditional posterior of the unknown parameters has been determined, the Gibbs sampler can be used to

obtain the marginal posterior distributions of the variance components as well as the fixed and random effects. The Gibbs sampler's main prerequisite is that all conditional densities must be accessible so that random variates can be simulated from them. The Gibbs sampling procedure is easy to implement and effectively generate samples. MATLAB R2022b was used to run the Gibbs sampler in order to obtain the marginal posterior densities of the unknown parameters. Starting from period 4, the growth period following canopy closure, the marginal posterior densities were simulated using the differences in circumference, calculated between adjacent growth periods of the individual stems planted on plot 9

The first step when implementing the Gibbs sampling procedure is to generate random numbers from the required distributions. The iterative process for the burn-in-period is started by specifying initial values $u^{(0)}, \sigma_s^{2(0)}$ and $\sigma_\varepsilon^{2(0)}$ to draw $\beta^{(1)}$. The obtained values were substituted into the full conditional posterior distribution of the unknown parameters to draw (sample) $u^{(1)}, \sigma_s^{2(1)}$ and $\sigma_\varepsilon^{2(1)}$. The full conditional posterior distributions were updated after every iteration. The results from the burn-in period were obtained after running the procedure 500 times and retaining simulated values obtained from every 20^{th} draw. The reason for retaining simulated values from only every 20th draw, is since the Gibbs sampling procedure produce dependent draws. By retaining simulated values from every 20^{th} draw only, the dependency between the simulated values will be reduced to a minimum. The values simulated on the final iteration of the Burn-in period, are then used as starting values to run the Gibbs sampler in order to obtain the marginal posterior distributions of the unknown parameters (Hugo, 1998). Therefore, the values obtained on the last iteration of the Burn-in period, i.e., the last set of retained simulated values from the Burn-in period, were then used as starting values for the Gibbs sampling procedure. The Burn-in period is necessary to ensure convergence of the simulated values before starting the actual Gibbs simulation procedure.

The marginal posterior distributions $p(\beta|y)$, $p(u|y)$, $p(\sigma_s^2|y)$ and $p(\sigma_\varepsilon^2|y)$ were obtained using the Gibbs sampler. Estimates from the marginal posterior densities of the fixed and random effects, as well as estimates from the marginal posterior

densities of the variance components and functions thereof, were therefore easily obtained (Hugo, 1998). A complete Bayesian solution to the mixed linear model can therefore be obtained using the Gibbs sampling procedure. Using the Gibbs sampling procedure, the following results were obtained:

4.5 Estimation of the Variance Component

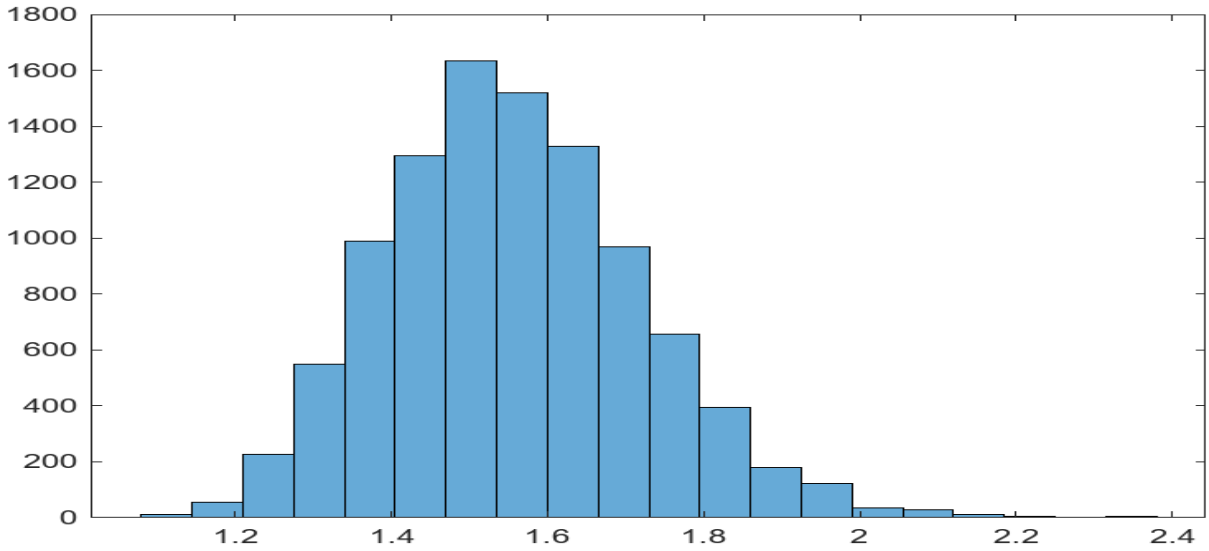

Figure 4.2: Histogram of the Estimated Marginal Posterior Density of the Error Variance σ_{ε}^{2}

Figure 4.2 depicts the histogram of the estimated marginal posterior density of the error variance simulated using the Gibbs sampling procedure, implemented for the randomly selected group of 25 trees on plot 9. From the histogram it can be seen that the estimated marginal posterior density of the error variance is slightly positively skewed. This is due to the high number of degrees of freedom associated with the error variance. The median is 1.543 cm with 95% equal tails credibility interval given by [1.5477 ; 1.5542].

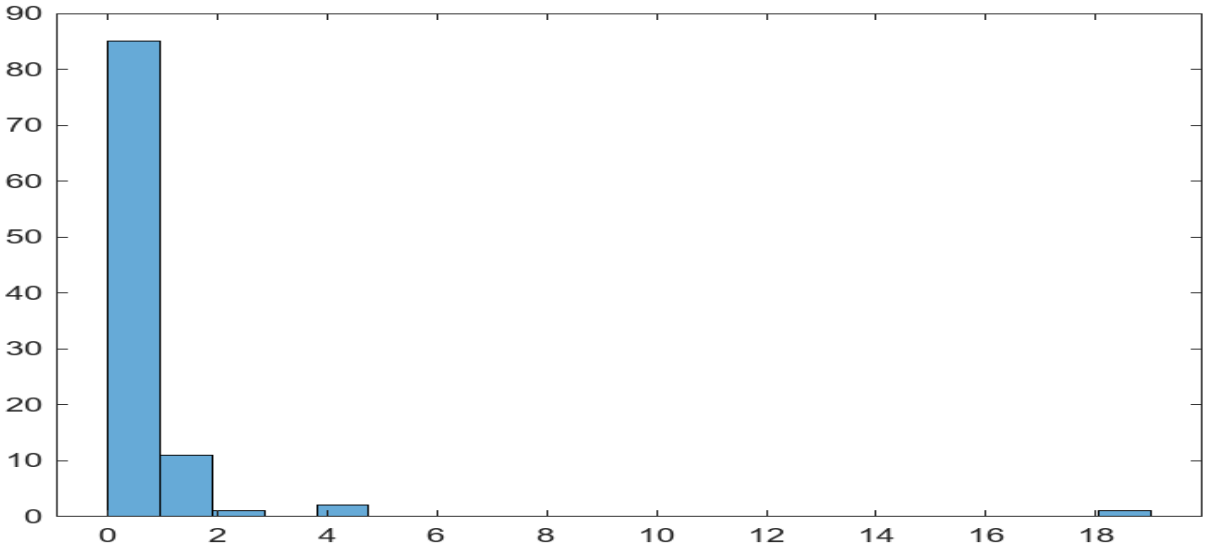

Figure 4.3: Histogram of the Estimated Marginal Posterior Density for the Tree Variance σ_s^2

Figure 4.5 depicts the histogram of the estimated marginal posterior density ~~for~~ of the tree variance simulated using the Gibbs sampling procedure, implemented for the randomly selected group of 25 trees on plot 9. From the histogram, it can be seen that the estimated marginal posterior density of the tree variance is positively skewed. This is due to the low number of degrees of freedom associated with the tree variance, since only 4 target trees were identified from the 25 selected trees. The median is 0.22871 cm with 95% equal tails credibility interval given by [0.9558 ; 2.1580].

4.6 Estimation of Marginal Posterior Density of Random and Fixed Effects

4.6.1 Random Effects Distributions

As mentioned, the Gibbs sampler can also be used to simulate the marginal posterior densities of the random effects (selected trees). The results for the marginal posterior densities of the 4 selected target trees, i.e., tree 182, tree 184, tree 214 and tree 216 are depicted in Figures 4.4, 4.5, 4.6 and 4.7, respectively.

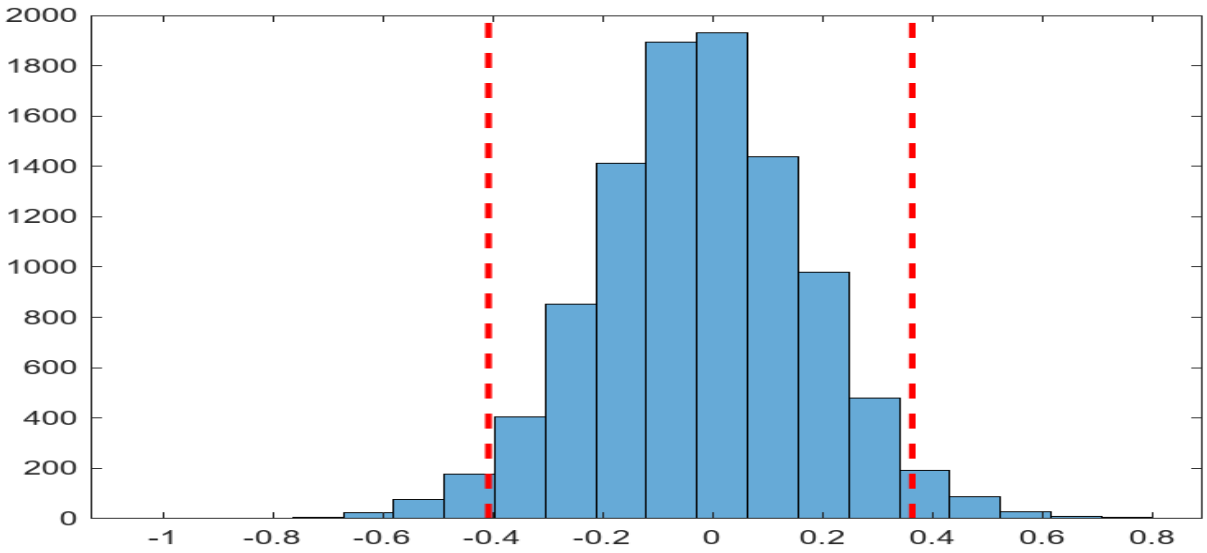

Figure 4.4: Histogram of the Estimated Marginal Posterior Density of Tree 182 $(\boldsymbol{u_1})$

Figure 4.6 shows the histogram of the estimated marginal posterior density for the growth index for tree 182 $(\boldsymbol{u_1})$**,** obtained using the Gibbs sampling procedure. The histogram of the estimated marginal posterior density of tree 182 is symmetrical with mean = -0.020153 cm and 95% equal tails credibility interval given by [-0.407995 ; 0.363461] From Figure 4.6 as well as the 95% equal tails credibility interval, it can also be seen that zero is contained in the interval. This indicates that there is no significant difference between the average growth of tree 182, and the average growth of the remaining 24 trees planted on plot 9.

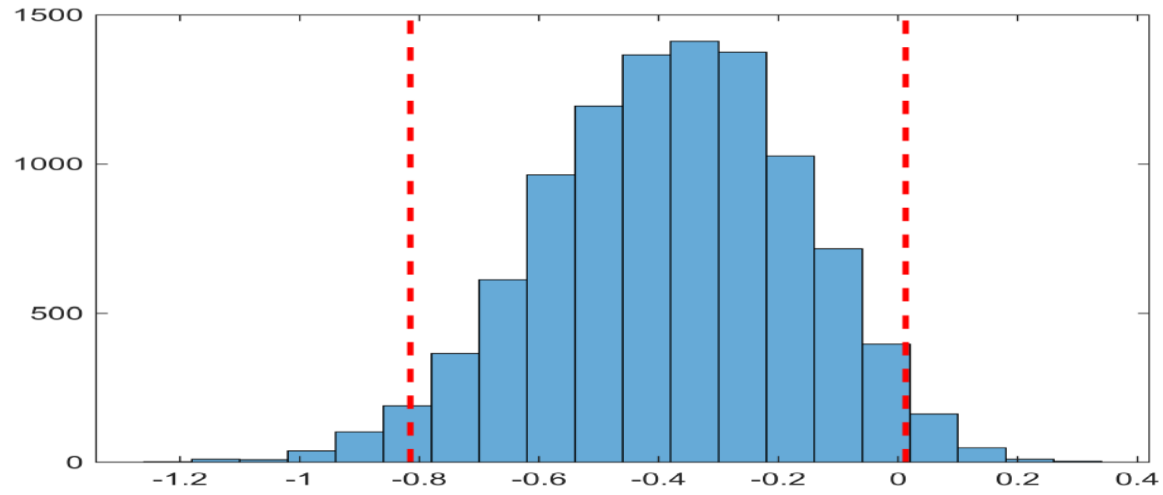

Figure 4.5: Histogram of the Estimated Marginal Posterior Density of Tree 184 $(\boldsymbol{u_2})$

Figure 4.5 indicates the histogram of the estimated marginal posterior density for the growth index for tree 184 ($\boldsymbol{u_2}$) using Gibbs sampling. It can be seen that the estimated marginal posterior density of tree 184 is symmetrical with mean = -0.38493 cm and 95% equal tails credibility interval given by [-0.819739 ; 0.010393]. Zero is also contained in the interval. This indicates that there is no significant difference between the average growth of tree 184, and the average growth of the remaining 24 trees planted on plot 9. By considering the 90% equal tails credibility interval however given by [-0.746170 ; -0.042693], it can be seen that zero does not fall within this interval, thus indicating that a significant difference exists between the average growth of tree 184 and the average growth of the remaining 24 trees planted on plot 9, at a 90% credibility level. Since both the lower and upper 90% equal tails credibility limits are negative, it can be seen that the average growth of tree 184 is significantly less than the average growth of the remaining 24 trees planted on plot 9.

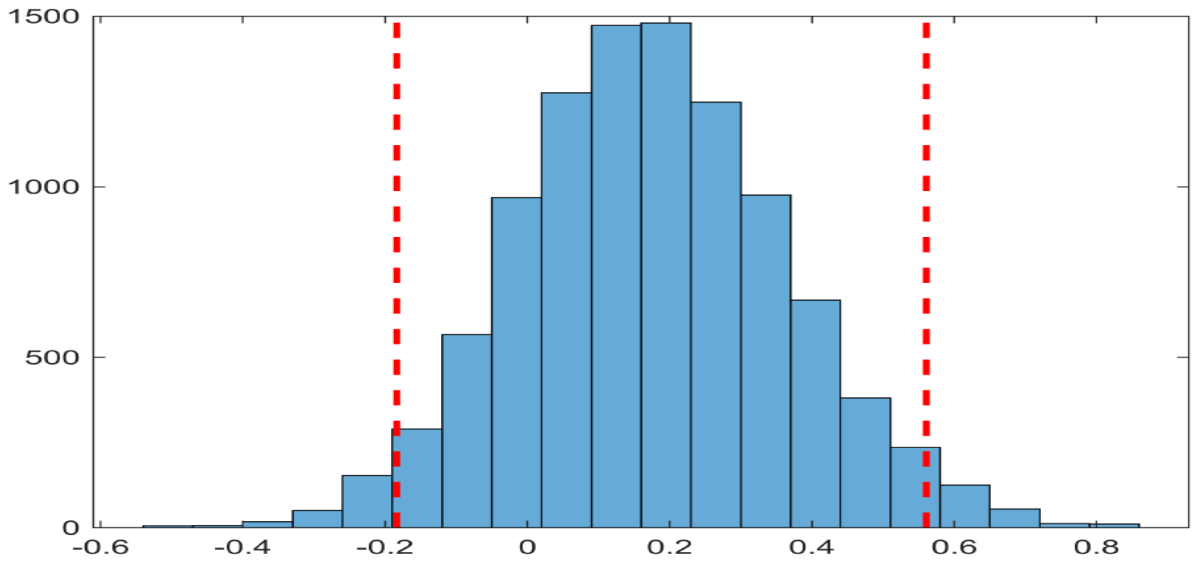

Figure 4.6: Histogram of the Estimated Marginal Posterior Density of Tree 214 ($\boldsymbol{u_3}$)

Figure 4.6 depicts the histogram of the estimated marginal posterior density for the growth index for tree 214 ($\boldsymbol{u_3}$) using Gibbs sampling. From this figure, it can be seen that the estimated marginal posterior density of tree 214 is symmetrical with mean = -0.20614 cm and 95% equal tails credibility interval given by [-0.155962 ; 0.606178]. From Figure 4.6 it can be seen that zero is contained in the interval. This indicates that

there is no significant difference between the average growth of tree 214, and the average growth of the remaining 24 trees planted on plot 9.

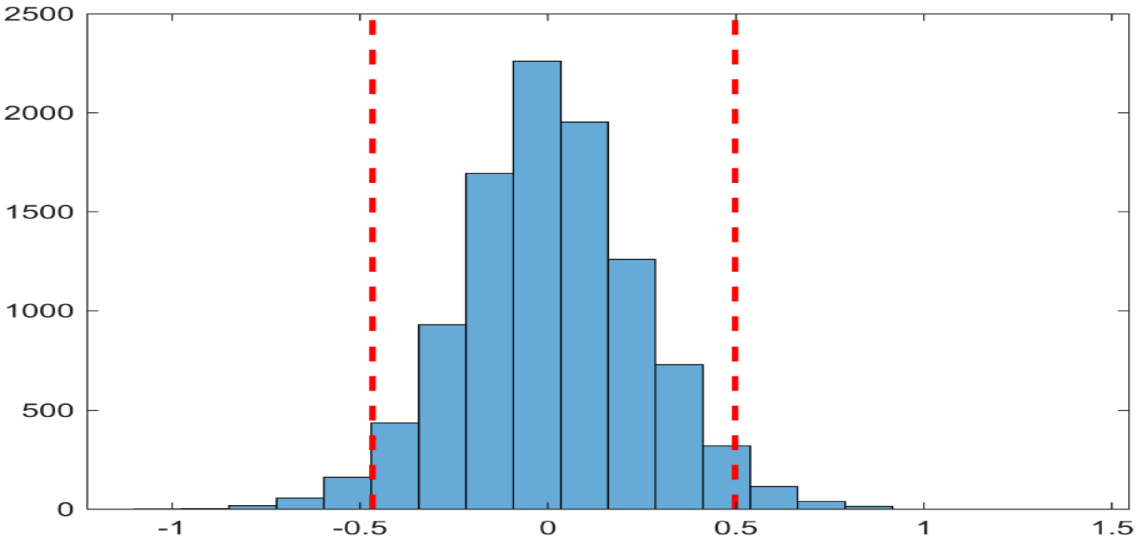

Figure 4.7: Histogram of the Estimated Marginal Posterior Density of Tree 216 (u_4)

Figure 4.7 shows the histogram of the estimated marginal posterior density for the growth index for tree 216 (u_4) using Gibbs sampling. It can be seen that the estimated marginal posterior density of tree 216 is symmetrical with mean = -0.033722 cm and 95% equal tails credibility interval given by [-0.539304 ; 0.472515]. Similar to Figures 4.4, 4.5 and 4.6, zero is also contained in the interval . This indicates that there is no significant difference between the average growth of tree 216, and the average growth of the remaining 24 trees planted on plot 9.

4.6.2 Unconditional or Marginal Posterior Distributions of the Random Effects

Using the Rao-Blackwell method (Gelfand and Smith, 1990), the unconditional or marginal posterior densities of the random effects can also be determined. These marginal posterior distributions of the random effects (tree effects) are depicted in Figures 4.8 – 4.11. From Figures 4.4 – 4.7, as well as Figures 4.8 – 4.11, it can be seen that the unconditional or marginal posterior densities correspond well with the histograms of the estimated marginal posterior densities of the random or tree effects, thus indicating that both methods can be used in order to obtain the estimated marginal

posterior distributions. This is also evident from the means and 95% equal tails credibility intervals obtained using both methods.

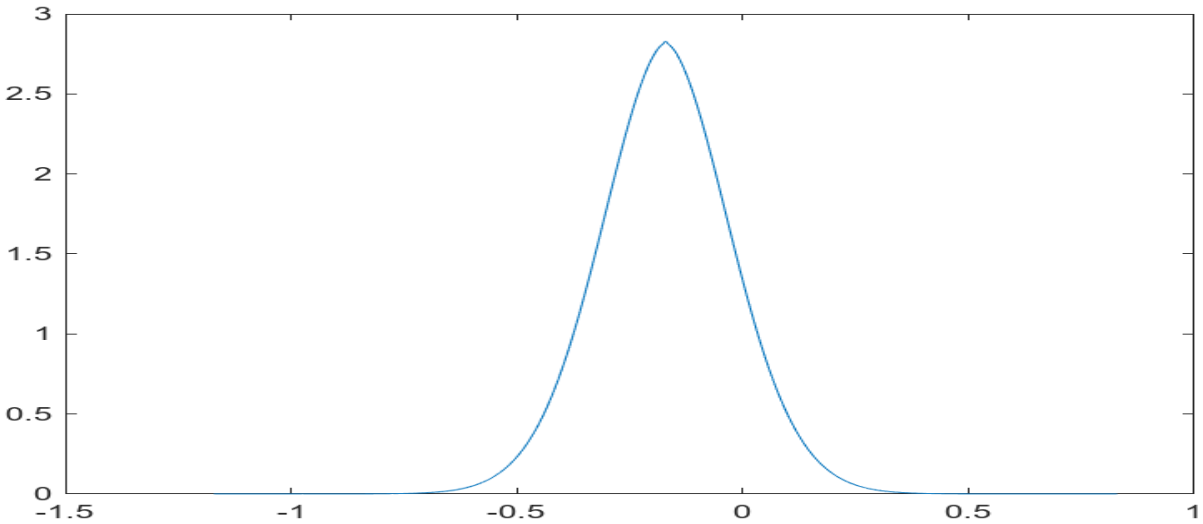

Figure 4.8: Estimated Marginal Posterior Density of Tree 182 (u_1)

Figure 4.8 shows an unconditional or estimated marginal posterior density of tree 182 determined using Rao-Blackwell method. The unconditional or estimated marginal posterior density of tree 182 is symmetrical with mean = -0.020153 cm and 95% equal tails credibility interval given by [-0.40828 ; 0.363316]. It can be seen that the interval corresponds with histogram of the estimated marginal posterior density of tree 182. The same conclusion can therefore be reached as in the corresponding histogram given in Figure 4.4.

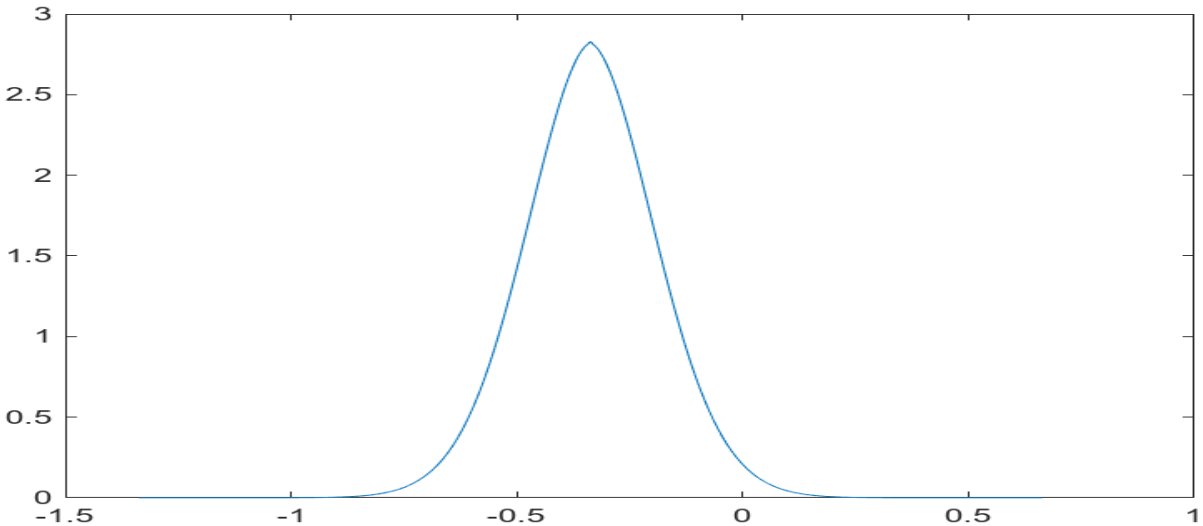

Figure 4.9: Estimated Marginal Posterior Density of Tree 184 (u_2)

Figure 4.9 illustrates the unconditional or estimated marginal posterior density of tree 182 determined using the Rao-Blackwell method. The mean value of this symmetrical density is -0.38493 cm, with a 95% equal tails credibility interval given by [-0.819920 ; 0.010359]. Notably, this interval corresponds to the histogram representing the estimated marginal posterior density of tree 184. By considering the 90% equal tails credibility interval given by [-0.961553 ; -0.6700073]. It can be seen that zero does not fall within the interval. The same conclusion can therefore be reached as in the corresponding histogram given in Figure 4.5.

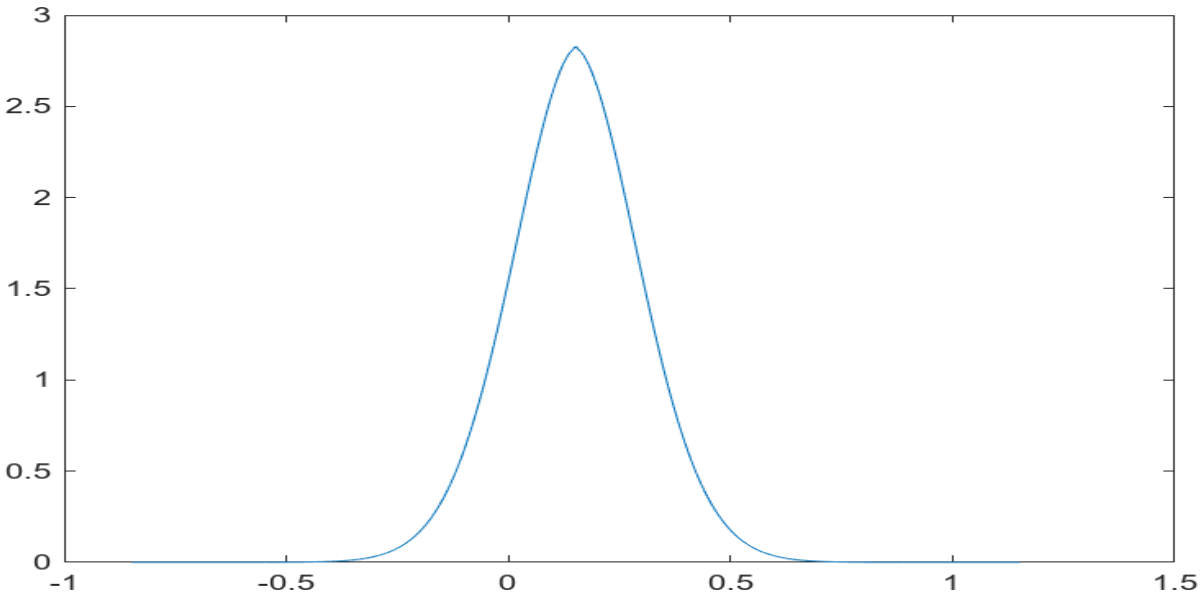

Figure 4.10: Estimated Marginal Posterior Density of Tree 214 $(\mathbf{u_3})$

In Figure 4.10, the unconditional marginal posterior density for tree 214, estimated using the Rao-Blackwell method, is displayed. This density is symmetric, with a mean = - 0.20614 cm and a 95% equal tails credibility interval given by [-0.156149 ; 0.605767]. This interval aligns with the histogram of the estimated marginal posterior density for tree 214. The same conclusion can therefore be reached as in the corresponding histogram given in Figure 4.6.

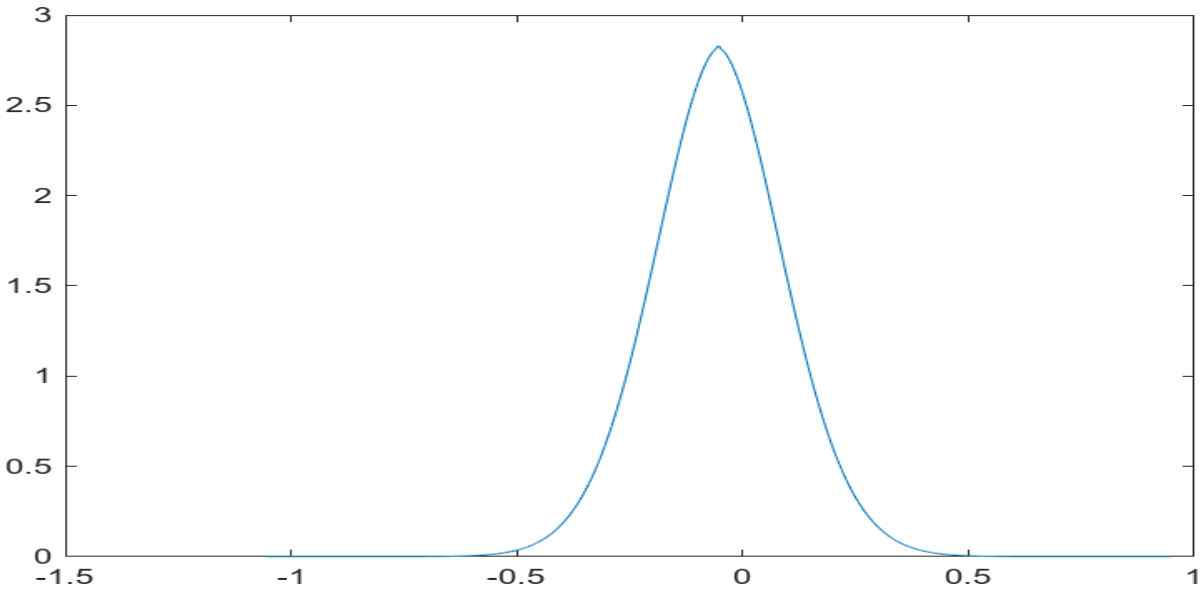

Figure 4.11: Estimated Marginal Posterior Density of Tree 216 (u_4)

Figure 4.11 presents the unconditional marginal posterior density of tree 216, determined through the Rao-Blackwell method. It can be seen that the density of tree 216 symmetry and has a mean = -0.033722 cm, along with a 95% equal tails credibility interval given by [-0.539589 ; 0.472419]. Remarkably, this interval matches the histogram of the estimated marginal posterior density for tree 216. The same conclusion can therefore be reached as in the corresponding histogram given in Figure 4.7.

4.6.3 Marginal Posterior Distribution of the fixed Effects

The Gibbs sampler can also be used to simulate the marginal posterior densities of the fixed effects. For this study, the fixed effects were represented by the growth period (measured at 8 levels), the number of normal growing trees planted around a specific tree (measured at 5 levels) and whether a specific tree itself, was suppressed or not (measured at two levels).

As mentioned, for this study, growth period was measured at 8 levels. The growth period included were, growth period 2-3, growth period 3-4, growth period 4-5, growth period 5-6, growth period 6-7, growth period 7-8, growth period 8-9 and growth period 9-10. For this study, growth period 1 – 2 (period between year 1 and 2) was however

excluded, since during this period, the trees were not yet at breast height. Also, for the fixed effect growth period, period 2-3 was considered the base level, since as mentioned earlier, according to literature, competition only starts to set in after canopy closure. For this study, canopy closure occurred during growth period 2-3, and as a result, competition would only start to set in during growth period 3-4.

As mentioned, the number of normal growing trees around a specific tree represented the second fixed effect. For this second fixed effect, 5 levels were observed. These were 8 normal growing trees, 7 normal growing trees, 6 normal growing trees, 5 normal growing trees and 4 normal growing trees. Since no tree had less than 4 normal growing trees around it, no additional level of this fixed effect, was considered. For this fixed effect, 4 normal growing trees, growing around a specific tree, was considered the base level. This level was selected as base level, since trees with only 4 normal growing trees around it, potentially, would then represent a tree with access to the highest amount of nutrients on the specific area the tree is located, given that all other conditions on the plot are the same.

The last fixed effect considered, was whether a specific tree on the plot was suppressed or not. A suppressed tree would represent a tree that is alive, but is either due to natural conditions, or human intervention, not growing any further at all. DBH for these trees would therefore remain constant from the time when suppression sets in.

For the fixed effects mentioned above, β_0 therefore represents the average growth of trees with a combination of base levels, i.e., trees with only 4 normal growing trees growing around these trees, trees which are not suppressed trees and with growth measured during growth period 2-3 (growth year 2). Here, $\beta_1, \dots, \beta_7$ represents the difference in the amount of average growth observed between growth periods following the base level period, and the average amount of growth observed for trees with a combination of base levels. It must be noted however that the amount of growth is modelled, and not the actual circumferences of the trees. The amount of growth is

therefore determined by subtracting the circumference observed for a specific tree in a given growth period, from the observed circumference of the same tree in the growth period following the given growth period.

Similarly, $\beta_8, \ldots, \beta_{11}$ represents the difference in the average amount of growth observed between trees with more than 4 normal growing trees around them, and the average amount of growth observed for trees with a combination of base levels. Here β_8 for example, will represent the difference in the average amount of growth observed between a tree with 5 normal growing trees around it, and the average growth observed of trees with a combination of base levels. Also, β_9 for example, will represent the difference in the average amount of growth observed between a tree with 6 normal growing trees around it, and the average growth observed of trees with a combination of base levels, and so on. It must be noted also that β_{12} represents the difference in the average amount of growth observed between suppressed trees, which should for all practical purposes be zero, and the average amount of growth observed between trees with a combination of base levels.

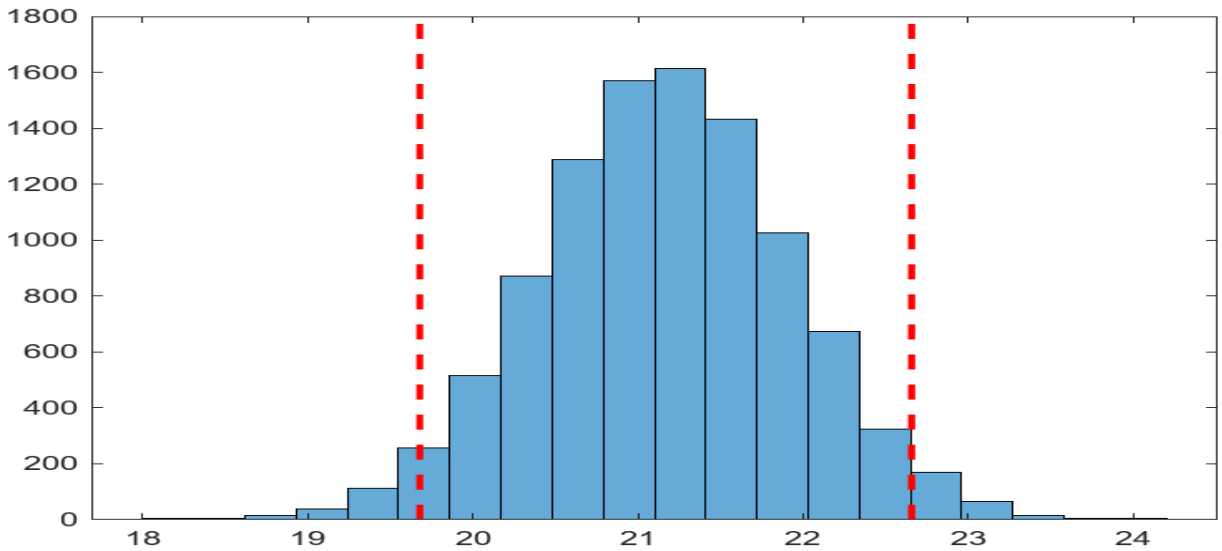

Figure 4.12: Histogram of the Estimated Marginal Posterior Density of β_0

Figure 4.12 represents the estimated marginal posterior density of β_0, i.e., the average observed growth rate of trees growing in growth period 2-3, with 4 normal growing trees growing around these trees and where the trees themselves, are not suppressed. From Figure 4.12 it can be seen that the histogram of the estimated

marginal posterior density of β_0 is for all practical purposes symmetrical. The average growth rate for these trees growing with a combination of the mentioned base levels, is 21.161 cm with a 95% equal tails credibility interval given by [19.678429 ; 22.656783].

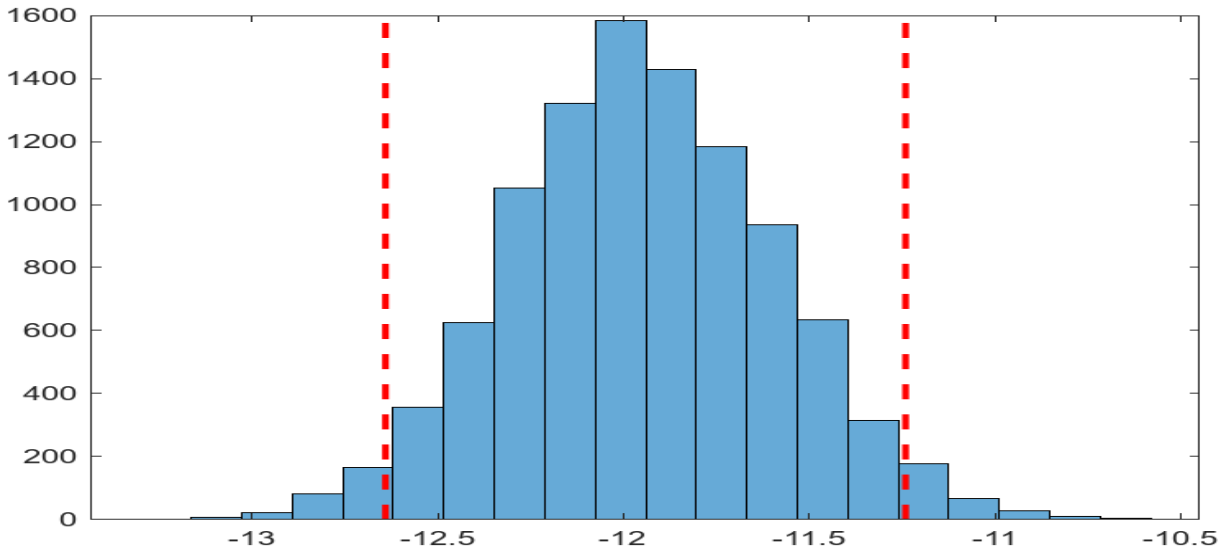

Figure 4.13: Histogram of the Estimated Marginal Posterior Density of $\boldsymbol{\beta_1}$

Figure 4.13 represents the histogram of the estimated marginal posterior density of β_1. As mentioned previously, β_1 represents the expected difference in the average amount of growth observed of the selected group of trees during growth period 3-4, and the average observed amount of growth of the trees growing under the mentioned base level conditions. From figure 4.13 it is therefore evident that the average growth observed during growth period 3-4, differ significantly from the average amount of growth observed for trees growing under base level conditions, since the 95% equal tails credibility interval given by [-12.640807 ; -11.240331], does not contain zero. The mean difference in the amount of growth observed, was -11.9589 cm.

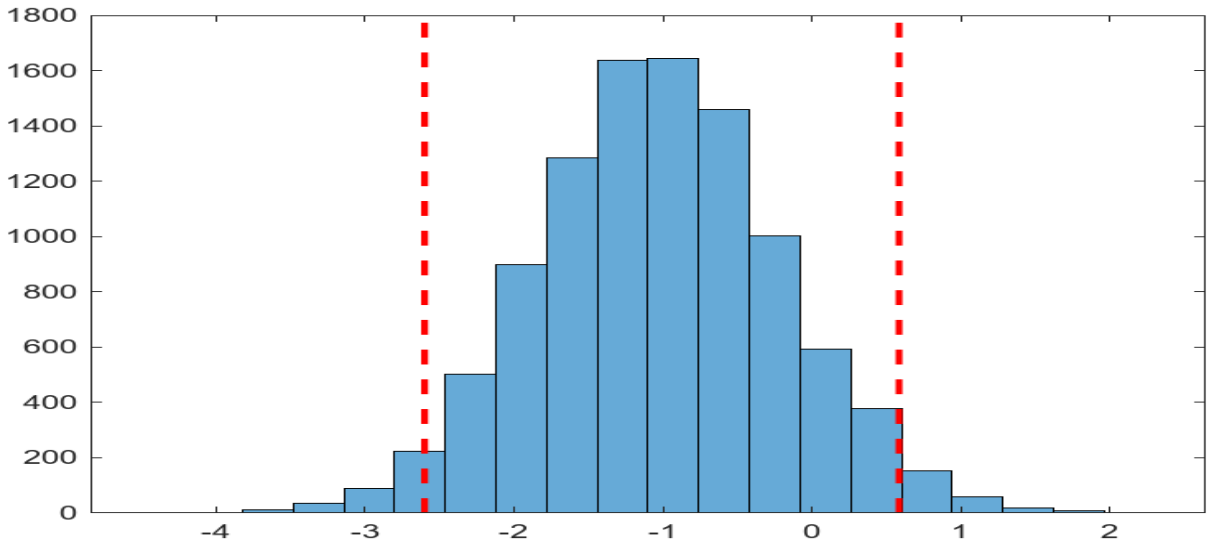

Figure 4.14: Histogram of the Estimated Marginal Posterior Density of β_8

Figure 4.14 represents the histogram of the estimated marginal posterior density of β_8. As mentioned previously, β_8 represents the expected difference in the average amount of growth observed between a tree with 5 normal growing trees around it, and the average amount of growth observed of trees growing under a combination of the mentioned base levels. From Figure 4.14 it is therefore evident that the average growth observed between a tree with 5 normal growing trees around it, is not significantly different from the average amount of growth observed for trees growing under base level conditions, since the 95% equal tails credibility interval given by [-2.599029 ; 0.582817], contains zero. The mean difference in the amount of growth observed, was -1.0368 cm.

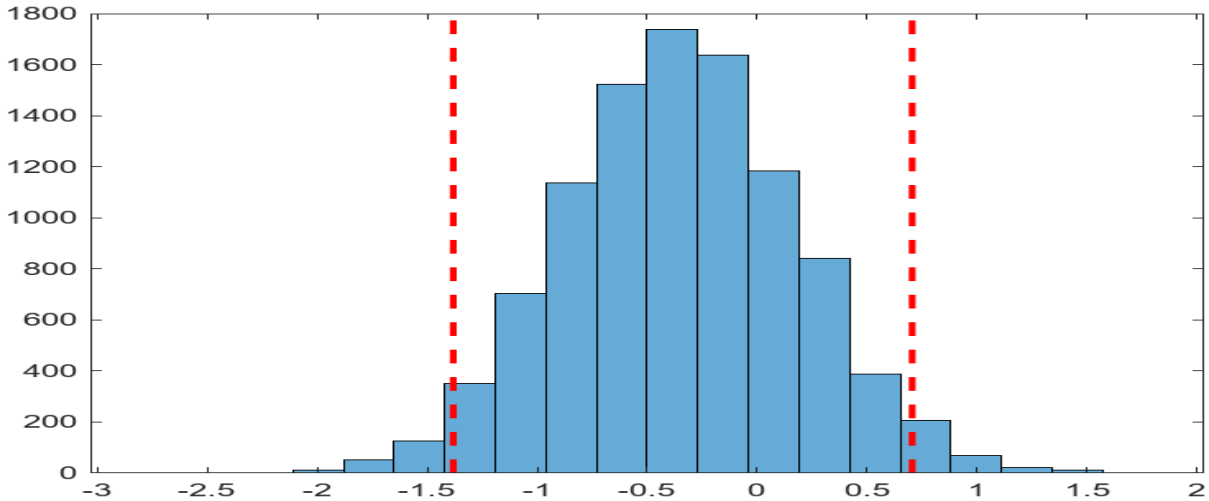

Figure 4.15: Histogram of the Estimated Marginal Posterior Density of β_{12}

Figure 4.15 represents the histogram of the estimated marginal posterior density of β_{12}. As mentioned previously, β_{12} represents the difference in the average amount of growth observed between suppressed trees, and trees growing under a combination of base levels. From Figure 4.15 it is therefore evident that the average growth observed between suppressed trees, is not significantly different from the average amount of growth observed for trees growing under base level conditions, since the 95% equal tails credibility interval given by [-1.380814 ; 0.703737], contains zero. This is to be expected, since, in order for a suppressed tree to have a DBH measurement, that tree must have reached at least breast height before it was suppressed. Also, period 2-3 represented the first period when all the trees on the plot had reached breast height. During period 1-2, some of the trees had not reached breast height, and as a result, do not have a DBH measurement. The histogram of the marginal posterior density of β_{12} therefore represents a comparison between the average observed growth of suppressed trees at breast height, and the average observed growth of trees that just reached breast height. The mean difference in the amount of growth observed however, was -0.35526 cm.

Table 4. 4: Estimated Values of Fixed Effects as well as the 95% Equal Tails Credibility Interval

Fixed Effects	Mean Difference in Observed Growth (cm)	95% Equal Tails Credibility Intervals (cm)
β_0	21.161	[19.678429 ; 22.656783]
β_1	-11.9589	[-12.640807 ; -11.240331]*
β_2	-15.845	[-16.539250 ; -15.150906]*
β_3	-17.7365	[-18.418174 ; -17.039680]*
β_4	-18.2456	[-18.937356 ; -17.555619]*
β_5	-17.8309	[-18.523065 ; -17.141632]*
β_6	-17.9204	[-18.608482 ; -17.215343]*
β_7	-18.9005	[-19.588926 ; -18.203006]*
β_8	-1.0368	[-2.599029 ; 0.582817]
β_9	-0.95159	[-2.453286 ; 0.581641]
β_{10}	-1.7219	[-3.236566 ; -0.215750]*
β_{11}	-1.5407	[-2.978742 ; -0.139725]*
β_{12}	-0.35526	[-1.380814 ; 0.703737]

* Indicate that a significant difference exists, since zero is not contained within the 95% equal tails credibility interval.

In Table 4.4 the posterior means and 95% equal tails credibility intervals of all fixed effects are provided. Note that a negative posterior mean does not indicate that a tree is in fact thinner than during a previous growth period, it represents the difference in the observed growth between a specific growth period and the base level growth period. Therefore, for example, during the base level period, the average growth (increase in circumference from the first year of growth to the second year of growth) measured in cm, was 17.3919 cm. During the following year (growth period 3-4), the average increase in diameter of the tress, was only 6.4214cm. Although the diameter of the trees was higher during growth period 3-4, the average increase in diameter was less than during the base level period (period 2-3). The average increase in circumference, or observed growth, is therefore compared, and not the actual average circumference of the trees during these periods.

4.7 Probability Distribution of the Rank Positions for trees 182, 184, 214 and 216 located on Plot 9

Simulated values from the marginal posterior densities of the variance components, random effects as well as fixed effects can also be used to make probability statements about the individual stems located on plot 9. Figure 4.16, 4.17, 4.18 and 4.19 respectively, represents the probability distribution of the rank positions for trees 182, 184, 214 and 216 located on the plot. Figure 4.16 for example, therefore, represents the rank position of the 4 target trees with regards to the weakest grower of the 4. Therefore, if a tree has the highest probability indicated in Figure 4.16, it means that this specific tree, has the highest probability of being the weakest grower of the 4 target trees. Figures 4.17 – 4.19 have similar interpretations with regards to the remaining rank positions.

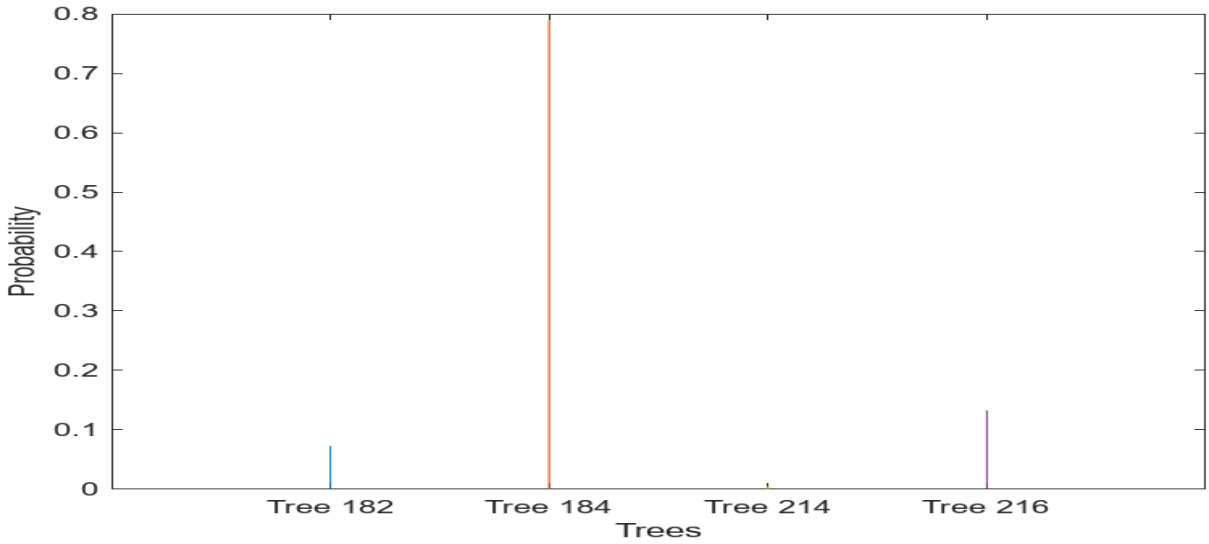

Figure 4.16: Probability of the Weakest Grower of the Group Selected

From Figure 4.16, it can be seen that tree 184 has the highest probability of being the weakest grower of the group of 4 selected target trees located on plot 9, with a probability of being the weakest grower, given by 0.7895 cm. This confirms the findings obtained in both Figures 4.5 and 4.9, since tree 184 had the lowest mean growth and the 95% equal tails credibility interval almost did not contain zero. By considering the 90% equal tails credibility interval given by [-0.746170 ; -0.042693] obtained for tree 184, it can be seen that this credibility interval does not contain zero, indicating that tree 184 has significantly weaker growth than the 3 other target trees located on plot 9.

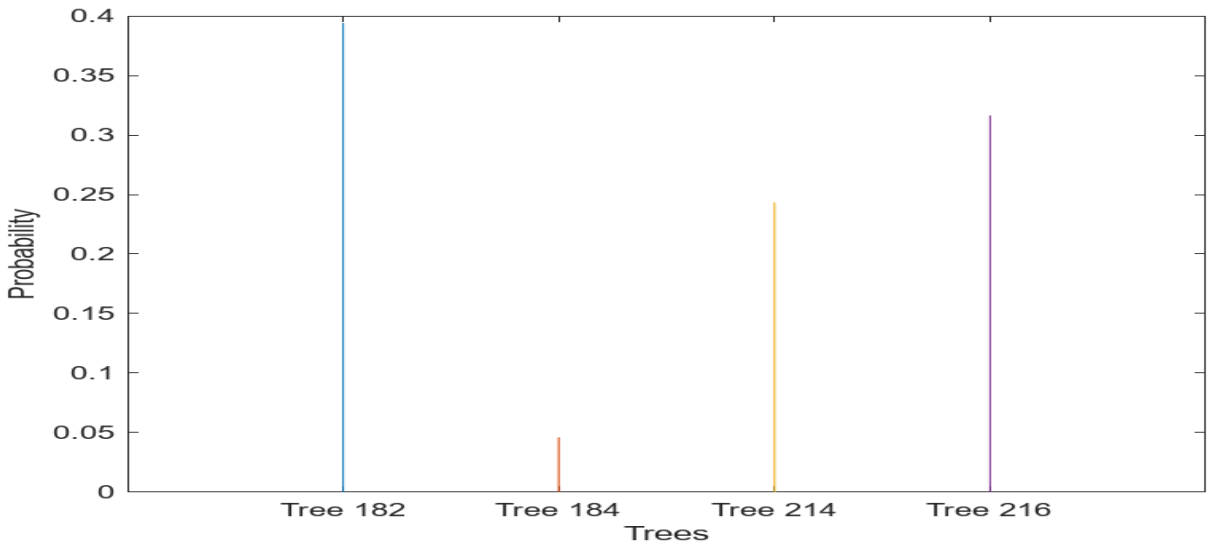

Figure 4.17: Probability of the Second Weakest Grower of the Groups Selected

Figure 4.17 depicts that tree 182 has the highest probability of being the second weakest grower of the group of 4 selected target trees located on plot 9, with a probability of being the second weakest grower, given by 0.3941 cm. This confirms the findings obtained in both Figures 4.4 and 4.8, since tree 182 had the second lowest mean growth. By considering the 95% equal tails credibility interval given by [-0.407995 ; 0.363461], obtained for tree 182, it can be seen that this credibility interval contains zero. This indicates that, although tree 182 had the second weakest growth rate, the growth rate for tree 182 did not differ significantly from the growth rates of the other 2 target or subject trees (i.e., tree 214 and 216). By considering Figures 4.4 – 4.11, also note the position of zero within this 95% equal tails credibility interval relative to the positions of zero within the other 95% equal tails credibility intervals for the remaining target or subject trees (i.e., trees 214 and 216). This confirms the probability obtained for tree 182 indicated in Figure 4.17.

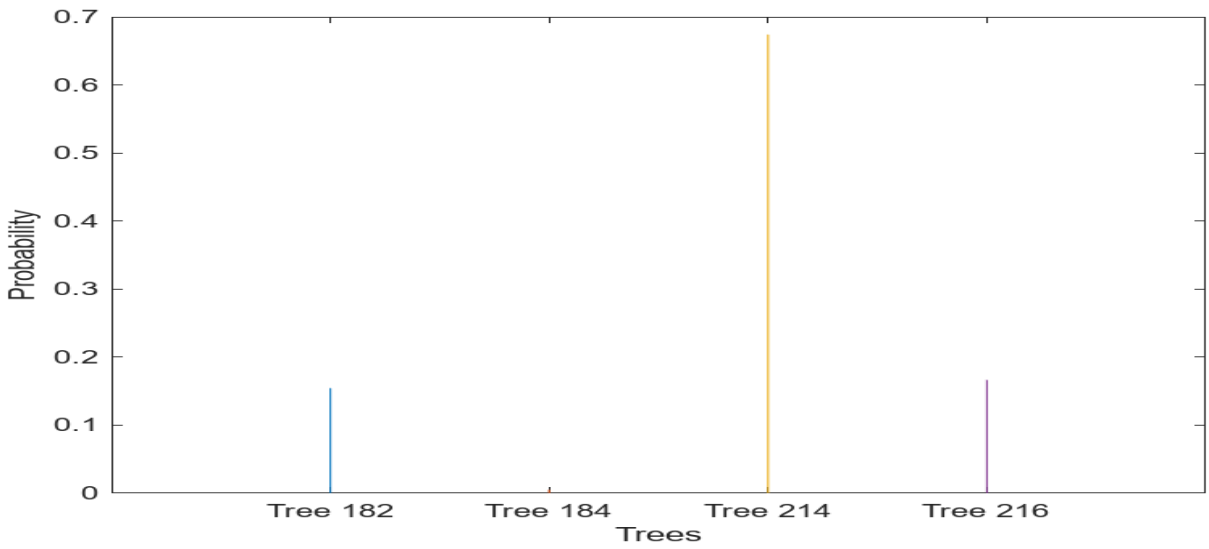

Figure 4.18: Probability of the Strongest Grower of the Group Selected

Figure 4.18 indicates that tree 214 has the highest probability of being the strongest grower of the group of 4 selected target trees located on plot 9, with a probability of being the strongest grower, given by 0.6741 cm. This confirms the findings obtained in both Figures 4.6 and 4.10, since tree 214 had the highest mean growth. By considering the 95% equal tails credibility interval given by [-0.155962 ; 0.606178], obtained for tree 214, it can be seen that this credibility interval however contains zero. By considering Figures 4.4 – 4.11, also note the position of zero within this 95% equal

tails credibility interval relative to the positions of zero within the other 95% equal tails credibility intervals for the remaining target or subject trees (i.e., trees 182 and 216). This confirms the probability obtained for tree 214 indicated in Figure 4.18.

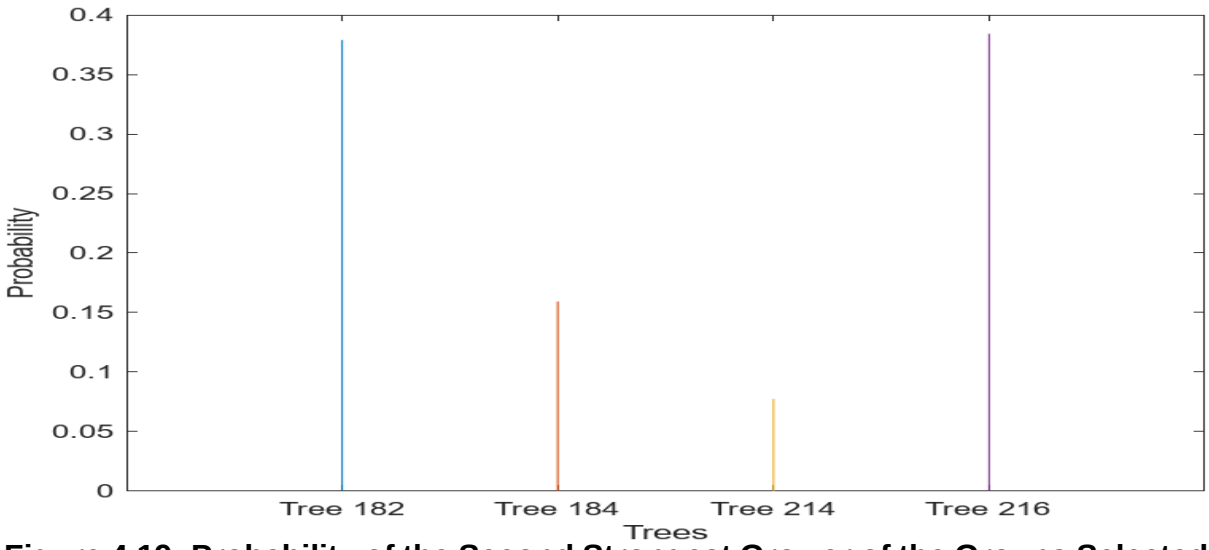

Figure 4.19: Probability of the Second Strongest Grower of the Groups Selected

From Figure 4.19 it can be seen that tree 216 has the highest probability of being the second strongest grower of the group of 4 selected target trees located on plot 9, with a probability of being the second strongest grower, given by 0.3904 cm. Figure 4.19 confirms the findings obtained in both Figures 4.7 and 4.11, since tree 216 had the second highest mean growth. By considering the 95% equal tails credibility interval given by [-0.539304, 0.472515] obtained for tree 214, it can be seen that this credibility interval however contains zero. By considering Figures 4.4 – 4.11, also note the position of zero within this 95% equal tails credibility interval relative to the positions of zero within the other 95% equal tails credibility intervals for the remaining target or subject trees (i.e., trees 182 and 214). This confirms the probability obtained for tree 216 indicated in Figure 4.19.

4.8 Estimation of Marginal Posterior Density for Random and Fixed Effects using a Non-Spatial Competition Index

Section 4.8 presents results pertaining to application of the non-spatial competition index: In section 4.4 the results were obtained after assuming that there is no relationship of competition between the trees, where the numerator relationship matrix

A was represented by an identity matrix. However, in this section it will be assumed that there is competition or relationship between the trees and the numerator relationship matrix will now be represented by the results in Table 4.6. The Gibbs sampler will also be used in this section to derive the marginal posterior distributions of the variance components as well as the fixed and random effects.

4.8.1 Lorimer (1983) Competition Index

Using equation 3.12 and the process discussed in section 3.9 for generating a new numerator relationship matrix consider the following examples:

1. The diagonal element for tree 182 (a_{11}) is given by:

$$a_{11} = 1 + 0.25 \times Sdr_{11} = 1 + 0.25(0.160634858) = 1.040087145$$

2. The off-diagonal element for trees 182 and 184 (a_{12}) is given by:

$$a_{12} = 0.5 \times Sdr_{12} + 0.25 \times Sdr_{21} = 0.5(0.163997652) + 0.25(0.163997652) = 0.122998239$$

Table 4. 5: Lorimer (1983) Matrix

	182	184	214	216
182	1.040087145	0.122998239	0.129887029	0.132971401
184	0.122998239	1.038595939	0.129372073	0.129179879
214	0.136460035	0.135866648	1.045421702	0.142717218
216	0.1405576	0.192092583	0.143670384	1.046483942

Table 4.6 shows the entries for numerator relationship matrix **A** using Lorimer index. The entries were calculated by summing up the circumference of the neighbouring trees divided by the subject tree's circumferences selected from the buffer in the plot and divide the sum by the area of the selected trees $(m^2 ha^{-1})$.

4.8.2 Estimation of the Variance Component

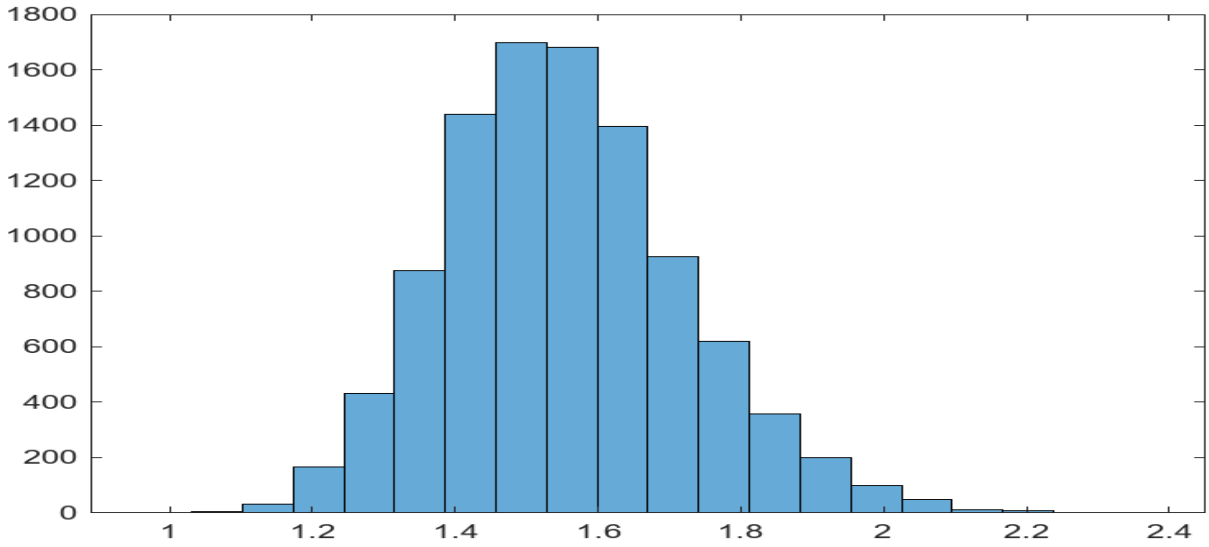

Figure 4. 20: Histogram of the Estimated Marginal Posterior Density of the Error Variance σ_{ε}^{2}

Figure 4.20 shows the histogram of the estimated marginal posterior density of the error variance simulated using the Gibbs sampling procedure, implemented for the randomly selected group of 25 trees on plot 9. From the histogram it can be seen that the estimated marginal posterior density of the error variance is slightly positively skewed. This is due to the high number of degrees of freedom associated with the error variance. The median is 1.5424 cm with 95% equal tails credibility interval given by [1.5496 ; 1.5562].

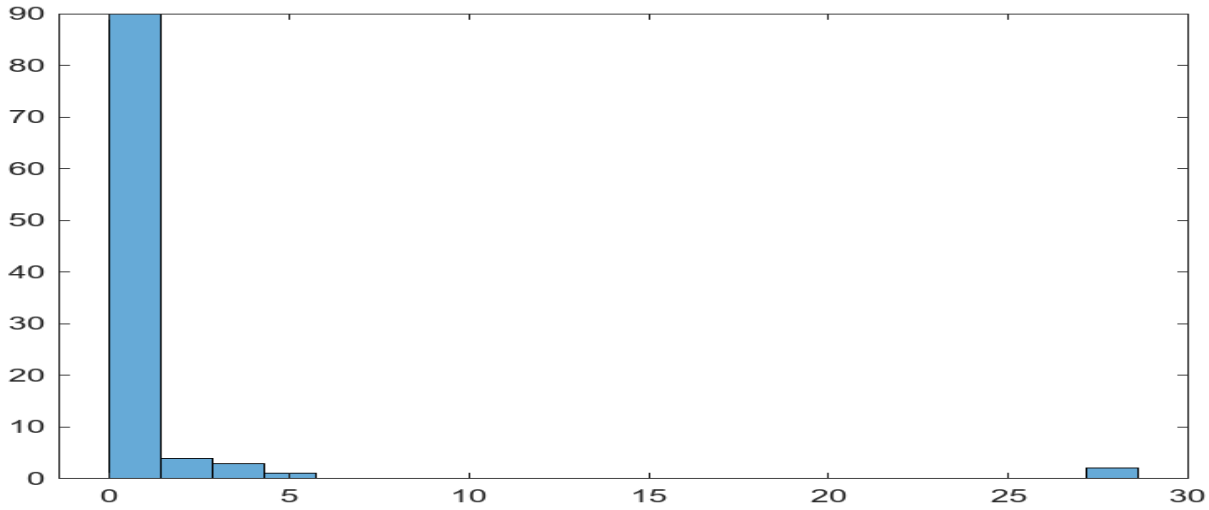

Figure 4. 21: Histogram of the Estimated Marginal Posterior Density for the Tree Variance σ_{s}^{2}

Figure 4.21 depicts the histogram of the estimated marginal posterior density of the tree variance simulated using the Gibbs sampling procedure, implemented for the randomly selected group of 25 trees on plot 9. From the histogram, it can be seen that the estimated marginal posterior density of the tree variance is positively skewed. This is due to the low number of degrees of freedom associated with the tree variance, since only 4 target trees were identified from the 25 selected trees. The median is 0.23376 cm with 95% equal tails credibility interval given by [0.9834 ; 2.7970].

4.8.3 Random Effects Distributions

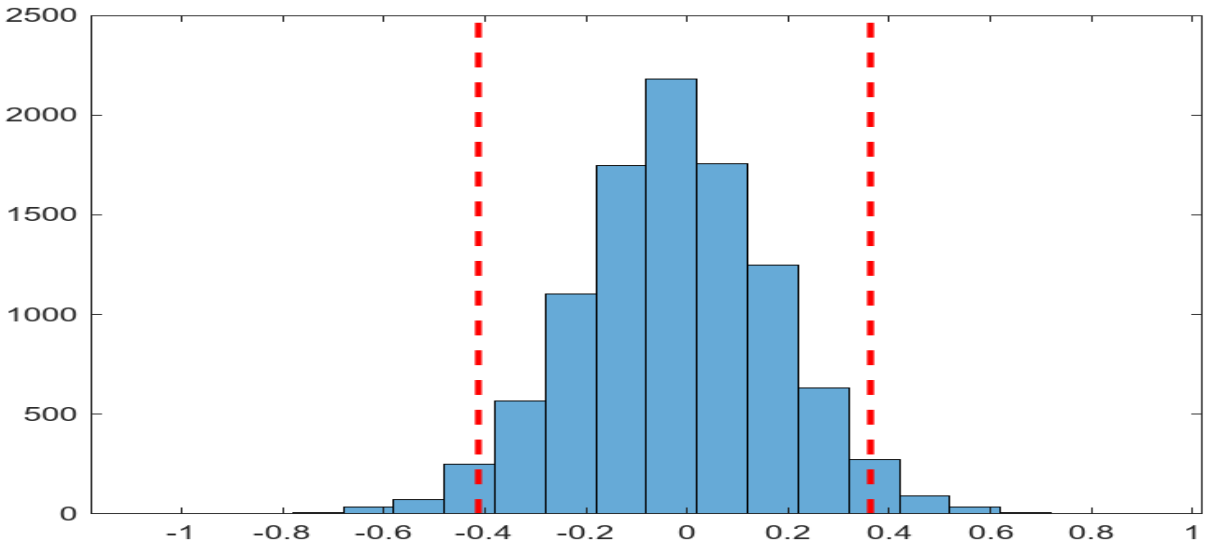

Figure 4. 22: Histogram of the Estimated Marginal Posterior Density of Tree 182 $(\boldsymbol{u_1})$

Figure 4.22 shows the histogram of the estimated marginal posterior density for the growth index for tree 182 $(\boldsymbol{u_1})$ using Gibbs sampling. The estimated marginal posterior density for tree 182 is symmetrical with mean = -0.023537 cm. From Figure 4.22, 95% equal tails credibility interval is given by [-0.412911 ; 0.362914] which contains zero. This indicates that there is no significant difference between the average growth of tree 182, and the average growth of the remaining 24 trees planted on plot 9.

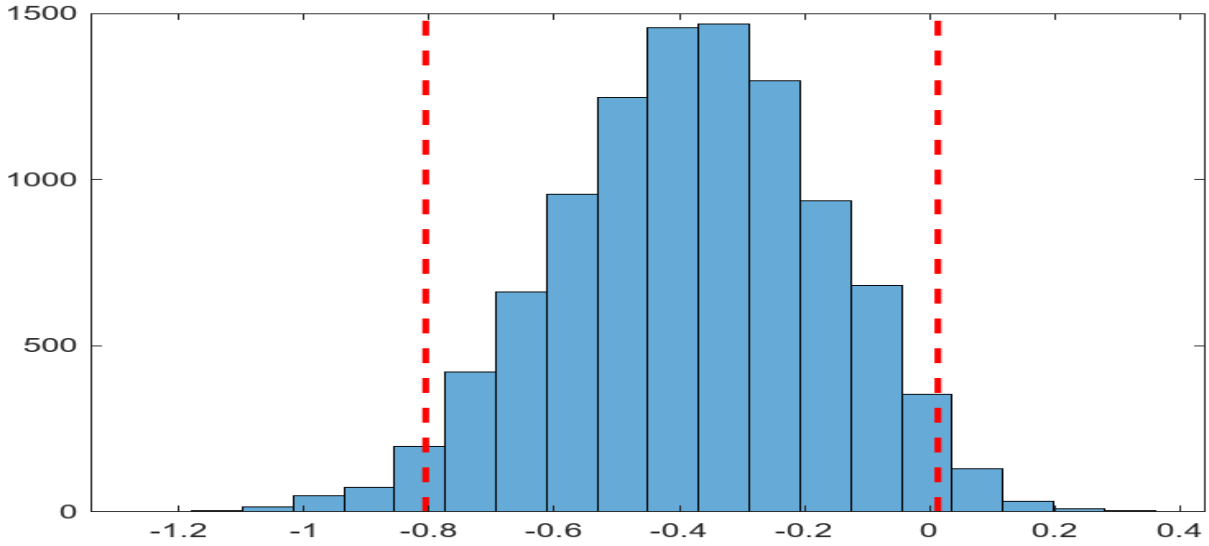

Figure 4. 23: Histogram of the Estimated Marginal Posterior Density of Tree 184 $(\boldsymbol{u_2})$

Figure 4.23 indicates the histogram of the estimated marginal posterior density for the growth index for tree 184 $(\boldsymbol{u_2})$ using Gibbs sampling. It can be seen that the estimated marginal posterior density of tree 184 is symmetrical with mean = -0.37951 cm and 95% equal tails credibility interval given by [-0.805306 ; 0.013159]. Zero is also contained in the interval. This indicates that there is no significant difference between the average growth of tree 184, and the average growth of the remaining 24 trees planted on plot 9. By considering the 90% equal tails credibility interval however given by [-0.749233 ; -0.038062], it can be seen that zero does not fall within this interval, thus indicating that a significant difference exists between the average growth of tree 184 and the average growth of the remaining 24 trees planted on plot 9, at a 90% credibility level. Since both the lower and upper 90% equal tails credibility limits are negative, it can be seen that the average growth of tree 184 is significantly less than the average growth of the remaining 24 trees planted on plot 9.

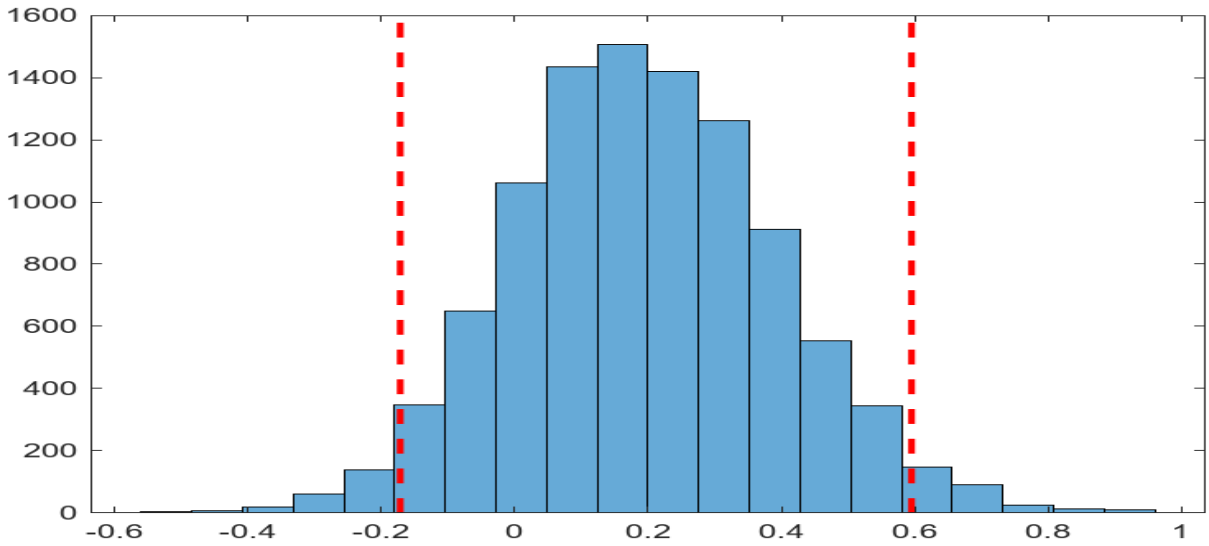

Figure 4. 24: Histogram of the Estimated Marginal Posterior Density of Tree 214 $(\mathbf{u_3})$

Figure 4.24 shows the histogram of the estimated marginal posterior density for the growth index for tree 214 $(\boldsymbol{u_3})$ using Gibbs sampling and estimated marginal posterior density for tree 214 is symmetrical with mean = 0.19531 cm and 95% equal tails credibility interval is given by [-0.171639 ; 0.595046]. It can also be seen that zero is contained in the interval which indicates that there is no significant difference between the average growth of tree 182, and the average growth of the remaining 24 trees planted on plot 9.

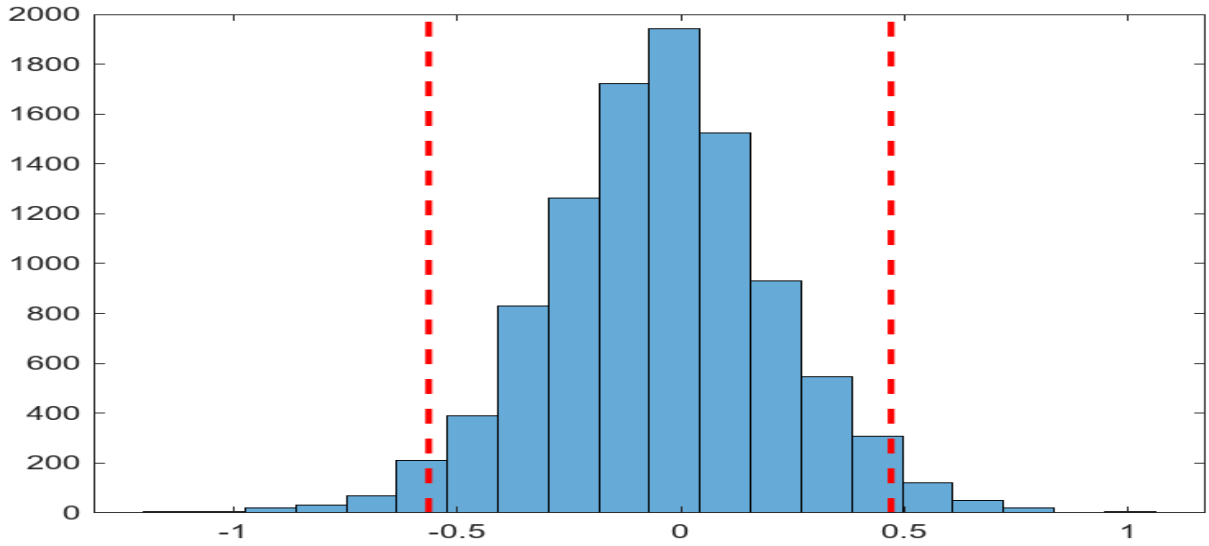

Figure 4. 25: Histogram of the Estimated Marginal Posterior Density of Tree 216 $(\boldsymbol{u_4})$

Figure 4.25 indicates the histogram of the estimated marginal posterior density for the growth index for tree 216 ($\boldsymbol{u_4}$) using Gibbs sampling and estimated marginal posterior density for tree 216 is symmetrical with mean = -0.045552 cm and 95% equal tails credibility interval is given by [-0.563765 ; 0.469610]. Zero is contained in the interval which indicates that there is no significant difference between the average growth of tree 182, and the average growth of the remaining 24 trees planted on plot 9.

4.8.4 Unconditional or Marginal Posterior Distributions of the Random Effects

Also, in this section the unconditional or marginal posterior densities of the random effects are determined using the Rao-Blackwell method mentioned in section 4.6.2. These marginal posterior distributions of the random effects (tree effects) are depicted in Figures 4.26 – 4.29. From Figures 4.22 – 4.25, as well as Figures 4.26 – 4.29, it can be seen that the unconditional or marginal posterior densities correspond well with the histograms of the estimated marginal posterior densities of the random or tree effects, thus indicating that both methods can be used in order to obtain the estimated marginal posterior distributions. This is also evident from the means and 95% equal tails credibility intervals.

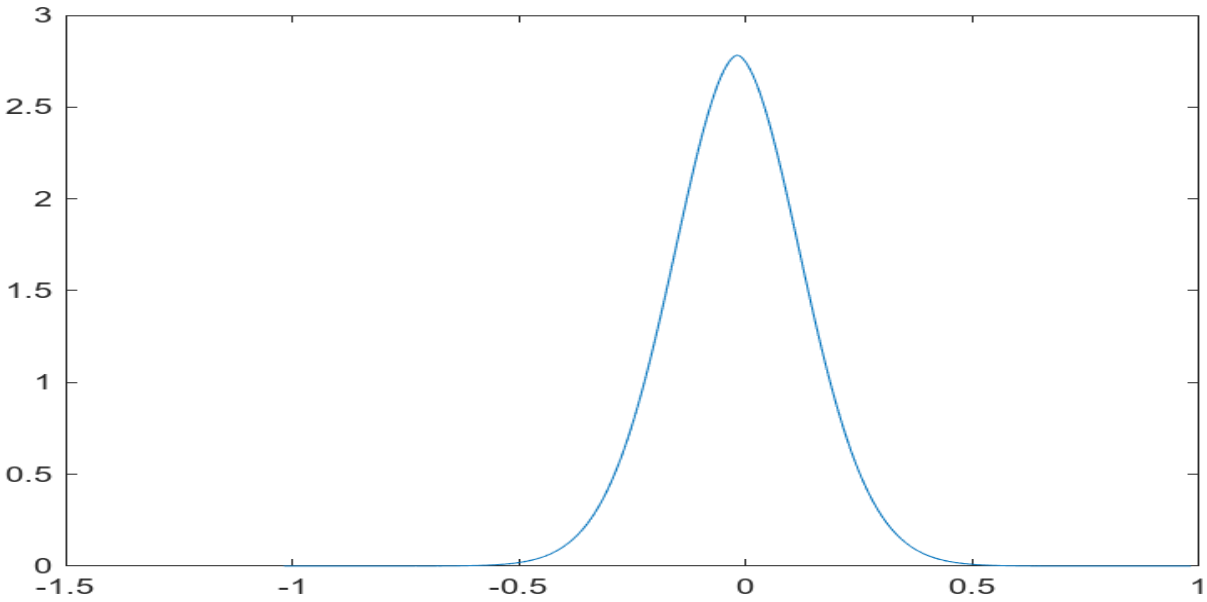

Figure 4. 26: Estimated Marginal Posterior Density of Tree 182 ($\boldsymbol{u_1}$)

Figure 4.26 shows an unconditional or estimated marginal posterior density of tree 182 determined using Rao-Blackwell method, when it was assumed that there is

competition between the trees in plot 9. The unconditional or estimated marginal posterior density of tree 182 is symmetrical with mean = -0.023537 cm and 95% equal tails credibility interval given by [-0.4372 ; 0.3105]. It can be seen that the interval corresponds with histogram of the estimated marginal posterior density of tree 182. The same conclusion can therefore be reached as in the corresponding histogram given in Figure 4.22.

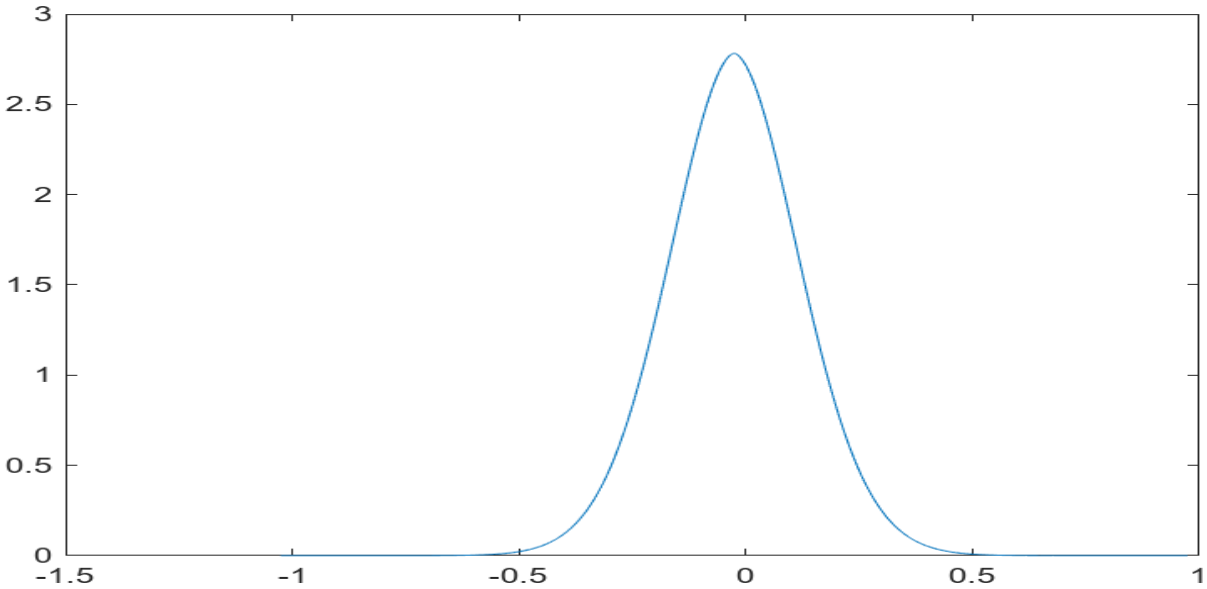

Figure 4. 27: Estimated Marginal Posterior Density of Tree 184 (u_2)

Figure 4.27 illustrates the unconditional or estimated marginal posterior density of tree 182 determined using the Rao-Blackwell method, when it was assumed that there is competition between the trees in plot 9. The mean value of the density is -0.3774 cm, with a 95% equal tails credibility interval given by [-0.8088 ; 0.0191]. This interval corresponds to the histogram representing the estimated marginal posterior density of tree 184. By considering the 90% equal tails credibility interval given by [-0.961553, -0.6700073]. It can be seen that zero does not fall within the interval. The same conclusion can therefore be reached as in the corresponding histogram given in Figure 4.23.

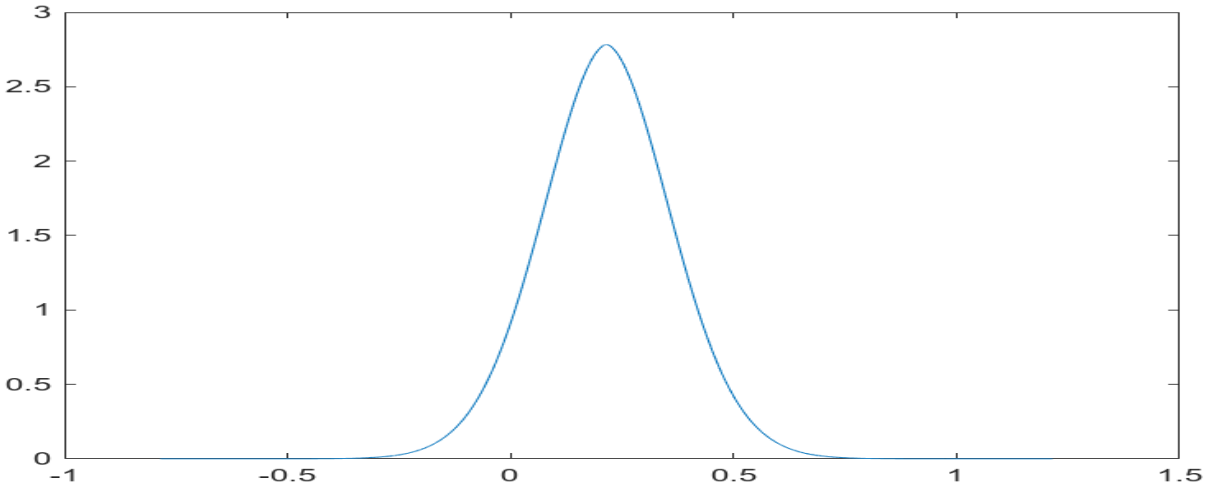

Figure 4. 28: Estimated Marginal Posterior Density of Tree 214 (u_3)

In Figure 4.28, the unconditional marginal posterior density for tree 214, estimated using the Rao-Blackwell method, is displayed, when it was assumed that there is competition between the trees in plot 9. This density is symmetric, with a mean = 0.17428 cm and a 95% equal tails credibility interval given by [-0.19998 ; 0.556]. This interval aligns with the histogram of the estimated marginal posterior density for tree 214. The same conclusion can therefore be reached as in the corresponding histogram given in Figure 4.24.

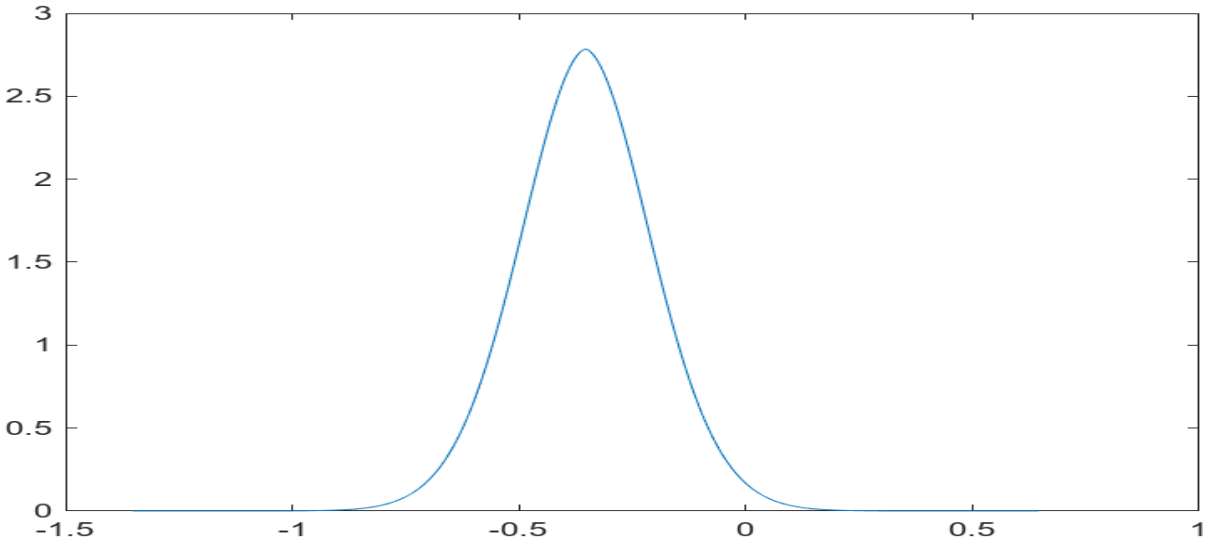

Figure 4. 29: Estimated Marginal Posterior Density of Tree 216 (u_4)

Figure 4.29 presents the unconditional marginal posterior density of tree 216, determined through the Rao-Blackwell method, when it was assumed that there is

competition between the trees in plot 9. It can be seen that the density of tree 216 symmetry and has a mean = -0.0017 cm, along with a 95% equal tails credibility interval given by [-0.4671 ; 0.4939]. Remarkably, this interval matches the histogram of the estimated marginal posterior density for tree 216. The same conclusion can therefore be reached as in the corresponding histogram given in Figure 4.25.

4.8.5 Marginal Posterior Distributions of the Fixed Effects

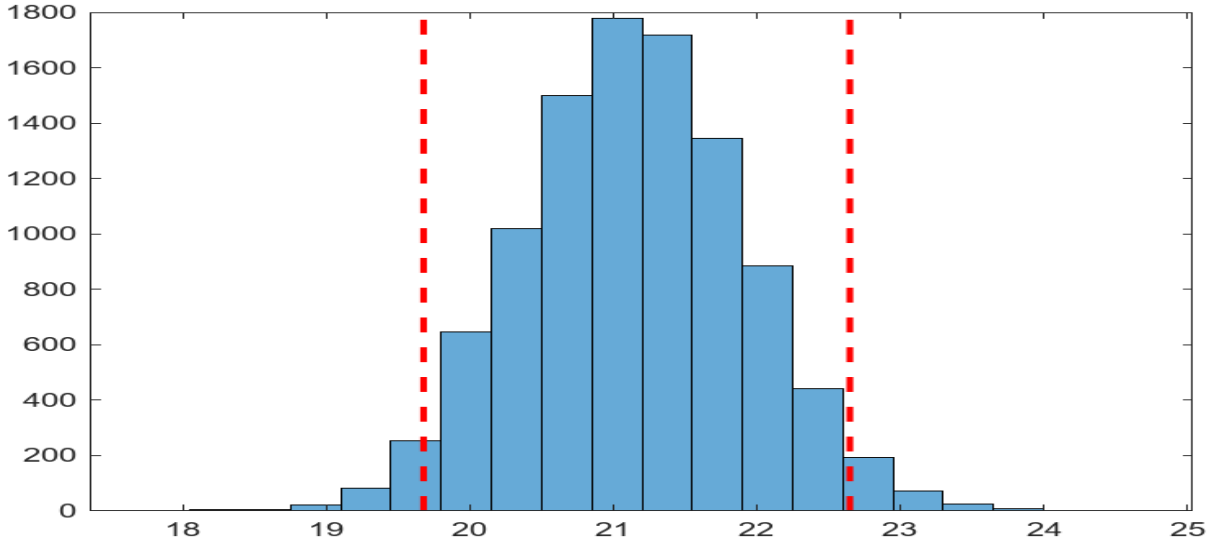

Figure 4. 30: Histogram of the Estimated Marginal Posterior Density of β_0

Figure 4.30 represents the estimated marginal posterior density of β_0, i.e., the average observed growth rate of trees growing in growth period 2-3, with 4 normal growing trees growing around these trees and where the trees themselves, are not suppressed. For these trees however, competition was assumed and determined using the Lorimer Competition Index as discussed earlier. From Figure 4.30 it can be seen that the histogram of the estimated marginal posterior density of β_0 is for all practical purposes symmetrical. Assuming competition as determined using the Lorimer Competition Index, the average growth rate for these trees growing with a combination of the mentioned base levels, is 21.135 cm with a 95% equal tails credibility interval given by [19.677431 ; 22.649052]. Since, as mentioned, competition will only set in after period 2-3, the histogram of the estimated marginal posterior density of β_0, assuming competition between the trees, and the histogram of the estimated marginal posterior density of β_0, assuming no competition between the trees

depicted in Figure 4.12, should for all practical purposes be the same. The same apply to the posterior means and 95% equal tails credibility intervals.

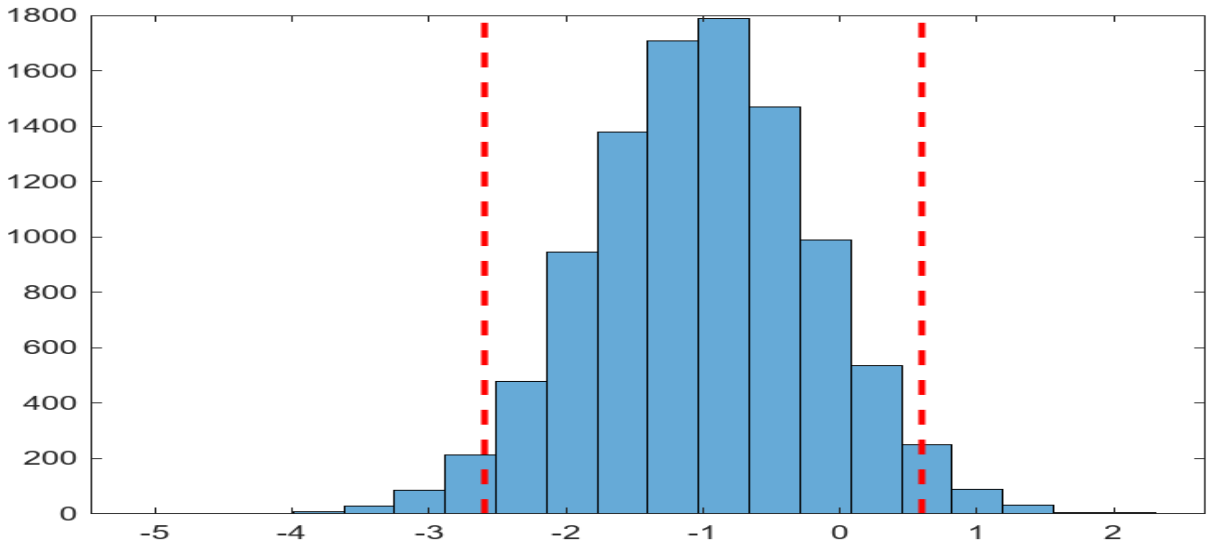

Figure 4. 31: Histogram of the Estimated Marginal Posterior Density of β_1

Figure 4.31 represents the histogram of the estimated marginal posterior density of β_1. β_1 represents the expected difference in the average amount of growth observed of the selected group of trees during growth period 3-4, and the average observed amount of growth of the trees growing under the mentioned base level conditions. For these trees however, competition was assumed and determined using the Lorimer Competition Index as discussed earlier. From figure 4.31 it is therefore evident that the average growth observed during growth period 3-4, differ significantly from the average amount of growth observed for trees growing under base level conditions, since the 95% equal tails credibility interval given by [-12.648124 ; -11.241807], does not contain zero. The mean difference in the amount of growth observed, was -11.9509 cm.

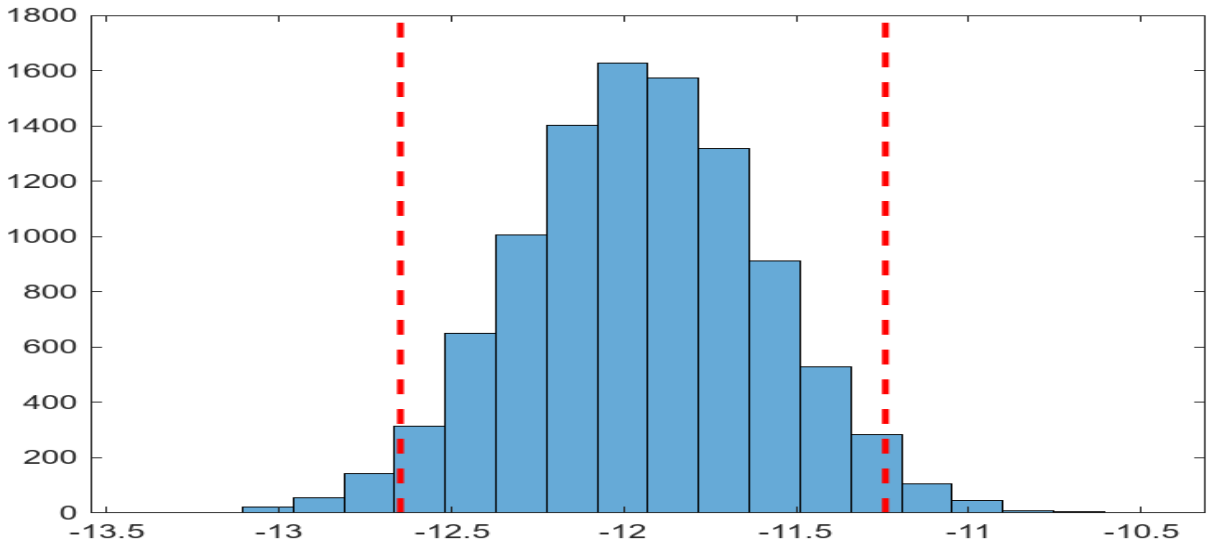

Figure 4. 32: Histogram of the Estimated Marginal Posterior Density of β_8

Figure 4.32 represents the histogram of the estimated marginal posterior density of β_8. β_8 represents the expected difference in the average amount of growth observed between a tree with 5 normal growing trees around it, , and the average amount of growth observed of trees growing under a combination of the mentioned base levels, assuming competition exist between the trees determined using the Lorimer Competition Index. From Figure 4.32 it is therefore evident that the average growth observed between a tree with 5 normal growing trees around it, is not significantly different from the average amount of growth observed for trees growing under base level conditions, since the 95% equal tails credibility interval given by [-2.594020 ; 0.598519], contains zero. The mean difference in the amount of growth observed, was -0.99699 cm.

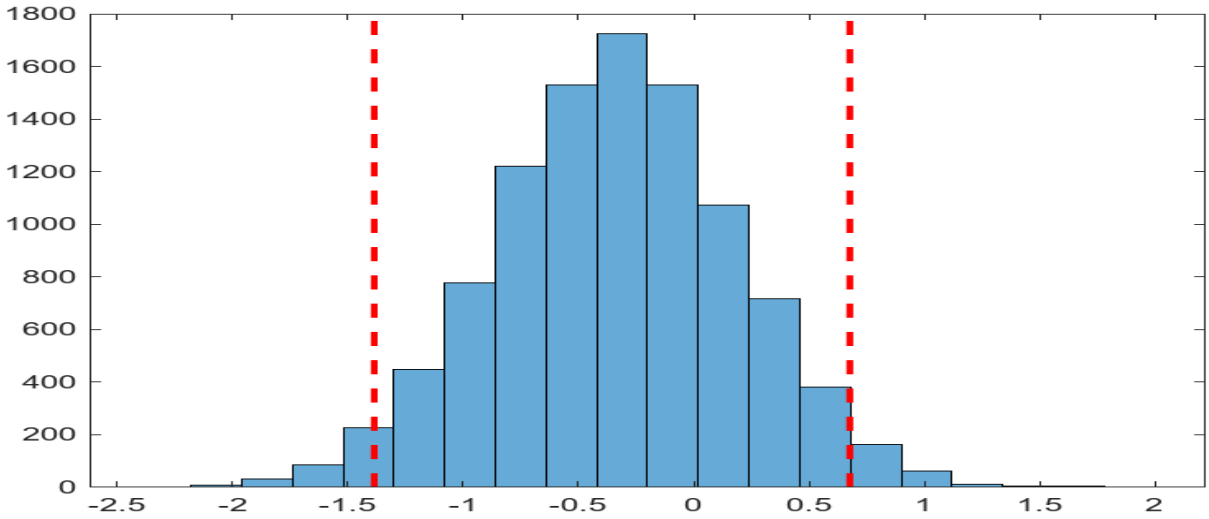

Figure 4. 33: Histogram of the Estimated Marginal Posterior Density of β_{12}

Figure 4.33 represents the histogram of the estimated marginal posterior density of β_{12}. β_{12} represents the difference in the average amount of growth observed between suppressed trees and trees growing under a combination of base levels, assuming competition exist between the trees determined using the Lorimer Competition Index. From figure 4.33 it is therefore evident that the average growth observed between suppressed trees, is not significantly different from the average amount of growth observed for trees growing under base level conditions, since the 95% equal tails credibility interval given by [-1.385304 ; 0.676956], contains zero. The mean difference in the amount of growth observed, was -0.33412 cm. This is to be expected, since, in order for a suppressed tree to have a DBH measurement, that tree must have reached at least breast height before it was suppressed. Also, period 2-3 represented the first period when all the trees on the plot had reached breast height. During period 1-2, some of the trees had not reached breast height, and as a result, do not have a DBH measurement. The histogram of the marginal posterior density of β_{12} therefore represents a comparison between the average observed growth of suppressed trees at breast height, and the average observed growth of trees that just reached breast height.

Table 4. 6: Estimated Values of Fixed Effects as well as the 95% Equal Tails Credibility Interval

Fixed Effects	Mean Difference in Observed Growth (cm)	95% Equal Tails Credibility Intervals (cm)
β_0	21.135	[19.677431 ; 22.649052]
β_1	-11.9509	[-12.648124 ; -11.241807]*
β_2	-15.8421	[-16.5523383 ; -15.148929]*
β_3	-17.7339	[-18.414096 ; -17.038416]*
β_4	-18.2439	[-18.943620 ; -17.570297]*
β_5	-17.8296	[-18.514906 ; -17.121045]*
β_6	-17.9217	[-18.606639 ; -17.208063]*
β_7	-18.9042	[-19.589742 ; -18.207729]*
β_8	-0.99699	[-2.594020 ; 0.598519]
β_9	-0.92219	[-2.437054 ; 0.579704]
β_{10}	-1.6821	[-3.196667 ; -0.203545]*
β_{11}	-1.5198	[-2.944861 ; -0.141670]*
β_{12}	-0.33412	[-1.385304 ; 0.676956]

* Indicate that a significant difference exists, since zero is not contained within the 95% equal tails credibility interval.

In Table 4.6 the posterior means and 95% equal tails credibility intervals of all fixed effects are provided assuming that there exists competition between the trees note that a negative posterior mean does not indicate that a tree is in fact thinner than during a previous growth period, it represents the difference in the observed growth between a specific growth period and the base level growth period. Therefore, for example, during the base level period, the average growth (increase in circumference from the first year of growth to the second year of growth) measured in cm, was 17.3919 cm. During the following year (growth period 3-4), the average increase in diameter of the tress, was only 6.4214 cm. Although the diameter of the trees was higher during growth period 3-4, the average increase in diameter was less than during the base level period (period 2-3). The average increase in circumference, or observed growth, is therefore compared, and not the actual average circumference of the trees during these periods.

4.8.6 Probability Distribution of the Rank Positions for trees 182, 184, 214 and 216 located on Plot 9

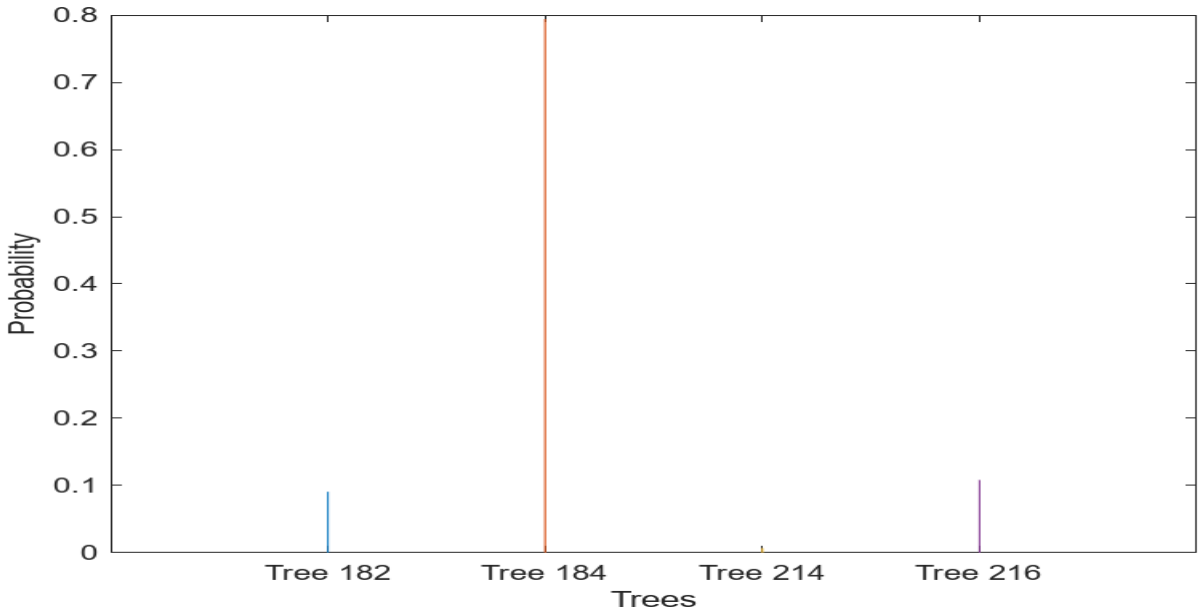

Figure 4. 34: Probability of the Weakest Grower of the Group Selected

From Figure 4.34, it can be seen that tree 184 has the highest probability of being the weakest grower of the group of 4 selected target trees located on plot 9, with a probability of being the weakest grower, given by 0.7867 cm. This confirms the findings

obtained in both Figures 4.23 and 4.27, since tree 184 had the lowest mean growth and the 95% equal tails credibility interval almost did not contain zero. By considering the 90% equal tails credibility interval given by [-0.171639, 0.595046] obtained for tree 184, it can be seen that this credibility interval does not contain zero, indicating that tree 184 has significantly weaker growth than the 3 other target trees located on plot 9.

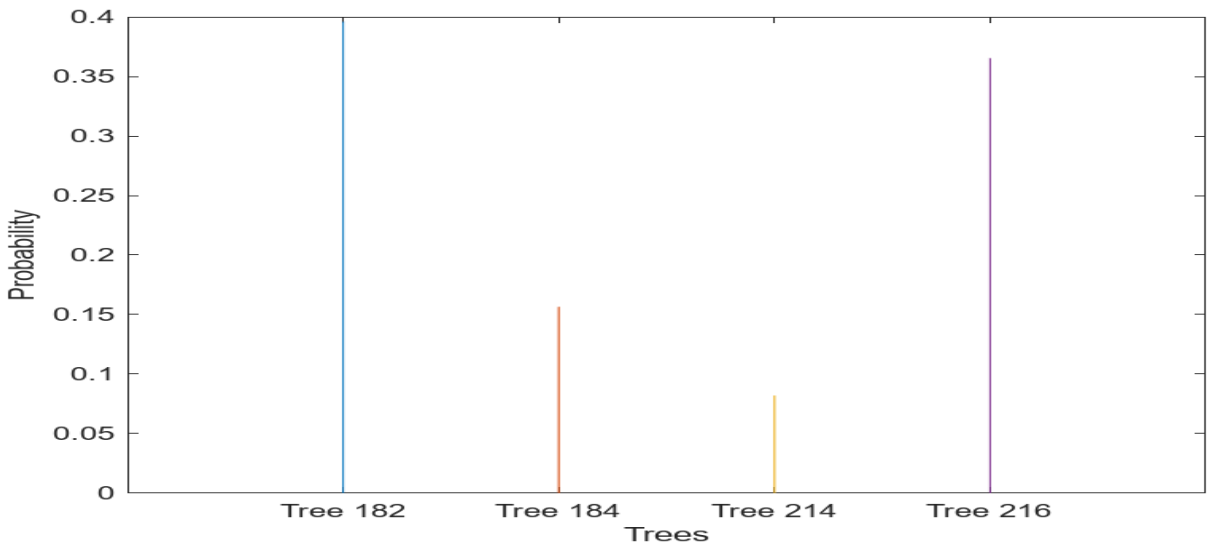

Figure 4. 35: Probability of the Second Weakest Grower of the Group Selected

Figure 4.35 depicts that tree 182 has the highest probability of being the second weakest grower of the group of 4 selected target trees located on plot 9, with a probability of being the second weakest grower, given by 0.396 cm. This confirms the findings obtained in both Figures 4.22 and 4.26, since tree 182 had the second lowest mean growth. By considering the 95% equal tails credibility interval given by [-0.412911, 0.362914] obtained for tree 182, it can be seen that this credibility interval contains zero. This indicates that, although tree 182 had the second weakest growth rate, the growth rate for tree 182 did not differ significantly from the growth rates of the other 2 target or subject trees (i.e., tree 184 and 216). By considering Figures 4.22 – 4.29, also note the position of zero within this 95% equal tails credibility interval relative to the positions of zero within the other 95% equal tails credibility intervals for the remaining target or subject trees (i.e., trees 184 and 216). This confirms the probability obtained for tree 182 indicated in Figure 4.35.

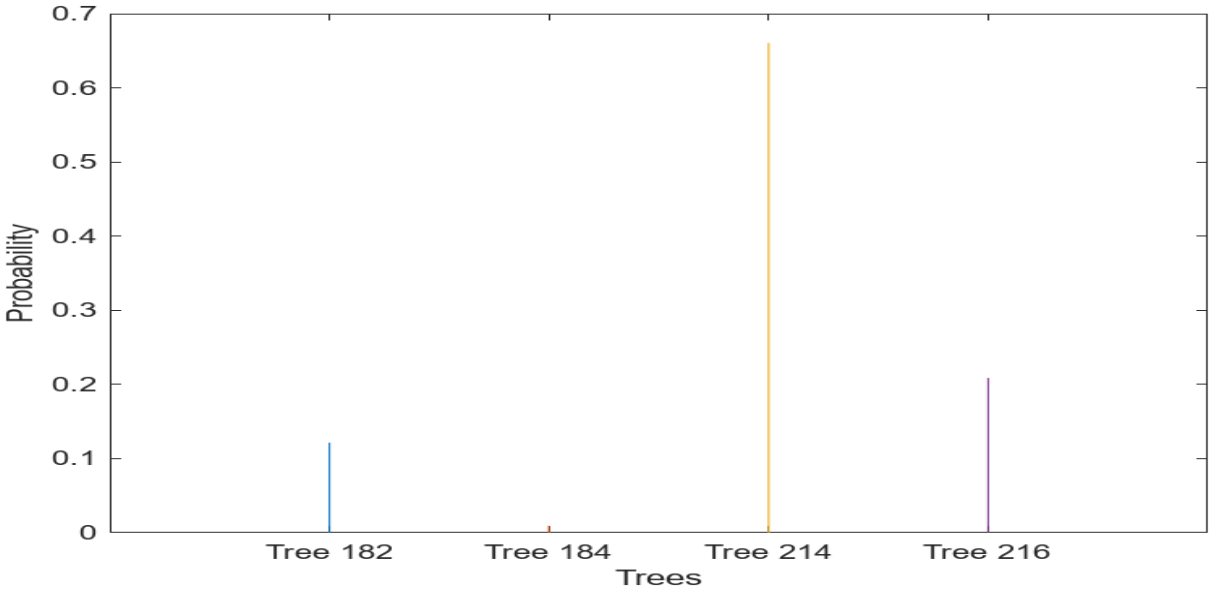

Figure 4. 36: Probability of the Strongest Grower of the Group Selected

Figure 4.36 indicates that tree 214 has the highest probability of being the strongest grower of the group of 4 selected target trees located on plot 9, with a probability of being the strongest grower, given by 0.6671 cm. This confirms the findings obtained in both Figures 4.24 and 4.28, since tree 214 had the highest mean growth. By considering the 95% equal tails credibility interval given by [-0.155962, 0.606178], obtained for tree 214, it can be seen that this credibility interval however contains zero. By considering Figures 4.22 – 4.29, also note the position of zero within this 95% equal tails credibility interval relative to the positions of zero within the other 95% equal tails credibility intervals for the remaining target or subject trees (i.e., trees 182 and 216). This confirms the probability obtained for tree 214 indicated in Figure 4.36.

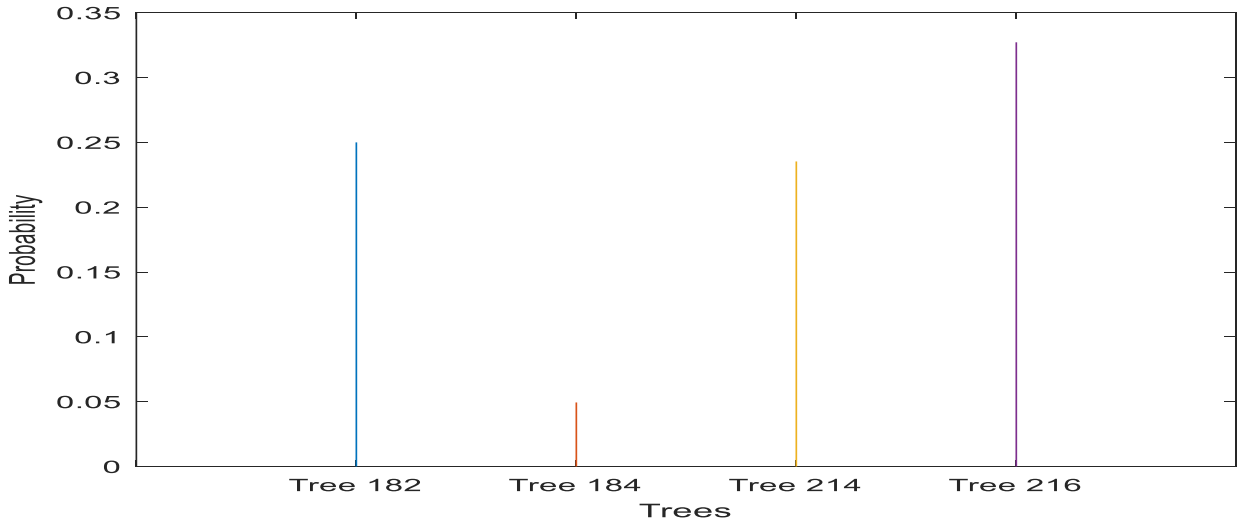

Figure 4. 37: Probability of the Second Strongest Grower of the Group Selected

From Figure 4.37 it can be seen that tree 216 has the highest probability of being the second strongest grower of the group of 4 selected target trees located on plot 9, with a probability of being the second strongest grower, given by 0.3272 cm. Figure 4.37 confirms the findings obtained in both Figures 4.25 and 4.29, since tree 216 had the second highest mean growth. By considering the 95% equal tails credibility interval given by [-0.563765, 0.469610] obtained for tree 216, it can be seen that this credibility interval however contains zero. By considering Figures 4.22– 4.29, also note the position of zero within this 95% equal tails credibility interval relative to the positions of zero within the other 95% equal tails credibility intervals for the remaining target or subject trees (i.e., trees 182 and 214). This confirms the probability obtained for tree 216 indicated in Figure 4.37.

CHAPTER 5

CONCLUSION AND RECOMMENDATIONS

5.1 Discussion and Conclusion

The conclusion, suggestions and topics for additional research are all covered in this chapter. The aim of the study was to evaluate individual tree growth present in eucalyptus plantations measured as a function of the amount of observed growth during a particular growth period, as well as individual competition that may be present during the mentioned growth periods. To determine the marginal posterior distributions of unknown parameters, and to provide an estimated growth coefficient of selected target or subject trees on a plot, a Bayesian re-purposed mixed effect variance component model, known as the Sire-Model in animal breeding problems was employed. The findings of this contribute significantly towards the advancement of Bayesian estimating techniques for actual tree competition issues observed in plantations.

In this study, the marginal posterior distributions of unknown variance components and fixed effects could easily be determined using the mentioned re-purposed Bayesian mixed effect variance component model known as the sire model, as originally proposed by Kepe et.al. (2019). It was also shown that the same model could be utilized in order to estimate marginal posterior distributions of growth indexes for specific target or subject trees in cases where no competition was assumed, as well as in cases where competition was assumed and determined using a non-spatial competition index, such as the Lorimer Index (1983). As a result, a complete Bayesian solution to a real-world problem, was provided. The study has shown that a straightforward and effective framework for calculating these distributions is provided by the Gibbs sampler, which is an adaptive Monte Carlo method. In this study it was also demonstrated that, in addition to the estimation of individual tree growth indices, probability statements about the growth of specific individual trees, were in fact also possible.

For the study, a eucalyptus tree stand was randomly selected with a planting density equivalent to 1959 stems planted per hectare. It must be noted here that the actual plot selected for the study, did not contain 1959 stems, it just had the same planting density as a plot with 1959 stems per hectare. In fact, the plot selected at random, only had 256 Eucalyptus hybrid clones planted on the plot, and these trees were for all practical purposes, subjected to the same environmental conditions. During the first phase of the study, growth was measured as the diameter at breast height. The average observed DBH was then determined and then plotted for the different growth periods, which ranged from year 1 (period 1-2) to year 9 (period 9-10). From Figure 4.1, it could then be seen that during the first two growth period, trees were growing fast until canopy closure, which for this plot, occurred at the end of growth period 2-3. This observation was confirmed by literature. For more information, see Morley et al. (2008). After canopy closure, a significant reduction in the amount of growth could however be observed, suggestion that competition between individual trees may, have started to set in.

Utilizing the re-purpose Bayesian mixed linear model and the Gibbs sampler, followed the initial phase of the study. Results from the Bayesian analysis was initially obtained assuming no competition between the individual trees. These results indicated that marginal posterior distributions of variance components and growth indices for individual target or subject trees could be determined, and that probability statements about individual subject trees could be made. It must be mentioned here that results obtained, were consistent with what was observed on the actual plot and also with what was expected, thus suggesting that the re-purposed Bayesian mixed effects model can be used as part of an investigation into individual tree growth.

The Bayesian analysis was then repeated assuming competition between individual trees. For this analysis, a non-spatial competition index known as the Lorimer index (1983), was used in the determination of the numerator relationship matrix A. Although results from this study was slightly different from the results obtained assuming no competition, the result were still consistent with what was observed and expected on the plot. It must be noted however that when competition was assumed, differences, especially in probability statements about individual target or subject trees, were more

clearly visible, thus suggestion that individual tree competition should be included as part of such an analysis. Posterior means obtained from the marginal posterior densities of the growth indices for individual subject or target trees, were also consistent with probability statements made about these trees. The Bayesian framework, and specifically the re-purposed sire model, allows specifically for the inclusion of these types of non-spatial or distance independent individual tree competition.

Using the Bayesian re-purposed sire model, marginal posterior densities of fixed effects could also easily be determined. From the results obtained assuming both no competition between individual trees, and competition between individual trees, it can be concluded that the average difference in growth observed from one period to the next, was significantly different from the average growth observed for trees growing with reference to base level conditions, and therefore specifically during the base level period. this suggests that the differences in the average growth observed after canopy closure, was significantly less than the average growth observed before canopy closure. This can be concluded since the 95% equal tails credibility intervals of the marginal posterior densities for $\beta_1, \dots, \beta_7$ did not contain zero.

Similar to the above, it can also be seen from the estimated marginal posterior densities of the fixed effects related to the number of normal growing trees that grow around a specific subject tree or target tree, i.e., the estimated marginal posterior densities of $\beta_8, \dots, \beta_{11}$, that significant differences existed between the average growth observed for trees with both 7 and 8 normal trees growing around a specific target or subject tree, and the average growth observed for trees growing with reference to the base level conditions (average observed growth was significantly less in both cases). This can be concluded, since the 95% equal tails credibility intervals for both the estimated marginal posterior densities of β_{10} and β_{11}, did not contain zero. No significant differences were however observed between the average growth observed for trees with 5 and 6 normal trees growing around a specific subject or target tree, and the average growth observed of tree growing with reference to base level conditions, i.e., 4 normal trees growing around a specific subject tree or target tree, since zero is contained within the 95% equal tails credibility intervals for both the

estimated marginal posterior densities of β_8 and β_9. This suggests that the optimal number of normal growing trees, growing around a specific subject tree or target tree, planted on a plot with a planting density of 1959 stems per hectare, is less than 7.

From Figure 4.15 it could also be concluded that the average growth observed between suppressed trees, is not significantly different from the average amount of growth observed for trees growing under base level conditions, since the 95% equal tails credibility interval contained zero. As mentioned earlier, this was to be expected, since, in order for a suppressed tree to have a DBH measurement, that tree must have reached at least breast height before it was suppressed. Also, the difference in growth measured during growth period 2-3, represented the difference in growth for the first period when all the trees on the plot had reached breast height.

The overall results of this study therefore provided a better understanding of observed differences in growth, subject to distance independent individual tree competition in eucalyptus stands/plantations.

5.2 Recommendations for Future Research

For future research, it is therefore recommended that more fixed effects be considered. These would include different planting densities, weeding of plots (removing weeds between the growing trees) and burning plots before new stems are planted on a plot. Distance dependent competition indices may also be considered. Since the findings from this study are intended to enhance awareness and understanding of the competition that exists among trees, it is therefore hoped that results from this study will assist to facilitate plantations like those found in the Kwa-Zulu Natal Midlands, in improving their mitigation strategies in order to improve yield on these plantations for a sustainable future.

REFERENCES

Albaugh, J.M., Dye, P.J. and King, J.S., 2013. Eucalyptus and water use in South Africa. International Journal of Forestry Research, 2013 pp.1-11.

Baayen, R.H., 2012. Mixed-effects models. The Oxford handbook of laboratory phonology, pp.668-677.

Batish, D.R., Singh, H.P., Kohli, R.K. and Kaur, S., 2008. Eucalyptus essential oil as a natural pesticide. Forest Ecology and Management, 256(12), pp.2166-2174.

Bayle, G.K., 2019. Ecological and social impacts of eucalyptus tree plantation on the environment. Journal of Biodiversity Conservation and Bioresource Management, 5(1), pp.93-104.

Berger, U., Piou, C., Schiffers, K. and Grimm, V., 2008. Competition among plants: concepts, individual-based modelling approaches, and a proposal for a future research strategy. Perspectives in Plant Ecology, Evolution and Systematics, 9(3-4), pp.121-135.

Bhandari, S.K., Veneklaas, E.J., McCaw, L., Mazanec, R. and Renton, M., 2021. Investigating the effect of neighbour competition on individual tree growth in thinned and unthinned eucalypt forests. Forest Ecology and Management, 499, pp.119637.

Bhandari, S.K., Veneklaas, E.J., McCaw, L., Mazanec, R., Whitford, K. and Renton, M., 2021. Individual tree growth in jarrah (Eucalyptus marginata) forest is explained by size and distance of neighbouring trees in thinned and non-thinned plots. Forest Ecology and Management, 494, pp.119364.

Box, G.E. and Tiao, G.C., 1973. Some comments on “Bayes” estimators. *The American Statistician*, *27*(1), pp.12-14.

Brooks, S., 1998. Markov chain Monte Carlo method and its application. Journal of the Royal Statistical Society: series D (the Statistician), 47(1), pp.69-100.

Chu, S., Ouyang, J., Liao, D., Zhou, Y., Liu, S., Shen, D., Wei, X. and Zeng, S., 2019. Effects of enriched planting of native tree species on surface water flow, sediment, and nutrient losses in a Eucalyptus plantation forest in southern China. Science of the Total Environment, 675, pp.224-234.

Contreras, M.A., Affleck, D. and Chung, W., 2011. Evaluating tree competition indices as predictors of basal area increment in western Montana forests. Forest Ecology and Management, 262(11), pp.1939-1949.

Curto, R.D.A., de Mattos, P.P., Braz, E.M., Canetti, A. and Netto, S.P., 2020. Effectiveness of competition indices for understanding growth in an overstocked stand. Forest Ecology and Management, 477, pp.118472.

Dale, V.H., Doyle, T.W. and Shugart, H.H., 1985. A comparison of tree growth models. Ecological Modelling, 29(1-4), pp.145-169.

de Oliveira, E.K.B., Rezende, A.V., Mazzei, L., Júnior, L.S.M., Castro, R.V.O., d'Oliveira, M.V.N. and Barros, Q.S., 2021. Competition indices after reduced impact logging in the Brazilian Amazon. Journal of Environmental Management, 281, p.111898.

Dong, L., Pukkala, T., Li, F. and Jin, X., 2021. Developing distance-dependent growth models from irregularly measured sample plot data–A case for Larix olgensis in Northeast China. Forest Ecology and Management, 486, pp.118965.

Dunson, D.B., 2001. Commentary: practical advantages of Bayesian analysis of epidemiologic data. American journal of Epidemiology, 153(12), pp.1222-1226.

Eaves, L., Erkanli, A., Silberg, J., Angold, A., Maes, H.H. and Foley, D., 2005. Application of Bayesian inference using Gibbs sampling to item-response theory modelling of multi-symptom genetic data. Behavior Genetics, 35(6), pp.765-780.

Gearhart, C. and Kasturiratna, D., 2018. Implementation of Gibbs sampling within Bayesian inference and its applications in actuarial science. SIAM Journal, pp.219-231.

Gelfand, A.E., 2000. Gibbs sampling. Journal of the American Statistical Association, 95(452), pp.1300-1304.

Gelfand, A.E. and Smith, A.F., 1990. Sampling-based approaches to calculating marginal densities. *Journal of the American statistical association*, *85*(410), pp.398-409.

Gelman, A., Carlin, J.B., Stern, H.S., Dunson, D.B., Vehtari, A. and Rubin, D.B., 2014. Bayesian data analysis. 3rd edition. CRC press Taylor and Francis Group. Boca Raton, USA. pp.1-4.

Glickman, M.E. and Van Dyk, D.A., 2007. Basic Bayesian methods. Topics in Biostatistics, pp.319-338.

Hastings, W., 1970. Monte Carlo sampling methods using Markov chains and their applications. Biometrika, 57(1), pp.97-109.

https://cdn.britannica.com/25/196825-050-E354355B/Eucalyptus-trees-plantation-Australia.jpg

https://images.mapsofworld.com/south-africa/south-africa-political-map.jpg

Hugo, J., 1998. A Bayesian Statistical Evaluation of the Elsenburg Dormer Stud Using a Sire Model (Master's dissertation, University of the Orange Free State).

İlseven, S. and Baştaş, M., 2018. The place of eucalyptus within the vegetation of Mesaoria plain (Cyprus) and the views of vegetation geography lecturers. EURASIA Journal of Mathematics, Science and Technology Education, 14(7), pp.3381-3388.

Kahriman, A., Şahin, A., Sönmez, T. and Yavuz, M., 2018. A novel approach to selecting a competition index: the effect of competition on individual-tree diameter growth of Calabrian pine. Canadian Journal of Forest Research, 48(10), pp.1217-1226.

Kepe, L., Little, K. and Hugo, J., 2019. An Investigation into Tree Growth Modelling. A Bayesian Approach. Programme and Abstracts. 61st Annual Conference of the South African Statistical Association, Nelson Mandela University, Port Elizabeth, South Africa, 25 – 29 November, 2019, p32. https://drive.google.com/file/d/1kJDnYhFV4et9EIaBbM1P-GJCi63-hMFN/view?hl=en_GB&pli=1

King, G.B., Lovell, A.E., Neufcourt, L. and Nunes, F.M., 2019. Direct comparison between Bayesian and frequentist uncertainty quantification for nuclear reactions. Physical review letters, 122(23), pp.232502.

Linck, J.A. and Cunnings, I., 2015. The utility and application of mixed-effects models in second language research. Language Learning, 65(1), pp.185-207.

Luu, T.C., Binkley, D. and Stape, J.L., 2013. Neighbourhood uniformity increases growth of individual Eucalyptus trees. Forest Ecology and Management, 289, pp.90-97.

Maleki, K., Kiviste, A. and Korjus, H., 2015. Analysis of individual tree competition on diameter growth of silver birch in Estonia. Forest Systems, 24(2), p.1-3.

Martins, F.B., Soares, C.P.B. and Silva, G.F.D., 2014. Individual tree growth models for eucalyptus in northern Brazil. Scientia Agricola, 71, pp.212-225.

Mary, O.O. and Oluremi, A.P., 2019. Assessment of Some Inter-Tree Competition Measures for Predicting Individual Stem Volume of Tectona Grandis (Lin. F.) Stands in Ibadan, South Western Nigeria. International Journal of Research Studies in Science, Engineering and Technology 6(8), pp.19-27.

Melesse, S.F. and Zewotir, T., 2017. Variation in growth potential between hybrid clones of Eucalyptus trees in eastern South Africa. Journal of Forestry Research, 28(6), pp.1157-1167.

Mohammed, H.M. and Röhle, H., 2011. Studying the competition in natural stands of Acacia seyal Del. variety seyal. Forestry Ideas, 17(1), pp.34-44.

Morley, T. A., Little, K. M. and Rolando, C. A., 2008. Enhancing the benefits of stand management: Background to improved understanding of individual tree growth. ICFR Bulletin Series 11/2008. Institute for Commercial Forestry Research, Pietermaritzburg, South Africa.

Mugayi, E., 2019. Impacts of Eucalyptus plantation on soil physico-chemical properties in Bamunanika sub-county, Luwero district, Uganda (Doctoral dissertation, Makerere University).

Myburg, A.A., Grattapaglia, D., Tuskan, G.A., Hellsten, U., Hayes, R.D., Grimwood, J., Jenkins, J., Lindquist, E., Tice, H., Bauer, D. and Goodstein, D.M., 2014. The genome of Eucalyptus grandis. Nature, 510(7505), pp.356-362.

Nazir, N., Mir, A.H. and Khan, A.A., 2011. Bayesian analysis of mixed effect models and its applications in agriculture. Electronic Journal of Applied Statistical Analysis, 4(2), pp.164-171.

Orso, G.A., Mallmann, A.A., Pelissari, A.L., Behling, A., Figueiredo, A. and Machado, S.D.A., 2020. How competition indices behave at different neighbourhood coverages and modifications in a natural araucaria forest in Southern Brazil. Cerne, 26, pp.293-300.

Paine, T.D., Steinbauer, M.J. and Lawson, S.A., 2011. Native and exotic pests of Eucalyptus: a worldwide perspective. Annual Review of Entomology, 56, pp.181-201.

Peet, R.K. and Christensen, N.L., 1987. Competition and tree death. *Bioscience*, *37*(8), pp.586-595.

Peng, H. and Lu, Y., 2012. Model selection in linear mixed effect models. Journal of Multivariate Analysis, 109, pp.109-129.

Perry, D.A., 1985. The competition process in forest stands. In: Cannel, M.G.R. and Jackson, J.E. Attributes of trees as crop plants, pp.481-506. Institute of Terrestrial Ecology. Huntingdon, England. pp.481-506.

Qian, S.S., Stow, C.A. and Borsuk, M.E., 2003. On monte carlo methods for Bayesian inference. Ecological Modelling, 159(2-3), pp.269-277.

Quiñonez-Barraza, G., Zhao, D., Héctor, M. and Corral-Rivas, J.J., 2018. Considering neighbourhood effects improves individual DBH growth models for natural mixed-species forests in Mexico. Annals of Forest Science, 75(3), pp.1-11.

Rivas, J.C., González, J.Á., Aguirre, O. and Hernandez, F.J., 2005. The effect of competition on individual tree basal area growth in mature stands of Pinus cooperi Blanco in Durango (Mexico). European Journal of Forest Research, 124(2), pp.133-142.

Rouvinen, S. and Kuuluvainen, T., 1997. Structure and asymmetry of tree crowns in relation to local competition in a natural mature Scots pine forest. Canadian Journal of Forest Research, 27(6), pp.890-902.

Rubio, G., Walk, T., Ge, Z., Yan, X., Liao, H. and Lynch, J.P., 2001. Root gravitropism and below-ground competition among neighbouring plants: a modelling approach. Annals of Botany, 88(5), pp.929-940.

Rupp, A.A., Dey, D.K. and Zumbo, B.D., 2004. To Bayes or not to Bayes, from whether to when: Applications of Bayesian methodology to modelling. Structural Equation Modelling, 11(3), pp.424-451.

Sahney, S., Benton, M.J. and Ferry, P.A., 2010. Links between global taxonomic diversity, ecological diversity and the expansion of vertebrates on land. Biology Letters, 6(4), pp.544-547.

Sehlabana, M.A., 2020. Modelling malaria in the Limpopo Province, South Africa: comparison of classical and Bayesian methods of estimation (Master's dissertation, University of Limpopo).

Sumner, M.D., Wotherspoon, S.J. and Hindell, M.A., 2009. Bayesian estimation of animal movement from archival and satellite tags. PLoS One, 4(10), p.e7324.

Sun, C., Madsen, P., Nielsen, U.S., Zhang, Y., Lund, M.S. and Su, G., 2009. Comparison between a sire model and an animal model for genetic evaluation of fertility traits in Danish Holstein population. Journal of Dairy Science, 92(8), pp.4063-4071.

Sun, S., Cao, Q.V. and Cao, T., 2019. Evaluation of distance-independent competition indices in predicting tree survival and diameter growth. Canadian Journal of Forest Research, 49(5), pp.440-446.

van de Schoot, R., Depaoli, S., King, R., Kramer, B., Märtens, K., Tadesse, M.G., Vannucci, M., Gelman, A., Veen, D., Willemsen, J. and Yau, C., 2021. Bayesian statistics and modelling. Nature Reviews Methods Primers, 1(1), pp.1.

Vecchio, M.G., Loganes, C. and Minto, C., 2016. Beneficial and healthy properties of Eucalyptus plants: A great potential use. The Open Agriculture Journal, 10(1), pp.52-57.

Wade, P.R., 2000. Bayesian methods in conservation biology. Conservation Biology, 14(5), pp.1308-1316.

Weigelt, A. and Jolliffe, P., 2003. Indices of plant competition. Journal of Ecology, 91(5), pp.707-720.

Westera, W., 2021. Comparing Bayesian Statistics and Frequentist Statistics in Serious Games Research. International Journal of Serious Games, 8(1), pp.27-44.

Yildirim, I., 2012. Bayesian inference: Gibbs sampling. Technical Note, University of Rochester, delivered August 2012.

Zanella, G., 2020. Informed proposals for local MCMC in discrete spaces. Journal of the American Statistical Association, 115(530), pp.852-865.

Zegeye, H., 2010. Environmental and socio-economic implications of Eucalyptus in Ethiopia. Ethiopian Institute of Agricultural Research, 2010, pp.184-205.

Zerga, B., 2015. Ecological impacts of Eucalyptus plantation in Eza Wereda, Ethiopia International Invention Journal of Agricultural and Soil Science, 3(4), pp.47-51.

APPENDIX

SOME SELECTED MATLAB R2022b CODES

MATLAB R2022b codes for descriptive statistics

```
T1= readtable("plot9.txt");

Avg1 = mean(T1{:,{'dbh1', 'dbh2', 'dbh3', 'dbh4', 'dbh5', 'dbh6', 'dbh7', 'dbh8', 'dbh9',
'dbh10'}});

var1 = var(T1{:,{'dbh1', 'dbh2', 'dbh3', 'dbh4', 'dbh5', 'dbh6', 'dbh7', 'dbh8', 'dbh9',
'dbh10'}});

SD1 = std(T1{:,{'dbh1', 'dbh2', 'dbh3', 'dbh4', 'dbh5', 'dbh6', 'dbh7', 'dbh8', 'dbh9',
'dbh10'}});

cv1 = ((SD1)./(Avg1)).*100;

t1 = table(Avg1, var1, SD1, cv1); disp(' Mean Variance SD C.V'),
% Displays the plot figure

disp([Avg1' var1' SD1' cv'])
plot(Avg1)
```

MATLAB R2022b codes for Gibbs Sampling Program 1

```
clear
clc

% Running simulations for the Burnin period

format long
Program1

OE = 0.825887603859672; % Starting value for Burn in Period
OS = 0.095698083836992; % Starting value for Burn in Period
k = [-1 -1 1 1 ]; % Selected vector U for burn in period

l1 = min(size(X));
l2 = min(size(Z));
l3 = max(size(Y));

U = K';
RB = [];
RU = [];
RS = [];
RE = [];
```

```
randn('seed',sum(100*clock));
rand('seed',sum(100*clock));

for i = 1:500          % Repeat ____ times
    i
        for j = 1:20

            % Simulate Q
            Z1 = randn([l1,1]);                % Simulate standard normal numbers
            Q = ((sqrtm(OE*M)*Z1)) + (M*L') - (M*J*U);

            % simulate U
            Z2 = randn([l2,1]);
            U = (Z2'*(sqrtm(OE*(inv((I)+((OE/OS)*B))))))' + ((inv((I)+((OE/OS)*B)))*K') –
            ((inv((I)+((OE/OS)*B)))*J'*Q);

            % Simulate sigma squared S
            Z3 = randn([l2-2,1]);
            Z4 = (Z3.^2);
            V = sum(Z4);          % simulates chi squared with (q-2) degrees of freedom
            OS = ((U'*B*U)/V);

            % Simulate sigma squared E
            Z5 = randn([l3-2,1]);
            Z6 = (Z5.^2);
            W = sum(Z6);           % simulates chi squared with (n-2) degrees of freedom
            OE = ((Y-X*Q-Z*U)'*(Y-X*Q-Z*U))/W;

         End

        RB = [RB Q];
        RU = [RU U];
        RS = [RS;OS];
        RE = [RE;OE];
End

save D:\Program\Gibbs_Results0 RB RU RS RE
```

MATLAB R2022b codes for Gibbs Sampling program 2

```
clear
clc

% Running simulations for Gibbs Sampling
% Use result of gibbs1 from the burnin period

format long
```

Program1

```
load D:\Program\Gibbs_Results0

l1 = min(size(X));
l2 = min(size(Z));
l3 = max(size(Y));
l = max(size(RE))

OE = RE(l)
OS = RS(l)
U = RU(:,l)
RBB = [];
RUU = [];
ROS = [];
ROE = [];

randn('seed',sum(100*clock));
rand('seed',sum(100*clock));

for i = 1:10000        % Repeat ____ times
    i
      for j = 1:20

          % Simulate Q
          Z1 = randn([l1,1]);              % Simulate standard normal values
          Q = ((sqrtm(OE*M)*Z1)) + (M*L') - (M*J*U);

          % simulate U
          Z2 = randn([l2,1]);
          U = (Z2'*(sqrtm(OE*(inv((I)+((OE/OS)*B))))))' + ((inv((I)+((OE/OS)*B)))*K') –
          ((inv((I)+((OE/OS)*B)))*J'*Q);

          % Simulate sigma squared S
          Z3 = randn([l2-2,1]);
          Z4 = (Z3.^2);
          V = sum(Z4);         % simulates chi squared with (q-2) degrees of freedom
          S = ((U'*B*U)/V);

          % Simulate sigma squared E
          Z5 = randn([l3-2,1]);
          Z6 = (Z5.^2);
          W = sum(Z6);           % simulates chi squared with (n-2) degrees of freedom
          OE = ((Y-X*Q-Z*U)'*(Y-X*Q-Z*U))/W;

      End

      RBB=[RBB Q];
      RUU=[RUU U];
      ROS=[ROS; OS];
```

```
    ROE=[ROE; OE];
End
save D:\Program\Gibbs_Results1 RBB RUU ROS ROE
```